Membrane-associated Periodic Skeleton: A developmental perspective

A thesis

submitted in partial fulfilment of the requirements for the degree of

Doctor of Philosophy

by

Shivani Bodas

20172011

Indian Institute of Science Education and Research Pune

2025

Membrane-associated Periodic Skeleton: A developmental perspective

A thesis

submitted in partial fulfillment of the requirements for the degree of

Doctor of Philosophy

विद्या वाचस्पति की उपाधि की अपेक्षाओं की आंशिक पूर्ती में प्रस्तुत शोध प्रबंध

by / द्वारा

Shivani Bodas / शिवानी बोडस

Registration No. / पंजीकरण सं.

20172011

Thesis Supervisor / शोध प्रबंध पर्यवेक्षक

Prof. Aurnab Ghose / प्रो. ऑर्नब घोष

Indian Institute of Science Education and Research Pune

भारतीय विज्ञान शिक्षा एवं अनुसन्धान संसथान पुणे

2025

Certificate

The work incorporated in this thesis entitled **'Membrane-associated Periodic Skeleton: A developmental perspective'** submitted by **Shivani Bodas** was carried out by the candidate under my supervision. The work presented here or any part of it has not been included in any other thesis submitted previously for the award of any degree or diploma from any other University or institution.

In my capacity as the supervisor of the candidate's thesis, I certify that the above statements are true to the best of my knowledge.

 23.06.2025

Prof. Aurnab Ghose

Declaration by Student

Name of Student: Shivani Bodas

Reg. No.: 20172011

Thesis Supervisor(s): Prof. Aurnab Ghose

Department: Biology

Date of joining program: 01/08/2017

Date of Pre-Synopsis Seminar : 30/07/2024

Title of Thesis: Membrane-associated Periodic Skeleton: A developmental perspective

I declare that this written submission represents my idea in my own words and where others' ideas have been included; I have adequately cited and referenced the original sources. I declare that I have acknowledged collaborative work and discussions wherever such work has been included. I also declare that I have adhered to all principles of academic honesty and integrity and have not misrepresented or fabricated or falsified any idea/data/fact/source in my submission. I understand that violation of the above will be cause for disciplinary action by the Institute and can also evoke penal action from the sources which have thus not been properly cited or from whom proper permission has not been taken when needed.

The work reported in this thesis is the original work done by me under the guidance of

Prof. Aurnab Ghose

Date:23/06/2025

Signature of the student

Dedication

To every challenge and every soul—human or canine—that shaped me, guiding me with lessons of resilience, compassion, and empathy.

Acknowledgements

Much like a neural network, my journey has been shaped by countless connections - each one strengthening my knowledge, resilience, and gratitude. This somewhat semi-formal note is to thank everyone I crossed paths with during this quest of knowledge and self.

I am deeply grateful to my mentor Prof. Aurnab Ghose for his constant guidance and support throughout this journey. His persistence in making me learn to think critically and encouragement during moments of doubt have been invaluable. During difficult phases such as dysfunction in the microscope that this study heavily relied on, his kind direction to help expand to alternate super-resolution imaging techniques have been crucial in bringing this project to its current form. His mentorship has not only shaped this work but also profoundly influenced my growth as a researcher and thinker. Importantly, his leadership style of letting people be who they are and giving advice from time to time (when we seemed lost). Having the space and liberty of learning by doing what I felt was ideal, has been instrumental in pushing me to expand the boundaries of my abilities and knowledge. I am truly appreciative for the opportunities of networking and collaborating that I got through him. For anyone joining Aurnab's lab please remember that while we (PhDs) think that all of us are lost (including boss-man), he has a plan brewing in this mind. So sit back, keep at it.

I express my sincere thanks to Prof. Pramod Pullarkat and his team at Raman Research Institute, Bangalore, especially Ashish Mishra who collaborated with us in this study and helped bring in an insightful biophysical perspective to the work.

I'm grateful to Dr. Nagaraj Balasubramanian and Dr. Nixon Abraham, my research advisory committee members, for taking out time for discussions on my project and progress. Their feedback has been vital in defining prospects in this work every so often. I would also like to thank Dr. Ramana Athreya for sharing enriching and uplifting conversations across various themes from astronomy to music. I acknowledge the neuro interest group (NIG) at IISER Pune for meetings to discuss and brainstorm about contemporary research in neuroscience through an interdisciplinary lens. As a part of NIG, I am also grateful to have had the opportunity to organize and host the No Garland Neuroscience conference 2023 at IISER Pune.

I genuinely thank all the present and former members of our neuronal connectivity lab for frequent elevating discussions, tea-time fun & frolic as well as creating a conducive environment or work.

I'd like to express special thanks to Dr. Dhriti Nagar, an excellent alumni of the lab and an important person of my life, who guided me through work with fruitful advice, constant motivation and help in learning new technique such as knockout generation which was crucial for this study. I would also like to thank her for providing me with circumstances which not only tested me but made me realize few crucial and fundamental things of human existence. I want to take this opportunity and thank her for loving and caring for me when she could.

I really admire the common lab atmosphere at IISER Pune that encourages resource sharing and fosters friendships as well as collaborations. I must intensely thank IISER Pune's fantastic support staff in all facilities - microscopy, cell culture, cell sorting, bio-office, proteomics, maintenance, repairs, security, administration and housekeeping. Special thanks to Vijay for all the help with microscope upkeep at all times. I acknowledge financial assistance from IISER Pune for funding my research fellowships during my tenure. I'm very thankful to DBT-CTEP for the generous travel award and to EMBO for inviting me to talk about my research and extending a fee waiver that helped me to present my work internationally.

I have made some great friends in IISER Pune who made experiences along the way fun and memorable. I extend a warm thanks to all my batch mates with whom studying felt like a joyride and many milestones were crossed together. To name a few friends, Gauri Patki, Raksha Bhansali, Somya Madan, Rajdeep Bhowmik, Jayashree Mahajan who have always been in my corner. I also want to thank my batchmates from MSU, Baroda who have been there when they could.

I'm deeply appreciative towards Dr. Himani Khurana for sharing laughs & blues as well as chatter & silences all the same with me, every step of the way. I'm especially grateful for her welcoming all my mischief, for editing my drafts me and for literally everything in between morning teas and evening dinner decision making. She has been one of the most substantial parts of my life, standing like a pillar through both health and sickness (literally). This journey would have been impossible without her. I will be forever grateful for her love, patience, and support.

Most importantly, I'd like to convey all my love and gratitude to aai, baba, tai and fluffy for their incessant warmth, unconditional support and firm faith in me. I recognize the personal growth this endeavor has brought me, through challenges and trials in ways I never expected. I am grateful to myself for staying committed to the process, learning from failures and navigating through challenges with an unwavering spirit. My persistence and grit have shaped this journey like a river carving its path through stone. Last but not the least, I am grateful for music and all the campus

dogs (too many to name) that kept me afloat through highs and lows.

Though this thesis marks an end to this chapter of life, the pursuit of knowledge is never truly finished. I look forward to the challenges and discoveries that lie ahead, knowing that the lessons from this journey and curiosity within me will continue to guide me.

To all the current and aspiring दर्दी PhDs reading this acknowledgment (and hopefully the entire thesis), please take care of your health through this journey of uncertainties. We often tend to overlook ourselves, as the project or the 50th attempt at a failing experiment somehow takes precedence over preservation of self. I've done that and I've suffered for it. All that said, If I had to summarize this journey, I will gladly stand on the shoulders of Urdu speaking literary friends I made in the last 7 years of my Integrated-PhD program.

During the PhD journey when me, the experiments and my life all were at the peak of uncertainty. I felt….

उम्र-ए-दराज़ माँग के लाई थी चार दिन
दो आरज़ू में कट गए दो इंतिज़ार में

- सीमाब अकबराबादी

Now that I am on the verge of finishing this degree, I feel…

मैं अकेला ही चला था जानिब-ए-मंज़िल मगर
लोग साथ आते गए और कारवाँ बनता गया

- मजरूह सुल्तानपुरी

Table of Contents

Abstract

The Membrane-associated Periodic Skeleton (MPS) is a critical cytoskeletal structure observed in diverse neuronal subtypes across multiple species. Since its identification in 2013, it has been demonstrated to be essential for neuronal stability, function, and circuit formation; however, the mechanisms underlying its assembly have remained elusive.

This study examined the developmental patterns and regulatory processes of MPS in embryonic chick dorsal root ganglia (DRG) neurons and in differentiating SH-SY5Y cells. Using STED, a super-resolution microscopy technique, we observed that MPS formation began as early as day-in-vitro-1 (DIV1) and progressed over time, as indicated by the enhanced autocorrelation and reduced dispersal in periodicity (spacing). Acute pharmacological treatments that disrupt actin and microtubule lead to MPS disruption. Chronic interference with microtubule dynamics hindered MPS formation at DIV2 and DIV4. Interestingly, MPS formation was found to be independent on chronic F-actin stabilization and myosin inhibition. Blocking the actin nucleators, Arp2/3 and Formins impeded MPS stability at DIV2 and DIV4 with a diminishing effect, indicating ongoing F-actin renewal and scaffold instability. However, MPS showed resistance to these inhibitors at DIV6, suggesting a more stable scaffold. FRAP analysis of βII-spectrin revealed reduced mobility during development, indicating its integration into the MPS scaffold. Latrunculin-A treatment increased βII-spectrin mobility in early stages but had no effect at DIV4, demonstrating that its reliance on cortical F-actin interaction is limited to early developmental phases. FRAP-based analysis of βII-spectrin domain mutants in differentiated SH-SY5Y βII-spectrin KO neurons showed that its plasma membrane and actin-binding activities are essential for its mobility and incorporation into the MPS, supporting the DRGs Lat-A-treated FRAP results.

To figure out the functional aspect of a forming MPS scaffold, we ablated axons and found a positive correlation between MPS assembly and axonal tension in DRGs. When βII-spectrin KO SH-SY5Y neurons were ablated, we observed a modest decrease in axonal tension, highlighting potential role in maintaining axonal tension. These discoveries offer new perspectives on the developmental assembly, regulatory mechanisms, and functional significance of MPS, underscoring the importance of cytoskeletal interactions in its formation and maintenance.

Synopsis

Discovered in axons in 2013, the periodic subcortical cytoskeleton was initially believed to offer structural support. However, current research has revealed its multifaceted nature. Recent studies (discussed in chapter 1) have broadened our comprehension of MPS's involvement in various neuronal functions like conduction, maintenance of axonal diameter, acting as a platform for sequestering signaling proteins etc. (Costa *et al.*, 2020; Zhou *et al.*, 2022). This developing understanding points to a more intricate role in axonal biology than previously thought, potentially influencing numerous neuronal processes at a circuit level. This becomes even more crucial as neurons are largely irreplaceable and must endure stretch deformation caused by various factors such as body movement, body growth, head impact, and injuries (Andrade et al., 2016; Bayly et al., 2005; Lillie et al., 2017; Phillips et al., 2004).

Interestingly, this periodic MPS arrangement in hippocampal neurons forms over time and increases its prevalence as the neuron matures (Zhong *et al.*, 2014; Qu *et al.*, 2017; Unsain *et al.*, 2018). This raises questions about the relationship between increasing MPS prevalence, development, and functionality. When the MPS is not present in early-stage neurons, what accommodates for its functionality? How is the system structurally stable when MPS is not formed? Is there a differential interplay between other cytoskeletal proteins and MPS as the neuron matures? Most of the studies use matured (late stage) neurons with established MPS, but how does MPS develop and how it gains different functionalities remains poorly understood. The current work is an attempt to tease out molecular mechanisms and understand how the MPS assembles and what are the variables that determine this process.

Chapter 1 of this thesis provides a comprehensive introduction describing how neurons form in the central and peripheral systems, followed by a detailed description of the components of the Membrane Periodic Skeleton (MPS) and the relevance of other neuronal cytoskeletons in the maintenance of MPS. This chapter also highlights the functional relevance of MPS.

Chapter 2 contains a detailed description of all methodologies, data-gathering techniques, and analytical procedures employed throughout the research process. It also includes specific information about the sources of all reagents utilized, both commercial and non-commercial, along with their respective vendor and catalogue information.

Chapter 3 serves as a concise bridge linking the previously reviewed literature in the introduction to the rationale behind the current study. This section sets the stage for the findings of the present

research, which are elaborated in subsequent chapters.

Chapter 4 discusses the results of experiments aimed at establishing a developmental timeline for MPS assembly in chick Dorsal Root Ganglion (DRG) neurons using super-resolution microscopy. This chapter also describes the potential differences in how MPS forms in DRGs and other neuronal types.

Chapter 5 explores the relationship between MPS with actin, microtubule and myosin throughout development. This section also emphasizes the importance of microtubule dynamics in MPS formation despite the absence of known direct interactions. This section has highlights how chronic stabilisation of F-actin or inhibition of contractility does not play a role in MPS formation.

Chapter 6 describes the relevance of Arp2/3 and Formins in regulating F-actin turnover and reveals differential effect on the MPS scaffold over development.

Chapter 7 examines the findings of FRAP experiments aimed at investigating the βII-spectrin mobility throughout the MPS assembly process. This section also explores how F-actin interactions influence the mobility of βII-spectrin. *This chapter also* outlines the procedure for creating and confirming a βII-spectrin knockout in the SH-SY5Y neuroblastoma cell line using the CRISPR-Cas9 gene-editing technique. Further, FRAP studies using βII-spectrin domain mutants demonstrate the importance of the plasma membrane and actin binding not only for mobility but also for incorporation into the MPS framework. Additionally, this chapter presents a novel finding demonstrating that differentiated SH-SY5Y axons exhibit MPS.

Chapter 8 examines the outcomes of an experiment involving axonal ablation in order to elucidate the relationship between MPS formation and axonal tension. Further, this section describes experiments conducted on DRGs and βII-spectrin knockout model that reveal potential functional importance in maintaining MPS and axonal tension.

Chapter 9 contains a brief summary of the findings described in the preceding chapters, a thorough discussion of our results in the context of the existing literature highlighting how this study propels our understanding of MPS formation and discusses how multiple variables dictate this process.

List of figures

Chapter 1. **Introduction**

Chapter 2. **Materials and methods**

Chapter 4. **Characterization of Membrane Periodic Skeleton (MPS) in chick DRG neurons**

Chapter 5. **Role of actin and microtubule dynamics in MPS formation and stability**

Chapter 6. **Role of Arp2/3 complex and Formin in maintenance of MPS**

Chapter 1

Introduction

The nervous system, an intricate web of neurons and auxiliary cells, controls the organism's capacity to perceive, react, and adjust to its surroundings. It is primarily separated into two key components: the central nervous system (CNS) and the peripheral nervous system (PNS). These two systems collaborate to synchronize sensory inputs, motor outputs, and advanced cognitive functions. The formation of the CNS and PNS is an exceptionally complex and regulated process, initiating early in embryonic development and persisting after birth, with distinct yet interrelated pathways that mould their structure and operation. This section explores the formation of the CNS and PNS, followed by components of membrane periodic skeleton and its functional relevance

1.1 Development of the Central Nervous System (CNS) and Peripheral Nervous System (PNS)

The central nervous system (CNS), comprising the brain and spinal cord, originates from the neural tube, formed during neurulation. This process starts with the neural plate, a thickened ectodermal area, influenced by signalling molecules like Sonic Hedgehog (Shh), Bone Morphogenetic Proteins (BMPs), and Fibroblast Growth Factors (FGFs) (Levine and Brivanlou, 2007; Ulloa and Martí, 2010). These signals from the notochord and mesoderm establish a dorsoventral gradient that patterns the neural tube into distinct regions. As the neural plate folds and fuses to form the neural tube, neuroepithelial cells lining its walls multiply and differentiate into various neuronal and glial types. This process is regulated by transcription factors, including Pax, Nkx, and Olig families, determining cell fates in the developing CNS. Along the rostro caudal axis, the neural tube segments into the forebrain (prosencephalon), midbrain (mesencephalon), and hindbrain (rhombencephalon). These mature brain structures like the cerebral cortex, basal ganglia, thalamus, and cerebellum.

Radial glial cells (RGCs) are crucial in CNS development, acting as progenitors for neurons and glia and as scaffolding for migrating neurons (Götz and Huttner, 2005; Kriegstein and Alvarez-Buylla, 2009). Cortical development relies on radial migration, where new neurons move outward to create the six-layered cerebral cortex. Axon guidance and synaptogenesis, facilitated by cues such as netrins, slits, semaphorins, and ephrins, ensure precise neural circuit formation (Yuasa-Kawada *et al.*, 2023). After birth, the CNS refines through synaptic pruning, myelination, and plasticity. Myelination by oligodendrocytes increases signal conduction speed, while synaptic pruning removes unnecessary synapses, optimizing neural connectivity.

After birth, the central nervous system (CNS) undergoes refinement through various processes, including synaptic pruning, myelination, and plasticity. Oligodendrocytes facilitate myelination, which boosts signal transmission speed, while synaptic pruning eliminates unnecessary or inefficient synapses, thereby improving neural connections.

The peripheral nervous system (PNS), which includes sensory, motor, and autonomic nerves, develops from two distinct embryonic structures: neural crest cells and placodes. Neural crest cells, a versatile cell population, emerge at the neural plate edges and extensively migrate throughout the embryo (Bronner and LeDouarin, 2012). These cells differentiate into various types, such as sensory neurons, sympathetic and parasympathetic neurons, and Schwann cells, depending on their migration paths and environmental signals. Placodes, which are thickened areas of ectoderm adjacent to the neural crest, contribute to cranial sensory ganglia formation. Together, neural crest cells and placodes give rise to the peripheral ganglia and related structures, enabling the PNS to transmit sensory information to the CNS and execute motor commands.

Axonal outgrowth in the PNS is guided by molecular cues similar to those in the CNS. Schwann cells, the myelinating glia of the PNS, play a crucial role in axonal insulation and repair following injury (Jessen and Mirsky, 2016). Unlike the CNS, the PNS exhibits a higher regenerative capacity, attributed to the intrinsic plasticity of Schwann cells and a supportive extracellular environment (Hoffman, 2010; Varadarajan *et al.*, 2022).

1.2 Structure of a Neuron

Neurons, the functional units of the nervous system, are specialized for rapid communication. Despite their diversity in shape and size, neurons share a fundamental structure comprising three main regions: the soma (cell body), dendrites, and axon.

As the basic building blocks of the nervous system, neurons exhibit a highly specialized structure that facilitates efficient information transmission and processing. The cell body, or soma, contains the nucleus, which houses genetic material and acts as the command center for cellular operations. Various organelles essential for protein production, energy generation, and other crucial cellular processes surround the nucleus within the cell body. The most characteristic components of neurons are their axons and dendrites, which extend outward from the soma and create complex networks.

Axons, generally longer and slenderer, transmit electrical signals away from the cell body to other neurons or target tissues. These structures can range in length from a few micrometers to over a meter in some instances. In contrast, dendrites are typically shorter and more extensively branched, forming tree-like structures that receive incoming signals from other neurons. This unique cellular arrangement enables neurons to establish intricate neural circuits, facilitating the integration and processing of information across extensive networks within the nervous system.

The cytoskeleton, an intricate and ever-changing network of protein, is crucial for preserving cell structure, facilitating internal transport, and enabling mechanical signal transduction. In nerve cells, this framework is vital for establishing and sustaining cellular asymmetry, fostering the growth of axons and dendrites, and allowing for synaptic adaptability. These processes are fundamental to neuronal operations and the formation of interconnected neural networks (Fletcher and Mullins, 2010; Coles and Bradke, 2015).

1.3 The neuronal cytoskeleton

Microtubules are structures made up of α- and β-tubulin heterodimers that provide structural support and enable intracellular transport via motor proteins like kinesin and dynein. These components are critical for transporting organelles, vesicles, and signaling molecules within axons, thus maintaining neuronal balance (Cooper, 2000). The polarity of microtubules, with minus ends near the cell body and plus ends extending towards the axonal or dendritic periphery, determines the direction of cargo transport within cells (Kapitein and Hoogenraad, 2015).

Neurofilaments, which are the main type of intermediate filaments in neurons, are vital for maintaining axonal structural integrity. Proper development of axon diameter is crucial for the nervous system to function normally, as the size of an axon significantly influences the speed at which nerve signals travel along it (Gasser and Grundfest, 1939; Arbuthnott *et al.*, 1980; Sakaguchi *et al.*, 1993). It becomes even more important as neurofilaments are known to determine axonal diameter (Sakaguchi *et al.*, 1993b; Križ *et al.*, 2000). Irregularities in neurofilaments function have been associated with various neurodegenerative disorders, such as amyotrophic lateral sclerosis (ALS) and Charcot-Marie-Tooth disease (Fuchs and Cleveland, 1998; Yuan *et al.*, 2017). These cellular elements collaborate to regulate neuronal shape, internal transport, and responses to mechanical stimuli, thereby ensuring proper neuronal function and adaptability.

F-actin, or actin filaments, are dynamic structures primarily found at the edges of neurons,

including growth cones, dendritic spines, and presynaptic terminals. These structures play essential roles in cellular movement, internal transport, endocytosis, and synaptic plasticity (Rust and Maritzen, 2015; Chakrabarti *et al.*, 2021; Gentile *et al.*, 2022; Schneider *et al.*, 2023) . The dynamics of actin are controlled by various proteins that bind to it, such as cofilin, profilin, and the Arp2/3 complex, which manage the assembly, branching, and breakdown of filaments (Blanchoin *et al.*, 2000; Liman *et al.*, 2020). Moreover, the way F-actin is organized within dendritic spines is crucial for the strength and plasticity of synapses during learning and memory formation (Hotulainen and Hoogenraad, 2010).

1.4 Actin-Spectrin Cytoskeleton

While F-actin is known to interact with numerous proteins, this dissertation concentrates on its relationship with spectrin protein. Initially identified in red blood cells, the actin-spectrin cytoskeleton forms a highly structured, repeating network. In these cells, its primary function is to boost the mechanical strength and flexibility of the cell membrane, allowing erythrocytes to endure repeated shape changes as they circulate through the body (Bennett and Healy, 2008, 2009).

The actin-spectrin skeleton consists of actin strands capped by adducin and connected by spectrin tetramers. Each spectrin tetramer is composed of two α-spectrin and two β-spectrin units arranged in an antiparallel manner. Spectrin repeats, which are triple-helical clusters, are found in the central rod domain of spectrin and are crucial for the flexibility and extension of the tetramer (Bennett and Lorenzo, 2013). In cell types apart from RBCs, the structure of αII-Spectrin consists of 20 modular SRs repeats, along with several functional domains. Near its C-terminal end, it features a calcium-binding EF hand domain. Additionally, the protein incorporates an Src-homology 3 (SH3) domain and a region that binds to calmodulin (CaM). The typical βI–βIV-spectrins are composed of 16 complete spectrin repeats (SRs) and a partial 17th SR. They also feature two calponin homology (CH) domains at the N-terminus, a binding site for ankyrin in SR15, and a pleckstrin homology (PH) domain at the C-terminus. The CH domains facilitate interaction with actin, while the PH domain enables binding to lipids in membranes (Fig. 1.0). The formation of spectrin tetramers occurs through non-covalent, head-to-head interactions between partial repeats in the α-spectrin and β-spectrin subunits.

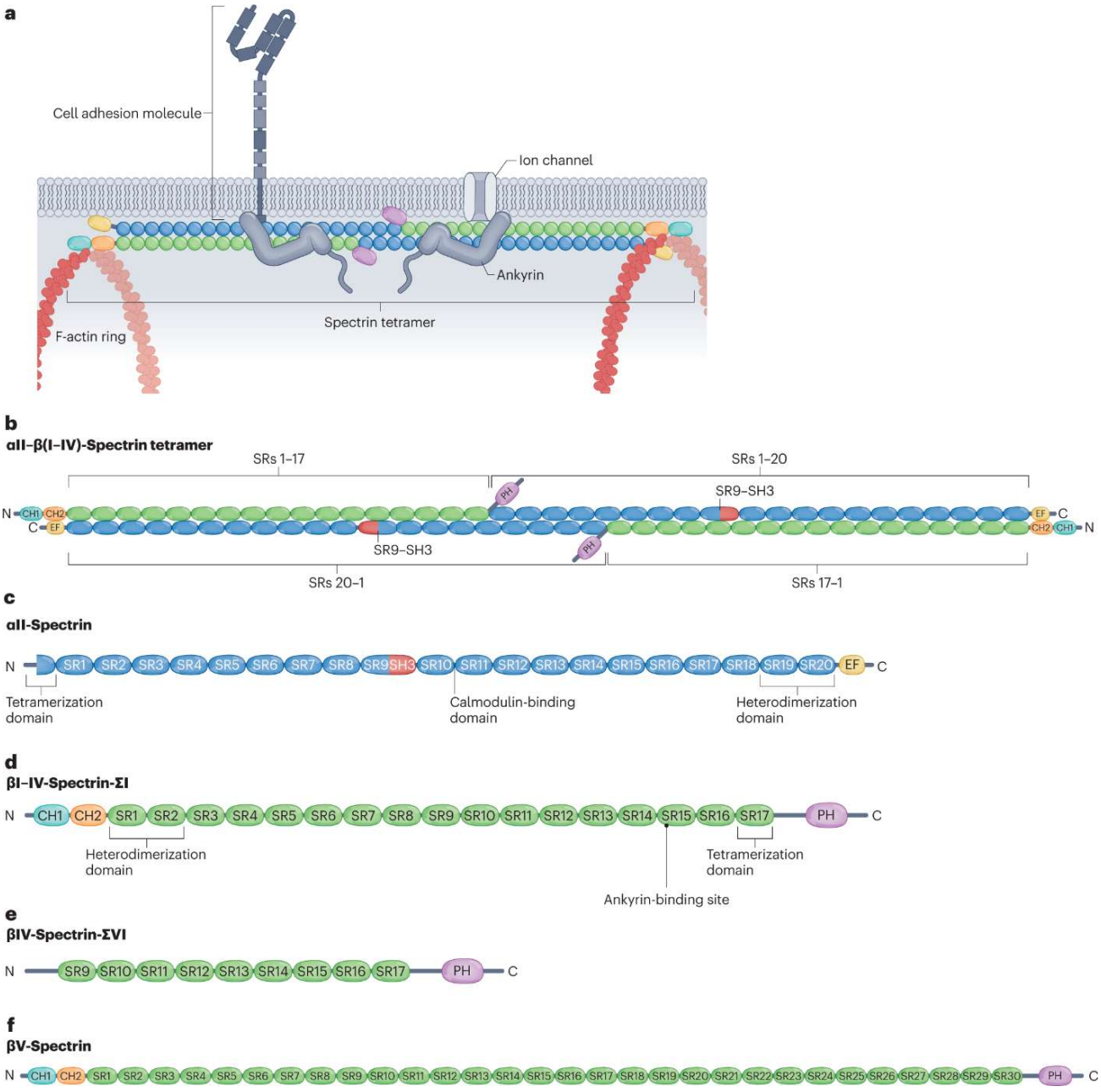

Figure 1.0 Tetrameric assembly and structural domains of neuronal spectrins. Adapted from Lorenzo, D.N., Edwards, R.J. & Slavutsky, A.L. Spectrins: molecular organizers and targets of neurological disorders. Nat Rev Neurosci 24, 195–212 (2023).

1.5 Axonal actin-spectrin Membrane Periodic Skeleton (MPS)

In 2013, researchers utilizing super-resolution microscopy identified a unique membrane-associated periodic skeleton (MPS) in neurons. This skeletal structure is composed of actin and spectrin proteins, which are positioned beneath the cell membrane at consistent intervals of about 190 nm along the axons (Xu *et al.*, 2013). Till now, MPS has been detected not only in axons but

also in dendritic region of neuron (Zhong *et al.*, 2014; Han *et al.*, 2017). In various neuron types, including cortical, hippocampal, touch receptor, and sensory neurons, spectrin can establish a comparable periodic structure. This organizational pattern has been identified in a range of organisms, such as *Caenorhabditis elegans*, *Drosophila, Gallus gallus, Mus musculus, and Homo sapiens* (D'Este *et al.*, 2015, 2017; Han *et al.*, 2017). The MPS has been observed in real-time using Sir-actin, a live imaging probe for F-actin, along with a GFP-tagged spectrin probe (D'Este *et al.*, 2015; Zhou *et al.*, 2022).

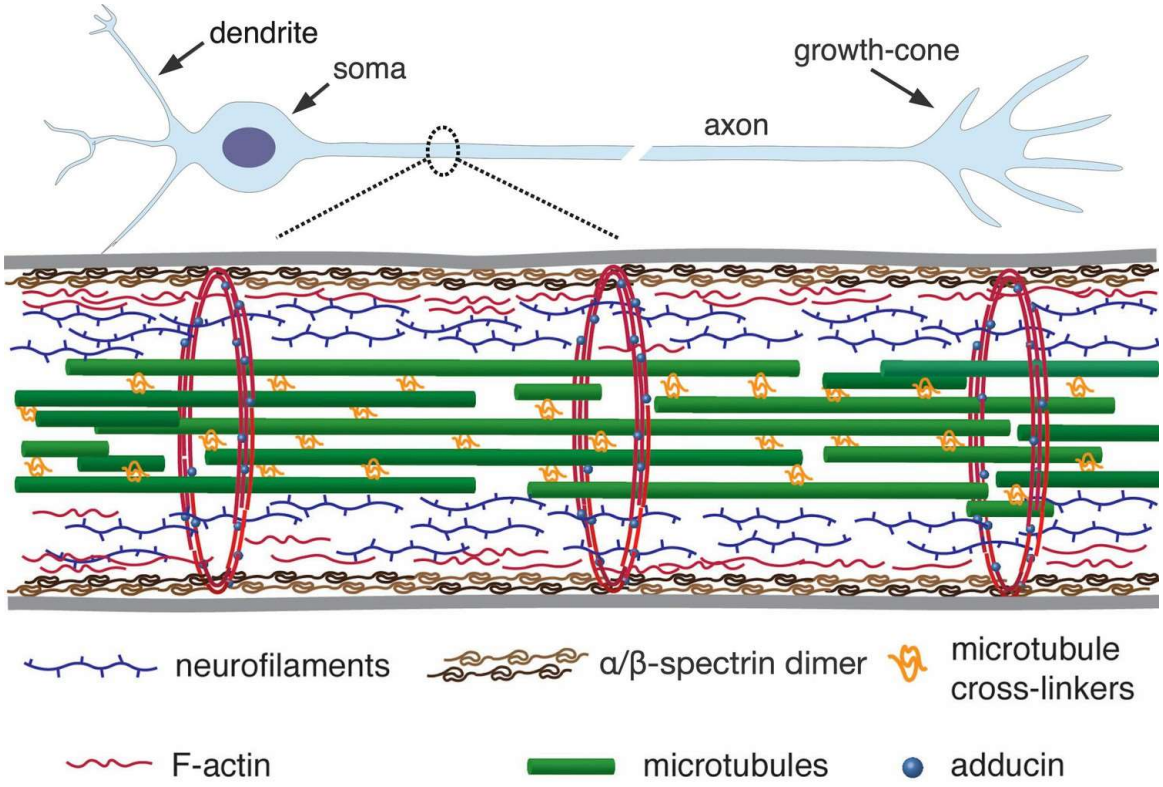

Figure 1.1 A simplified schematic of the axonal cytoskeleton. Adapted from Sushil Dubey, Nishita Bhembre, Shivani Bodas, Sukh Veer, Aurnab Ghose, Andrew Callan-Jones, Pramod Pullarkat (2020) The axonal actin-spectrin lattice acts as a tension buffering shock absorber eLife 9:e51772

1.6 How does MPS form over development?

There have been few studies that have contributed in understanding few aspects of MPS formation during early development. In hippocampal neurons, MPS has been observed shortly after axons begin to grow, primarily in areas close to the cell body at DIV2. As time progresses, this periodic structure extends towards the distal end of the axon. By DIV12, the MPS can be identified throughout the entire length of the axon (Zhong *et al.*, 2014). In contrast, Dorsal root ganglion (DRG) neurons exhibit minimal MPS in the proximal area, while it is abundant in the distal region

(Wang *et al.*, 2019). This pattern of development, moving from proximal to distal regions, requires further validation using unbiased sampling methods and quantitative analysis of the MPS across multiple neuronal types coming from both CNS and PNS.

In mouse cortical neurons, the MPS does not extend continuously into the growing axon but develops from patches of periodic βII-spectrin at the growth cone which grow and coalesce into a continuous scaffold from distal end to the proximal end. The researchers imaged the entire axon and propose the growth cone or its neck as a potential site for the formation of periodic patches. Their findings reveal periodic patches in the axonal region immediately adjacent to the GC. In parallel, they found that the GC contains a high concentration of spectrin, potentially serving as a reservoir for its incorporation into the expanding axon (Hofmann *et al.*, 2022). This hypothesis corroborates with more MPS observed in proximal region compared to distal region (Zhong *et al.*, 2014) but it needs to be further tested by live imaging since they were imaged from snapshot at DIV11 and we can't be sure if it forms from distal and then coalesce away from GC or it assembles in a proximo-distal direction.

Recent work (a pre-print) which used hippocampal neurons found that while the MPS was getting assembled near the soma-axon junction, distal axons exhibited discrete patches enriched with spectrins and adducin. They hypothesize that these patches serve as local reservoirs, providing the necessary components to facilitate the assembly of the MPS. They also found that the spectrin patches to be highly stable and solid-like. Their observations suggest that actin filaments play a role in the formation of the MPS. Spectrin/adducin patches tend to form in axonal regions with less F-actin, and deleting actin- and membrane-binding domains of βII-spectrin triggers phase separation. These findings indicate that the gradual accumulation of actin filaments in the distal axon may translocate spectrins and adducin from the axonal patches to the subplasmalemmal actin network, where they can assemble into the periodic lattice (Boyer *et al.*, 2024). While both the models hint towards assembly-post condensation/ coalescence, the directionality still remains to be unfurled. It is interesting and surprising that these discrete patches arise much later (DIV 6) compared to when MPS starts to assemble.

In contrast, (Gazal et al., 2025) report that in human motor neuron derived from iPSCs, spectrin patches primarily occur in mid-axon regions, with distal axons exhibiting continuous MPS. Moreover, they find that these patches do contain organized MPS, challenging the conclusions of the earlier study. According to the authors, the gap-and-patch pattern reflects an intermediate stage

of MPS assembly, with βII-spectrin incorporation into patches halting its diffusion and depleting adjacent regions. This dynamic assembly is actin-dependent and not a result of degeneration. This needs thorough investigation as different neuronal type show differences in assembly whereas the rate of formation can also vary.

Apart from this, Axonal Initial Segment (AIS), which develops near the proximal area of the axon as the neuron matures, also displays a periodic MPS structure (Leterrier *et al.*, 2015; Huang *et al.*, 2017). During neuronal development, the βII-spectrin is displaced from the proximal to distal axonal region, followed by the integration of βIV Spectrin into the periodic framework along with αII Spectrin (Zhong *et al.*, 2014). Nodes of ranvier demonstrate regular MPS patterns, while ankyrin G, neurofascin, and Nav channels also display periodic arrangements (Leterrier *et al.*, 2015a; D'Este *et al.*, 2016, 2017).

Multiple studies have tried to understand components of MPS that are essential for its assembly. Presence of spectrin-tetramer is essential for MPS formation (Lorenzo *et al.*, 2019) where was pharmacological destabilization of F-actin dynamics is detrimental to stability of MPS (Han *et al.*, 2017; Qu *et al.*, 2017; Wang *et al.*, 2019; Dubey *et al.*, 2020). βII-spectrin knock down affects periodic distribution of F-actin (Xu *et al.*, 2013; Zhong *et al.*, 2014). Where as knockout of one of the spectrin leads to downregulation of others (Lorenzo *et al.*, 2019).These studies highlight that neither F-actin nor spectrin tetramer can form the periodic structure alone.

The next few sections describe multiple components of the scaffold and their relevance in assembly as well as in functionality of the MPS

1.7 Actin binding/regulating proteins in MPS

Neuronal development relies heavily on the actin cytoskeleton, which is crucial for shaping cell morphology, facilitating intracellular transport, and enabling synaptic plasticity. The highly dynamic nature of the actin cytoskeleton is orchestrated by numerous actin-binding proteins (ABPs). These proteins regulate various processes, including the polymerization, depolymerisation, branching, severing, and cross-linking of actin filaments. In neurons, ABPs are essential for multiple functions, such as guiding axons, forming dendritic branches, establishing synapses, and modulating synaptic plasticity.

In addition to myosin and adducin, which control axonal diameter through their interaction with MPS via F-actin, other proteins also interact with F-actin and are found to be present in the MPS. Studies have revealed that the MPS contains a periodic arrangement of two proteins: dematin, which bundles and stabilizes F-actin, and tropomyosins (both 1 and 2), which interacts with both F-actin and myosin. Coronin also associates with MPS and exhibits a periodic arrangement. In neurons where tropomodulin 1 and dematin were depleted, MPS was either completely or partially disrupted. However, when ankyrin B, coronin 2B, or tropomodulin 2 were depleted, no significant disruption to the MPS was observed (Zhou *et al.*, 2022). These results highlight differential role of these proteins in MPS formation and functionality.

Actin Polymerization:

Profilin, a crucial actin-binding protein, enhances actin polymerization by attaching to G-actin and assisting its incorporation into F-actin at the barbed ends (Pollard & Cooper, 2009). In nerve cells, profilin plays a vital role in axon growth and the formation of dendritic spines. The Drosophila profilin null mutant, $Chic^{221}$, exhibited no decrease in MPS abundance in *Drosophila* neurons at 10 DIV. This observation suggests that Profilin does not play a role in F-actin dependent MPS regulation. In contrast, when Ena/Vasp (responsible for F-actin elongation) was reduced through the ena^{23} mutation, a notable decrease in MPS abundance was observed at 10 DIV (Qu *et al.*, 2017). This finding is unexpected, given that profilin and Ena/Vasp are known to collaborate (Bear and Gertler, 2009). The researchers suggest that actin nucleation might play a crucial role in MPS formation, where actin filaments are characterized by their short length and, consequently, are anticipated to be abundant in number (Qu *et al.*, 2017).

On the other hand, Formins are proteins that nucleate actin and promote filamentous F-actin formation. Formins attach to the fast-growing ends of filaments, shielding them from capping proteins while enabling the incorporation of actin monomers. In nerve cells, formins are essential for axon development, dendrite branching, and filopodia formation (Matusek *et al.*, 2008; Heiman and Shaham, 2010; Ganguly *et al.*, 2015; Sahasrabudhe *et al.*, 2016). Neurons with $DAAM^{Ex68}$ null mutation or those treated with the formin-inhibiting drug SMIFH2 exhibited a significant decrease in MPS quantity (Qu *et al.*, 2017). This seems intuitive as MPS structure would need more filamentous F-actin for the ring formation.

Actin Branching:

The Arp2/3 complex initiates new actin filaments from existing ones, creating a branched network

essential for dendritic spine structural plasticity (Korobova and Svitkina, 2008). Abnormalities in Arp2/3 complex regulation have been implicated in neurodevelopmental conditions, including autism spectrum disorders (Kim *et al.*, 2013). Neurons with Arp null mutation exhibited a significant decrease in MPS quantity (Qu *et al.*, 2017). This seems intriguing because branched F-actin is not seen to be a part of the MPS but it's possible this pool of actin is acting as a reservoir.

1.8 Adducin and myosin in MPS

Adducin and myosin are also part of MPS and are known to determine axonal diameter (Leite *et al.*, 2016; Costa *et al.*, 2020). α-adducin deletion leads to an MPS with enlarged diameter, although adducin integration into the MPS occurs in neurons at later stages (Zhong *et al.*, 2014; Leite *et al.*, 2016). It is possible that adducin might be maintaining the structural integrity of the MPS as the proportion of axonal segments with regular MPS in neurons lacking adducin is reduced. These findings indicate that while adducin is not essential for MPS formation, it plays a crucial role in regulating its diameter. In parallel, Non-muscle myosin II (NMII) filaments bind to the MPS and modulate circumferential contractility (Costa *et al.*, 2020; Zhou *et al.*, 2022) and in turn also maintain conduction.

1.9 Ankyrins in MPS

In the distal axonal compartment, two primary neuronal ankyrin-B variants (220 and 440 kDa) are found throughout the axon and play crucial roles in axonal development, guidance, and establishing proper structural connections (Lorenzo *et al.*, 2014; Yang *et al.*, 2019). STED images of axons labelled with a 440 kDa ankyrin-B-specific antibody shows ~190 nm periodicity, suggesting that 440 kDa ankyrin-B is a component of the MPS (Yang *et al.*, 2019). While pan-ankyrin-B antibody labelling reveaed that axonal ankyrin-B proteins form a partially periodic pattern (Xu *et al.*, 2013). Interestingly, eliminating both ankyrin-B isoforms does not disrupt the MPS formation (Lorenzo *et al.*, 2014).

In the AIS, Ank-G is a part of MPS and this scaffold is known to be resistant to actin and microtubule perturbation (Leterrier *et al.*, 2015). Interestingly, when the AIS morphology is disrupted by sudden Increase in intracellular calcium concentration, the MPS gets disassembled but AnkG localization remains undisturbed (Leterrier *et al.*, 2015a). The MPS in AIS scaffold seems to be more stable towards perturbation at least when it comes to cytoskeletal destabilization

than distal MPS.

1.10 Clustering of transmembrane proteins or signaling proteins in MPS

Advanced imaging techniques utilizing super-resolution have revealed the presence of various proteins within cellular structures. These include structural components like coronin, as well as proteins that span the cell membrane such as sodium and potassium ion channels, G protein-coupled receptors (GPCRs), and receptor tyrosine kinases (RTKs). Additionally, molecules involved in signalling processes that associate with the membrane, such as CAMK IIβ, have been observed (Zhou *et al.*, 2022).

1.11 Functional relevance of MPS

- **Axonal Contractility, Conduction, and Structural Stability**

As discussed earlier, the MPS is crucial for maintaining axonal circumferential contractility and conduction (Costa *et al.*, 2018, 2020; Zhou *et al.*, 2022).The spectrin cytoskeleton mitigates mechanical forces, preventing excessive deformation during neuronal activity and external stress (Krieg *et al.*, 2014a, 2017). Loss of spectrin results in axonal fragility, impaired signal transmission, lethality and eventual degeneration highlighting its structural importance (Hammarlund *et al.*, 2007a; Lorenzo *et al.*, 2019).

- **AIS formation and function**

MPS is vital for AIS development and operation, serving as an anchor for critical ion channels and scaffolding proteins (Zhong *et al.*, 2014; D'Este *et al.*, 2017b; Huang *et al.*, 2017). Spectrin forms a complex with ankyrin-G, which helps stabilize voltage-gated sodium (Nav1.6) and potassium (Kv7) channels, ensuring effective action potential generation (Huang *et al.*, 2017). The periodic structure of actin-spectrin is fundamental for preserving AIS integrity, preventing the displacement of ion channels and structural proteins (Zhong *et al.*, 2014). Disruption of spectrin at the AIS results in disorganized clustering of ion channels, compromising neuronal excitability and circuit function (D'Este *et al.*, 2017b). This can contribute to neurodevelopmental disorders, epilepsy, and intellectual disability (Cousin *et al.*, 2021).

- **Spectrin's mechanical resilience and elasticity**

The mechanical resilience of spectrin is essential for neuronal functionality, especially in axons that are constantly subjected to physical forces. Research utilizing atomic force microscopy has demonstrated that the tertiary configuration of spectrin repeats (SRs) contributes to the molecule's elasticity (Rief *et al.*, 1999). This elastic property allows spectrin to regain its form after being mechanically stretched, which is vital for its role in both red blood cells (RBCs) and axons (Krieger *et al.*, 2011; Krieg *et al.*, 2017). In RBCs, the unfolding and refolding of spectrin enable the cell membrane to endure shear stress during circulation (Rief *et al.*, 1999; Krieger *et al.*, 2011). Similarly, in neurons, spectrin's ability to stretch in response to mechanical tension ensures axonal durability, protecting against structural damage under stress (Krieg *et al.*, 2014, 2017; Dubey *et al.*, 2020). Consequently, spectrin's capacity to adapt to mechanical stress is crucial for maintaining both cellular integrity and neuronal function, ensuring long-term survival in dynamic environments.

- **MPS in Axonal Transport and Synaptic Function**

The MPS plays a crucial role in regulating intracellular transport, ensuring the efficient movement of organelles and vesicles within axons, which is essential for synaptic transmission, neuronal health, and plasticity (Lorenzo *et al.*, 2019; Wang *et al.*, 2019). Spectrin functions as a platform for microtubule-associated motor proteins, including dynein and kinesin, enabling bidirectional cargo transport (Lorenzo *et al.*, 2019). When spectrin is absent, synaptic vesicle trafficking is disrupted, resulting in synaptic dysfunction and imbalances in neurotransmitters (Wang *et al.*, 2019). Neurodevelopmental disorders and neurodegenerative diseases can arise from defects in axonal transport caused by mutations in spectrin (Cousin *et al.*, 2021).

- **MPS and neuro-degeneration**

Rapid and sustained reduction in the abundance and organization of the axonal MPS was observed after trophic factor deprivation. Fragmented axons completely lack this crucial structural element, and pharmacological stabilization of actin filaments prevents both MPS loss and axonal fragmentation. These findings strongly suggest that disassembly of the MPS is a prerequisite for the fragmentation of axons to occur (Unsain *et al.*, 2018).

In a similar study, depriving mouse sensory neurons of trophic support rapidly disassembled the MPS, preceding protein loss and occurring independently of caspase activation. Destabilization of

the actin cytoskeleton initiates retrograde signaling pathways required for degeneration, whereas stabilizing actin prevents MPS disassembly and related retrograde signaling during trophic deprivation. Importantly, depleting βII-spectrin, a key MPS component, suppressed retrograde signaling and protected axons from degeneration (Wang *et al.*, 2019).

- **MPS and microtubules**

In *Drosophila*, F-actin reduction resulted in gaps in microtubule bundles, reduced microtubule polymerization, and fewer axons, suggesting a role for the periodic membrane skeleton in microtubule organization. These effects were significantly exacerbated in neurons lacking the microtubule-stabilizing protein Short stop. Combining actin manipulations with Shot deficiency revealed a close relationship between MPS abundance and microtubule regulation (Qu *et al.*, 2017). Examining MT length and quantity in β-spectrin mutants indicates that the network formed by actin and spectrin provides sideways support, safeguarding the MT bundle from distortion (Krieg *et al.*, 2017). Interestingly, microtubules have no known direct interaction but they interact rather indirectly via intermediate proteins that connect microtubule to ankyrin and eventually to the MPS structure as shown by work in *C.elegans* (He *et al.*, 2020a).

In cultured neurons, high dose acute destabilization of microtubule by nocodazole in hippocampal neurons leads to reduction in MPS status while low dose chronic stabilization of microtubules by Taxol at DIV3 for 3 days lead to no change in MPS (Zhong *et al.*, 2014). DRG neurons pretreated with high dose Taxol showed resistance to degeneration upon trophic factor withdrawal and it is hypothesized that Taxol might be affecting microtubule dependent transport and stability (Unsain *et al.*, 2018). This needs further analysis to understand dependence of both components on each other.

Expanding research on membrane periodic skeleton (MPS) development is essential for numerous reasons:

1. **Neuronal functionality and neuro developmental conditions**: The MPS is critical for maintaining axonal structure, stability, and operation. Exploring its development may offer insights into how neurons establish and sustain their intricate architecture. Various neurodevelopmental disorders are linked to abnormalities in neuronal structure and function. Examining MPS development could uncover new mechanisms underlying these conditions and potential treatment targets.

2. **Synaptic adaptability:** The MPS may impact synaptic plasticity, which is fundamental for learning and memory. Investigating its development could shed light on synaptic function and plasticity mechanisms.

3. **Cellular mechanics:** The MPS contributes to axonal mechanical properties. Further study could at a whole-body scale could help us understand how MPS is contributing to circuit formation and how it could be relevant for keeping the nerves safe from breaking because of body movements.

4. **Therapeutic potential:** understanding MPS development and maintenance would enhance our understanding of complex protein interactions in neurons, potentially uncovering new therapeutic targets for neurological disorders. This could inform strategies to promote axonal regeneration following injury or in neurodegenerative diseases.

Taking all these possibilities into consideration, this thesis focuses on systematically understanding formation of this periodic scaffold and to also tries to understand its functional relevance during development of the neuron.

Chapter 2

Materials and method

Materials and Methods

The subsequent sections provide comprehensive details on the materials utilized throughout this thesis, as well as the methodologies employed. For items obtained from commercial sources, the relevant supplier information and product numbers are provided in brackets. Where applicable, appropriate acknowledgments and references have been included for external contributions or sources.

2.1 Constructs, cloning, and plasmids

The human βII-spectrin (SPTBN1) gene (Gene bank accession no – 6711) was inserted into pCAG-GFP for expression in bacteria. This construct served as a template for introducing modifications and deletions within the βII-spectrin gene. All gene insertion, mutation and deletion were performed using the PCR-based restriction-free cloning method. The following table includes all necessary details regarding the plasmids and primers used for cloning:

S.No.	Plasmid Name	Insert/deletion/ mutation	Vector	Primers
1	pCAG-GFP	NA	NA	
2	pCAG-FL-Spectrin-GFP	Full length SPTBN1 (Addgene : 31070)	pCAG-GFP	Insert (spectrin) Forward : AGTCGACGGTACCGCGGGCCCatgacgaccacagtagccaca Insert (Spectrin) Reverse : CATGGTGGCGACCGGTGGATCCCtccgcggtttctttttgccaaa Vector (pCAG) Forward : tttggcaaaaagaaaccgcggaGGGATCCACCGGTCGCCACCATG Vector (pCAG) Reverse : tgtggctactgtggtcgtcatGGGCCCGCGGTACCGTCGACT
3	pCAG-ΔABD-Spectrin-GFP	SPTBN1 825bp deletion at C Terminal (3-277 amino acid))	pCAG-FL-Spectrin-GFP	Forward : CGACGGTACCGCGGGCCCATGACGTCTAAGATGAAGGCCTT Reverse : AAGGCCTTCATCTTAGACGTCATGGGCCCGCGGTACCGTCG
4	pCAG-Spectrin-K2207Q -GFP	SPTBN1 with Point mutation in PH domain : K2207Q	pCAG-FL-Spectrin-GFP	Phmutant forward :ttcctcaatcggcagcacgagtg Vector Reverse : cactcgtgctgccgattgaggaa Vector forward : AATGCCCTGGCTCACAAATACCAC Phmutant Reverse : GTGGTATTTGTGAGCCAGGGCATT
6	pCAG-Spectrin-Y1874A -GFP	SPTBN1 with Point mutation in Ank domain : Y1874A	pCAG-FL-Spectrin-GFP	Ank Forward : tccaggcggccGCTgcgggtgacaa Ank Reverse : ttgtcacccgcAGCggccgcctgga Vector Frwd : CCACTCGTGCACCCAACTGATCTTC Vector Rev : GAAGATCAGTTGGGTGCACGAGTGG

Plasmid-prep: *E. coli* DH5α cells were utilized for the amplification and isolation of plasmids via the alkaline lysis method. The plasmids were subsequently purified using Miniprep columns (Qiagen, 27106) and stored at -20 ºC for future use. Sequencing was conducted to verify all clones.

2.2 DRG dissection and culture

Chick embryo Dorsal Root Ganglia (DRG) were extracted from 8-9-day old embryo using sterile Leibovitz's L-15 medium (Hi-Media, AL204A) for the dissection process. The procedure was conducted under a microscope within a laminar flow hood. Each embryo yielded approximately 12-16 DRGs in the L-15 medium. The mixture was then centrifuged at 3000 rpm for 3 minutes, and the supernatant was discarded. The DRGs in the resulting pellet were immersed in trypsin solution and kept at 37 °C for 30 minutes. Subsequently, another 3-minute centrifugation at 3000 rpm was performed to eliminate most of the trypsin solution, followed by a L-15 wash to remove any extra trypsin. The cell bodies, now separated, were plated on either just glass coverslips or glass-bottom dishes coated with Poly-D-lysine (0.1 mg/mL PDL; Merck, A-003-E) depending on the experimental requirement. The neurons were grown in a serum-free medium consisting of L-15 enhanced with 6 mg/mL glucose, 1× GlutaMAX (Gibco, 35050061), 1× B27 supplement (Invitrogen, A1895601), 50 ng/mL nerve growth factor (Gibco, 13290010), 0.006 g/ml methyl cellulose (34516, ColorconID), and 1× PenStrep (HiMedia, A001A). The cultures were maintained in an incubator without CO2 at 37 °C from DIV1 to DIV6. The medium was changed at DIV4.

2.3 Preparation on glass bottom coverslips

Neuronal cultures were cultured in 35mm plastic petri plates obtained from Laxbro Ltd. The petri plates were modified by creating a 12mm radius opening in the base, with the edges meticulously smoothened. This opening was subsequently covered using 18-22mm #1.5 glass coverslips, secured with Dow Corning 3145 RTV silicone adhesive. The containers were allowed to remain at ambient temperature overnight to ensure proper adhesive curing. The resulting glass-bottomed dishes underwent sterilization using ethanol and UV radiation for a duration of 15-20 minutes. For FRAP and STED experiments, the glass was treated with Poly-D-lysine (0.1 mg/mL PDL; Merck, A-003-E) to enhance neuronal attachment through non-specific electrostatic interactions. The dishes were then thoroughly washed with phosphate buffered saline (PBS, pH-7.4) to remove any extra PDL, as free PDL can be detrimental to cells. In the case of ablation experiments, neurons were seeded directly onto

the coverslip without any surface treatment.

2.4 Pharmacological treatment

Various pharmacological compounds known to disrupt actin and microtubules were administered to neuronal cultures. The specific agents and their corresponding treatment protocols are outlined in the accompanying table. Post-exposure, all cultures underwent fixation and subsequently were processed for immunofluorescence. Dimethyl sulfoxide (DMSO) was used as the solvent for the drugs, with DMSO-treated cultures functioning as vehicle controls for each experimental condition.

Drug	Source	Type of treatment	Time of addition	Concentration	Duration
Taxol	Santa Cruz (sc-201439)	Acute	DIV 1,2 & 4	10 µM	30 min
Nocodazole	Tocris Bioscience (2792)	Acute	DIV 1,2 & 4	20 µM	30 min
Latrunculin-A	Sigma Aldrich (L5163)	Acute	DIV 1,2 & 4	5 µM	15 min
Jasplakinolide	Tocris Bioscience (1228)	Acute	DIV 1,2 & 4	5 µM	30 min
Taxol	Santa Cruz (sc-201439)	Chronic	16 hrs post seeding	1 nM	Till DIV 2 or 4
Nocodazole	Tocris Bioscience (2792)	Chronic	16 hrs post seeding	10 nM	Till DIV 2 or 4
Jasplakinolide	Tocris Bioscience (1228)	Chronic	16 hrs post seeding	10 nM	Till DIV 2 or 4
Blebbistatin	Sigma Aldrich (B0560-1MG)	Chronic	16 hrs post seeding	10 µM	Till DIV 2 or 4
CK666	Merck (182515)	Acute	DIV 2,4 & 6	20 µM	30 min
SMIFH2	Merck (344092)	Acute	DIV 2,4 & 6	20 µM	30 min

2.5 Electroporation based transfection

The transfection procedure involved suspending cells in Optimem® (Gibco) medium with varying volume (contingent upon pellet size). Plasmid (15-20µg) was added and mixed via careful pipetting.

Subsequently, the cell suspension underwent electroporation utilizing a Super Electroporator NEPA21 Type II. The following parameters were used in all experiments:

Poring pulse:

- Voltage (V) – 125
- Pulse length (msec) – 5
- Pulse interval (msec) - 50
- Number of pulses - 2
- Decay rate (%) – 10
- Polarity - +

Transfer pulse:

- Voltage (V) - 20
- Pulse length (msec) – 50
- Pulse interval (msec) – 50
- Number of pulses - 5
- Decay rate (%) – 40
- Polarity - +/-

Post-electroporation, 400µl of culture medium was added to the cuvette. The resultant mixture was then transferred to glass-bottomed dishes and incubated at 37 °C. The incubation duration ranged from 24 to 144 h, contingent upon specific experimental requirements.

2.6 Fixation and Immuno-staining

Cultured neurons were fixed in 4% (w/v) paraformaldehyde (PFA) in phosphate-buffered saline (PBS) for 10 min at room temperature (RT). PFA was subsequently removed by washing with PBS, and the cells were permeabilized with 0.1% (v/v) Triton X-100 in PBS for 5 min at RT, followed by blocking with 3% (w/v) bovine serum albumin (BSA) in PBS for 1 hr at RT. The cells were then washed thrice with PBS and incubated with the primary antibody overnight at 4 °C. The primary antibody was removed the following day, followed by three PBS washes, and the cells were incubated with secondary antibody (1:1000 in blocking buffer) for 1 hr at RT. For super-resolution microscopy, neurons at different stages (days in vitro or DIV) were mounted in a mixture of 10% Mowiol 4–88 in poly (vinyl alcohol) (Sigma-Aldrich, 81381) and 2.5% (w/v) DABCO (1,4-diazabicyclo [2.2.2] octane; Sigma-Aldrich, D27802). The mounted samples were stored overnight in the dark at 4 °C before imaging. Primary antibodies: βII-spectrin 1:700 (BD bioscience; 612563), Anti-GFP 1:500 (Invitrogen; A11122) and βIII-tubulin 1:1000 (Santa-Cruz; sc-80005) were used. Alexa secondary antibodies against mouse and rabbit with fluorophore of variable wavelengths procured from Invitrogen.

2.7 FRAP and analysis

Electroporation was employed to transfect primary neurons and differentiated βII-Spectrin KO SH-SY5Y cells, which were subsequently utilized in experiments at various intervals ranging from 24 to 144 hours after transfection. The transfection process involved the use of several plasmids: pCAG-βII-Spectrin-GFP, pCAG-βII-Spectrin-K2207Q-GFP, pCAG-βII-Spectrin-Y187A-GFP, and pCAG-ΔABD-βII-Spectrin-GFP. Fluorescence recovery after photobleaching (FRAP) experiments were performed using a Zeiss LSM 710 confocal microscope. This instrument was equipped with a 488 nm Argon laser for bleaching and a temperature-controlled stage maintained at 37 °C with humidity control. GFP fluorescence was captured in time-lapse images at 2-second intervals. The imaging was conducted using a Zeiss Plan-Apochromatic 63x Oil DIC objective (N.A. = 1.4) with 3× optical zoom. Along the axon, rectangular region of interest (ROIs) measuring ~ 2 x 1 μm (height x width) were repeatedly photo-bleached for 50-100 iterations. This was achieved by scanning with a 488 nm laser at maximum power and a scanning speed of 6 μs/pixel.

The resulting images were then analysed using ImageJ software and GraphPad. In the analysis process, background fluorescence was subtracted from each ROI at every time point. To account for fluorescence loss during image acquisition, a reference region was used for normalization, adjusting it to the pre-bleaching intensity. The ROI intensities, after background correction and acquisition loss adjustment, were further normalized. This normalization set the pre-bleaching intensity to 100% and the immediate post-bleaching intensity to 0%. A single-phase association function was used to fit the recovery curve. The mobile fraction was calculated by taking the average of the intensities from the final five frames. F-test was performed for plateau values (Y_{max}) of the average curves to figure out if they are statistically different.

2.8 Stimulated emission depletion microscopy (STED) and analysis

2D-STED imaging of chick dorsal root ganglion (DRG) neurons and differentiated SH-SY5Y neurons was performed using a Leica TCS SP8 STED 3X microscope. An HC PL APO CS2 100x NA 1.4 STED WHITE oil immersion objective facilitated image capture in both confocal and STED modes. Acquisition parameters encompassed 16x line averaging and detector gating on a Hybrid Detector (HyD), with a gating range spanning 0.3 ns to 8 ns. The zoom factor was set ~ 6x, yielding a pixel less than 20 nm. STED 592 depletion laser was utilized for all image acquisitions, while other settings remained constant. Huygens Professional software was employed for image deconvolution before

analysis.

Medial axonal regions (unless mentioned otherwise) were segmented into approximately 3 µm segments, from which intensity versus distance profiles were derived. Autocorrelation functions were computed based on these profiles for each segment using MATLAB. The average autocorrelation function was calculated by combining autocorrelation curves from all selected axon segments for each experimental condition. Autocorrelation amplitude was defined as the difference between the first peak and the average of two adjacent valleys of the autocorrelation curve. The average periodicity of the membrane periodic skeleton (MPS) structure for each ~3 µm segment was determined by the first peak's position in the autocorrelation function. Diameter of each ~3 µm segment was assessed by measuring the distance between spectrin signals coming from edges.

2.9 SH-SY5Y differentiation

The SH-SY5Y cell line, which is of human origin, has been extensively used in scientific research. This cell line was established as a sub clone from the SK-N-SH cell line, which was originally obtained from a bone marrow biopsy of a four-year-old female patient diagnosed with neuroblastoma. To induce differentiation, researchers frequently employ a combination of retinoic acid (RA) and brain-derived neurotrophic factor (BDNF) (Encinas *et al.*, 2000; Murillo *et al.*, 2017; Şahin *et al.*, 2021). In this work, we have used differentiated SH-SY5Y cells which form axons and are known to express a lot of neuronal markers (Encinas *et al.*, 2000; Murillo *et al.*, 2017). For this thesis, we have changed the protocol as described in figure 2.0.

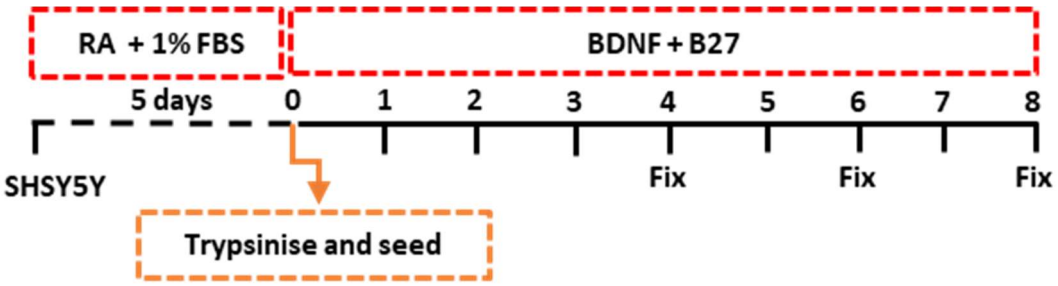

Figure 2.1: Schematic describing process of differentiation of SH-SY5Y cells

SH-SY5Y cells were cultured in 60 mm Petri dishes containing standard growth medium (DMEM/F12 enriched with 10% FBS and 1% penicillin-streptomycin) at 37 °C in a 5% CO2 incubator. When cell density reached 80–90% confluence, sub culturing was performed using trypsin-EDTA. Experiments were conducted exclusively with cells that had undergone fewer than 20 passages. The differentiation

process of SH-SY5Y cells into neuron-like cells, spanning 12-14 days, was modified the procedure from the a previously described protocol to accommodate FRAP and STED experiments that required us to transfect plasmid constructs in the middle of the protocol. Cells seeded on a 60mm plate were subjected to 5 days of 10 μM RA (Retinoic acid) treatment in DMEM/F12 enriched with 1% FBS and 1% penicillin-streptomycin. Cells were trypsinised (with or without transfection) and seeded on glass with 50 ng/ml Brain Derived Neurotrophic Factor (BDNF) in DMEM/F12 supplemented with 1% B-27 (Invitrogen) and 1% penicillin-streptomycin. These differentiated cells were further processed for super-resolution microscopy or FRAP experiments. Chapter 7 discusses about the procedure and validation of βII-Spectrin KO SH-SY5Y by CRISPR Cas-9 genome editing technique

2.10 Axonal ablation

DRG neurons were grown on a glass-bottom dish without any coating to obtain detached axons. Axons of DIV1, DIV2, and DIV4 neurons were subjected to laser ablation using a home-built laser ablation setup (by Ashish Mishra, RRI Bangalore). This setup consists of a 355 nm, 25 mJ, 350 ps pulsed laser (PowerChip PNV-M02510-100; Teem Photonics, Meylan, France) coupled to the side port of a Leica TCS SP8 confocal microscope using a custom filter-cube and focussed on the sample using 40x/0.75 dry Phase Contrast objective. A custom-made 90° rotated filter cube having a UV-reflecting dichroic filter (T387lp-UF3, Chroma) was used to reflect the laser light into the objective. During and after ablation, phase contrast images were recorded using a CCD camera (Phantom VRI-MICRO-C210-16GB-M, Vision Research) at 2000 fps for 0.8-1 second to capture the initial fast retraction process of the ablated axons. A custom MATLAB code was employed to quantify the evolving gap distance. The x- and y-coordinates obtained were converted to distance values and plotted using GraphPad software. Estimation statistics (Ho *et al.*, 2019; *Estimation Stats*), Cohen's d and two-sided permutation test between the final gap length post-ablation was determined. The F-test was used to compare the plateaus of the evolving curve after fitting the data to a single-phase association model.

2.11 βII-Spectrin intensity analysis across axonal segment

Axons from DIV 1, 2, and 4 were stained for βII-Spectrin and imaged using confocal microscopy with 20x, 0.4NA objective. Using Image-J, the entire axon was traced with a line similar to axonal thickness (from cell-body towards growth-cone). Intensity profile and axonal length was noted. Since the axonal length increases over DIVs, we normalised the lengths (0-100) and plotted intensity profiles of individual axons across DIVs. Apart from quantifying total axonal length we also calculated average

intensity of axonal regions after dividing the axon in 3 portions: proximal- near cell body (0-25%), middle (25-75%), and distal-near growth cone or some connection (75-100%). Majority of STED analysis is done on the middle segment of the axon and it's important to analyse and compare intensity per unit area of these middle regions across DIVs. To this end, we selected smaller section from middle region of all DIVs and processed it with ImageJ software for Otsu-based thresholding or manually. A particle analyser tool was used to estimate the integrated density and area of the axon, followed by CTCF calculation.

2.12 Statistical analysis

All statistical analyses and visual representations were conducted using GraphPad Prism 10 (10.4.0). In the figures, data are presented with a central line indicating the mean, along with error bars displaying the standard error of mean (SEM). The number of data points analyzed for each graph is indicated in the figure legends. Statistical test along with correction tests used for the analysis are mentioned in the figure legend.

Chapter 3

Brief rationale:

A PRELUDE TO THE RESULTS

3.1 Brief rationale: A prelude to the results

Ample literature sheds light on the fact that MPS is crucial not only for proper functioning of the neuron but also has consequences at the circuit level, which can lead to neurodevelopmental disorders or failure at circuit formation, as discussed in Chapter 1.

In 2020, our work (Dubey *et al.*, 2020) uncovered links between the mechanical responses of axons and their cytoskeletons. We demonstrated that in addition to microtubules, F-actin and spectrin play a significant role in axon mechanics. Our findings revealed that DIV4 axons displayed more prevalent MPS than DIV1 axons, which corresponded with an increase in axon elasticity. Interestingly, we also saw that disruption of F-actin not only led to loss of MPS but also had significant loss in elastic modulus while stabilization had the opposite effect. Our theoretical model suggests that the actin-spectrin network functions as a tension regulator in axons by allowing reversible unfolding of spectrin tetramer repeat domains, thereby alleviating excessive mechanical stress.

These findings, coupled with the fact that the majority of work in the field was conducted in neurons with already assembled MPS, presented an opportunity to characterize how the MPS forms during early neuronal development. The thesis is divided into the following broad objectives with rationale mentioned below each objective:

- **To systematically examine the time-line and directionality of MPS assembly during early development in Chick embryonic DRG neurons.**

  A comprehensive characterization of MPS formation during early development was lacking in the field, and it was essential to conduct a detailed analysis of MPS formation, including both the timeline and directionality in cultured embryonic chick DRG neurons, as this had not been previously investigated in this neuronal type.

- **To investigate the influence of actin, microtubule and myosin on the formation and maintenance of MPS during early development. To elucidate the role of actin regulators in MPS maintenance.**

  The dependency of MPS stability on F-actin and microtubules has been previously studied in various systems (as discussed in chapter 1); however, a detailed characterization during early development was missing. We aimed to determine if microtubule stability and dynamics facilitate MPS assembly during early time points. Additionally, only two reports (Qu *et al.*, 2017; Micinski and Hotulainen,

2024) have addressed the role of actin regulators in the process of MPS stability. We sought to elucidate the roles of the Arp2/3 complex and Formins in regulating and maintaining F-actin and, consequently, the MPS during early neuronal development.

Reports also highlight role of Myosin in maintaining axonal diameter but nobody has shown its relevance in MPS development. We have aimed to address the same in a developing DRG axons.

- **To examine the dynamics of βII-spectrin across development and potential domain-specific interactions that might influence protein mobility and recruitment in order to form the MPS**

In hippocampal neurons, βII-spectrin at DIV10 is extremely stable (immobile) (Zhong *et al.*, 2014), which was hypothesized to be due to its incorporation in the MPS. We aimed to determine if we would observe a decrease in mobility as the scaffold forms over DIVs and if this mobility is also dependent on F-actin interaction. Concurrently, we aimed to characterize the role of various βII-spectrin domains, such as actin-binding, plasma-membrane binding, and ankyrin binding, in facilitating mobility and recruitment.

- **To characterise role βII-spectrin in regulation of axonal tension**

Multiple studies across cell types have indicated that βII-spectrin is under tension (discussed in chapter 1), but we sought to determine if this phenomenon extends to axonal tension. Given our model demonstrating the formation of MPS over time, we utilized this system to investigate whether this architecture, particularly βII-spectrin, contributes to the maintenance of axonal tension

Chapter 4

Characterization of Membrane Periodic Skeleton (MPS) in chick embryonic DRG neurons

Research has shown that the Membrane Periodic Skeleton (MPS) is present in diverse neuronal types and across multiple organisms, including *Caenorhabditis elegans, Drosophila*, *Gallus gallus*, *Mus musculus*, and *Homo sapiens* (D'Este *et al.*, 2016; He *et al.*, 2016; Han *et al.*, 2017). The majority of these studies have utilized variable developmental time points to elucidate the role of MPS in the neuronal system; however, minimal research has been conducted on MPS formation during early DIVs when the axon is getting specified. Given the ubiquitous presence of MPS across diverse species and its critical function in neuronal development, our investigation focused on delineating the initial developmental progression of chick embryonic DRG neurons. It is to be noted that across this work we have imaged and analysed βII-spectrin as the key marker for MPS. We did not image F-actin as during early time period F-actin is difficult to detect is more labile and doesn't survive fixation step (Zhong *et al.*, 2014), whereas the spectrin tetramer forms a periodic structure only when it interacts with F-actin (discussed in chapter 1). βII-spectrin antibody is extremely specific and is much cleaner way of accessing MPS than F-actin staining as during early development there are multiple F-actin structure which are abundant and interfere with the analysis.

4.1 MPS starts to form at DIV1

In 2019, as part of a study, we imaged and analysed MPS from DIV1-DIV5 to quantify MPS qualitatively (Dubey *et al.*, 2020); however, as a part of this thesis we aimed to comprehensively establish a developmental timeline of MPS formation.To investigate the development of the membrane periodic skeleton in chick dorsal root ganglion (DRG) neurons, we fixed neurons at various time points, performed immunostaining against βII-spectrin, and imaged them in the middle region of the axon using super-resolution microscopy. We quantified the early stages by imaging axons in vitro on days 1, 2, 4, and 6, followed by periodicity, autocorrelation, and axon diameter analysis. Autocorrelation measures the relationship between a variable and itself across consecutive time periods. Values range from -1 to 1, with -1 indicating perfect negative correlation and 1 signifying perfect positive correlation. A positive peak above the horizontal axis suggests a recurring pattern at that specific lag. In this analysis, the punctate nature of βII-spectrin intensity is examined in relation to itself along the axonal length. Periodic repetition of βII-spectrin intensity over distance will result in high autocorrelation, which will fluctuate and gradually decrease as the distance increases. This was employed to extract values of periodicity (spacing between the beta spectrin rings) and autocorrelation amplitude of the first peak, which provides information about the periodicity that repeats with maximum strength, as indicated by its maximum amplitude. The measures of amplitude and periodicity tell us about ring development and organization.

The micrographs in Fig. 4.1 A illustrate the emergence and evolution of periodic membrane structures throughout development. Punctate spectrin localization was observed from DIV1; however, it did not exhibit periodicity. The localization became more structured with developmental progression (DIV2-DIV6). Quantification of the average autocorrelation curves across multiple axonal segments revealed that DIV1 exhibited periodic structures, albeit with a low autocorrelation amplitude. Over time, the average autocorrelation increased, indicating the formation of MPS. Furthermore, in addition to the first peak, the subsequent undulating peaks also demonstrated increased amplitude, suggesting the presence of MPS with higher probability, even at larger distances, thus highlighting higher abundance (Fig. 4B). DIV1 exhibited punctate spectrin localization, indicating initial recruitment to the cortex but not in the MPS scaffold. First peak autocorrelation amplitude showed increased a significant increase across DIVs (Fig. 4 C), which is expected considering the average autocorrelation curves also increase as time progresses (Fig.4 D).

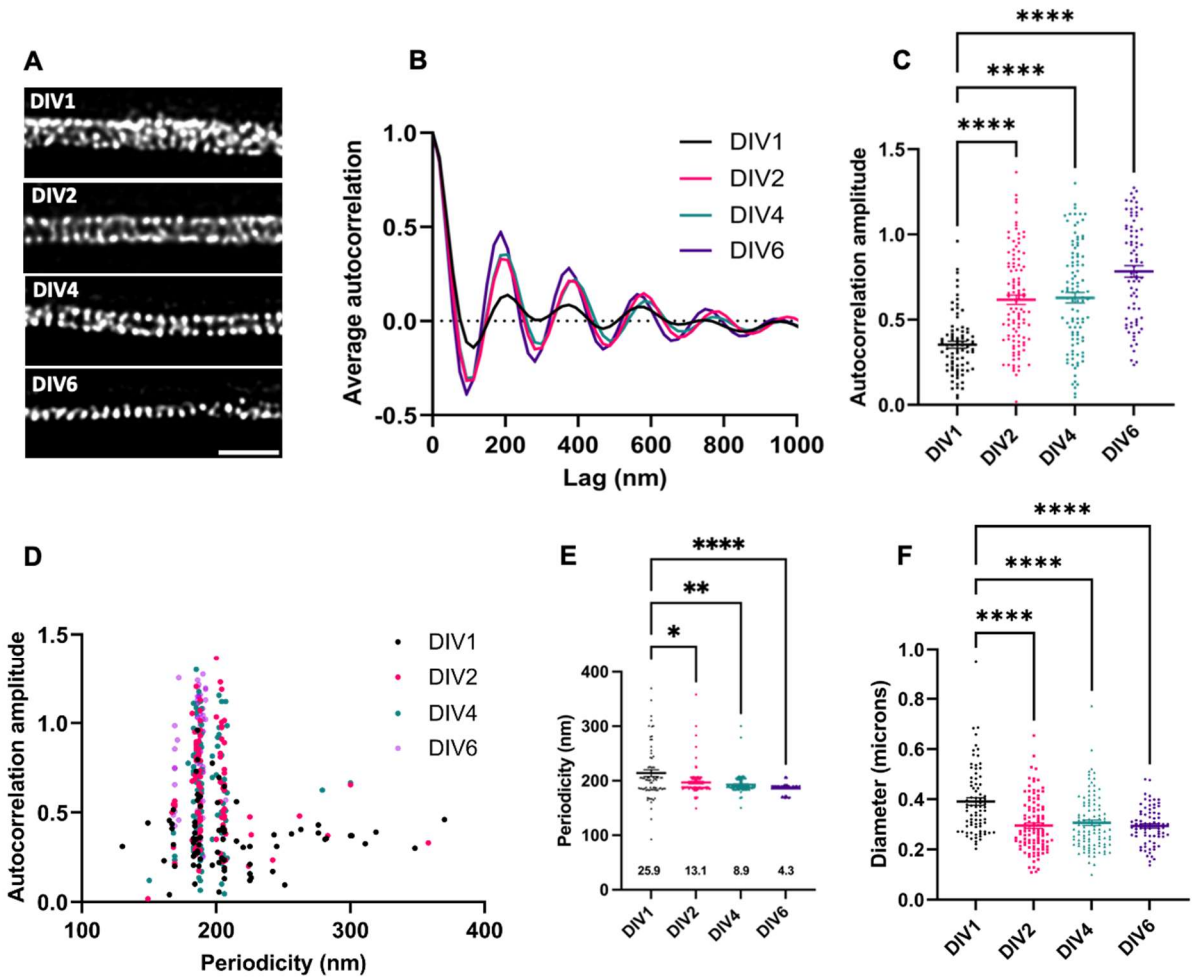

Figure 4.1 Formation of Membrane Periodic Skeleton (MPS) in chick DRG neurons (A) Representative 2D-STED micrographs of DIV1, DIV2, DIV4, and DIV6 chick DRG axons stained with βII-spectrin antibody.

Scale bar: 1 µm. (B) Average autocorrelation curves for multiple axonal regions across the DIVs. (C) The autocorrelation amplitudes of the βII-spectrin distribution were quantified as the difference between the first peak and average of the first two valleys of the autocorrelation curve. The data were analysed using the Brown-Forsythe and Welch ANOVA test with multiple comparisons corrected by Games -Howell's test. (D) Autocorrelation amplitude versus periodicity graph for all DIVs, indicating the degree and distribution of periodicity in MPS. (E) Periodicity across DIVs demonstrates a reduction in the coefficient of variation from 25.96% in DIV1 to 4.3% in DIV6. The data were analysed using the Brown-Forsythe and Welch ANOVA test with multiple comparisons corrected by Games -Howell's test. (F) Diameter analysis across DIVs was performed using βII-spectrin staining. The data were analysed using the Kruskal-Wallis test with multiple comparison corrected by Dunn's test. 80-100 axonal segments from 3 biological replicates for each DIV were analysed (ns, $p > 0.05$; *, $p \leq 0.05$; **, $p \leq 0.01$; ****, $p \leq 0.0001$).

Upon quantifying periodicities derived from the first peak of autocorrelation amplitude, a dispersed distribution was observed with decreasing variance across DIVs. DIV1 exhibited the largest distribution, which progressively decreased as the DIVs advanced (DIV2-DIV6). Variance was quantified, and the coefficient of variance decreased from 25.9% at DIV1 to 4.3% at DIV6, indicating that the MPS scaffold had become uniformly periodic over the course of development (Fig 4.1 D, E). These early time-point dispersion in periodicities were associated with lower autocorrelation amplitudes, which increased with development (Fig.4.1 D). This observation underscores that during the early developmental stages, the MPS undergoes organization, potentially exhibiting periodicities of approximately 180-200 nm while maintaining low autocorrelation amplitudes. Conversely, instances may occur where the periodicity deviates from the 180-200 nm range but demonstrates higher autocorrelation amplitudes. Over time, this process becomes more refined, with the majority of the periodicities converging around 200 nm and exhibiting an increase in amplitude. It is plausible that rudimentary scaffold proteins are recruited at DIV1, which may or may not exhibit periodicity initially, but subsequently arrange in a periodic fashion over time. Given that MPS is known to regulate axonal caliber (Costa *et al.*, 2020), we also sought to examine changes in axonal diameter as MPS forms and becomes more periodic. As anticipated, MPS formation correlated with a reduction in axonal caliber (Fig. 4.1 F).

4.2 MPS forms simultaneously across the axonal shaft

To determine whether MPS assembly occurs in a directional manner, we conducted imaging studies on chicken DRG neurons. We examined βII-spectrin stained DRG axons at their proximal, middle, and distal regions. It is to be noted that crowding and the ability of axons to align and merge into one

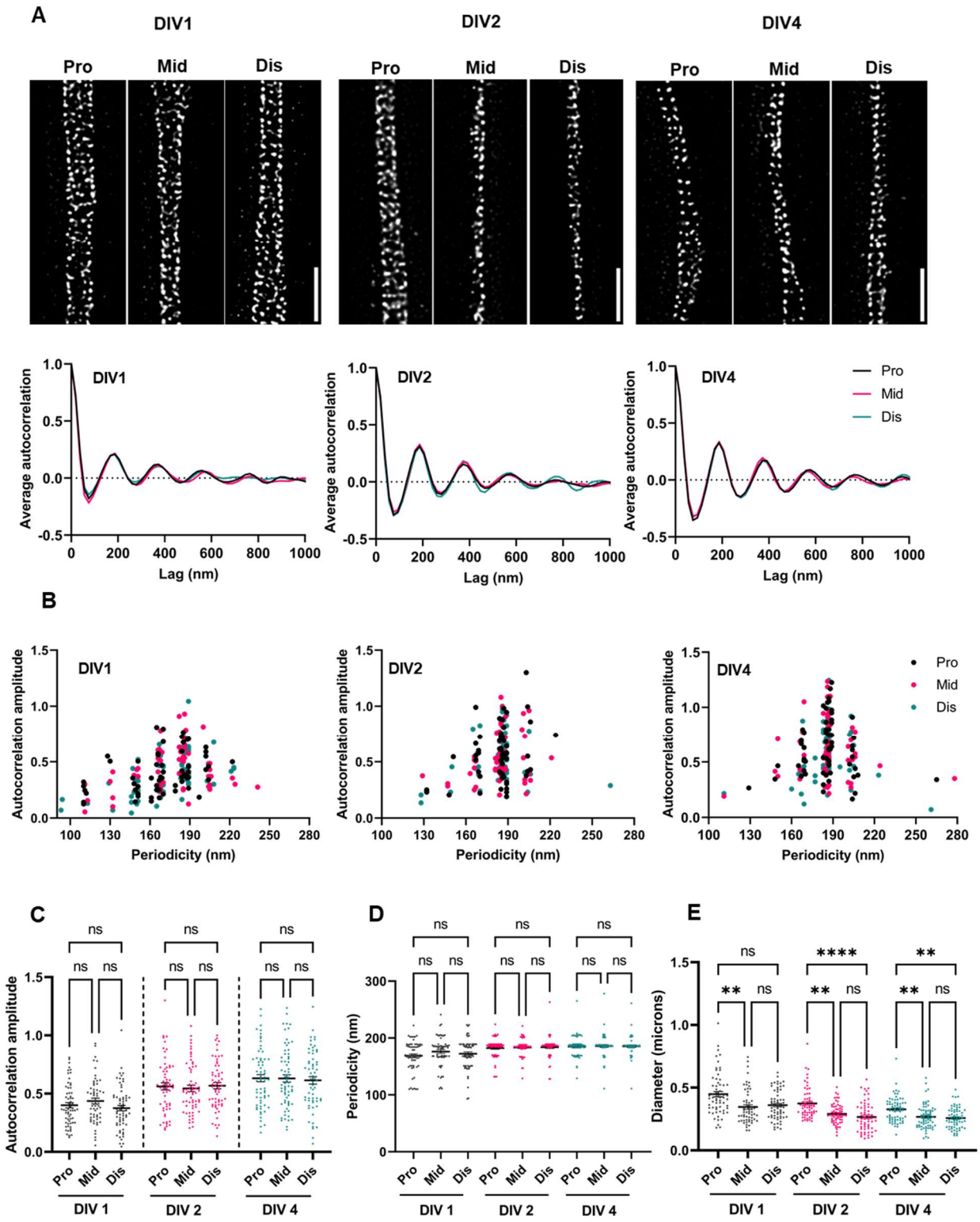

Figure 4.2 MPS forms uniformly along the axonal length in chick DRG neurons (A) Representative micrographs along with average autocorrelation curves for proximal (Pro), middle (Mid), and distal (Dis) axonal regions of βII-spectrin -stained DIV1, DIV2, and DIV4 neurons, demonstrating a similar degree of MPS formation. Scale bar: 1 µm (B) Autocorrelation amplitude versus periodicity graph for all DIVs, indicating an equivalent degree of periodicity of MPS across different regions of axons for individual DIVs. (C, D)

Quantification of autocorrelation amplitude and periodicity show no significant difference across segment. The data were analysed using the Brown-Forsythe and Welch ANOVA test with multiple comparisons corrected by Games -Howell's test. (E) Diameter across segment. Proximal region across DIV show higher diameter. The data were analysed using the Kruskal-Wallis test with multiple comparison corrected by Dunn's test. 60-90 axonal segments from 3 biological replicates for each segment and DIV were analysed (ns, $p > 0.05$; **, $p \leq 0.01$; ****, $p \leq 0.0001$).

another makes it difficult to understand the dorsal segment. We have tried to our best abilities to demarcate this region for this work. Representative micrographs are shown in Figure 4.2 A. Autocorrelation analysis was conducted on every imaged axonal segment. The averaged autocorrelation curves for all regions across DIVs were analysed, revealing no significant differences or biases (Fig. 4.2 A). Comparisons of the initial peak autocorrelation amplitude with corresponding periodicities showed no variations within each DIV (Fig. 4.2 A).

These findings demonstrated that MPS forms concurrently across the axonal shaft without directional bias. Subsequently, diameter analysis revealed a trend of the proximal region exhibiting larger diameter across DIVs, which is noteworthy given the absence of difference in MPS, which maintains axonal diameter. It is significant to observe that the overall diameter decreases across all segments as time progresses, indicating the potential influence of other components that contribute to this morphology in the proximal region.

4.3 βII-spectrin is equally distributed along the axon

Studies have shown that neurons when over-expressed with spectrin show increased or better MPS formation (Zhong *et al.*, 2014). Considering this information, along with our finding demonstrating no directionality bias towards MPS formation, we subsequently investigated the expression level of βII-spectrin to determine if it correlates with the MPS formation timeline and if it exhibits any bias towards a specific axonal region. To this end, we conducted an examination of βII-spectrin stained neurons across DIVs utilizing confocal imaging with a 20x objective to facilitate imaging of the entire axon. Although axonal length increases over time, the expression levels remain relatively constant across the axon and DIVs (Fig. 4.3 A, B). To quantify potential differences in spectrin intensity among various axonal regions, we normalized the axonal length and converted it into percentages. Subsequently, we divided the axon into three segments: proximal (0-25%), middle (25-75%), and distal (75-100%), and calculated the average intensity along these axonal segments. However, no significant difference was

observed even though there seems to be a trend average gray values between proximal and distal (Fig 4.3 C). Since majority of the STED analysis is restricted to imaging middle region of the axon, spectrin intensity per unit area was measured after selecting a region of the middle segment followed by measurement of Corrected Total Cell fluorescence (CTCF) (Fig.4.3D). There was no significant difference in spectrin intensity across middle segment of the axon over DIVs. Collectively, these findings suggest that spectrin is expressed at similar levels along the axon and across DIVs.

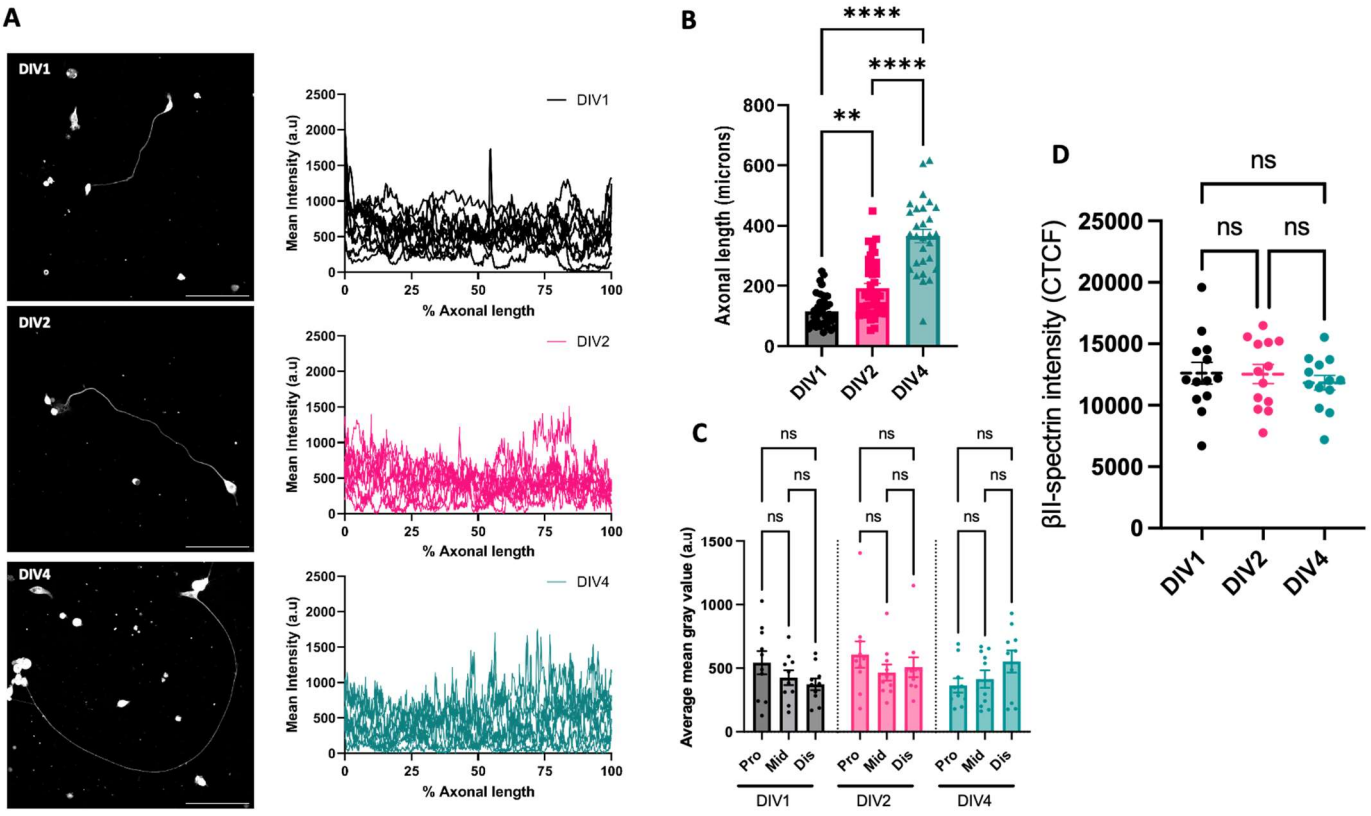

Figure 4.3 βII-spectrin intensity analysis across the axon (A) Representative micrographs of βII-spectrin -stained DIV1, DIV2, and DIV4 axons, accompanied by length-normalized intensity profiles across axonal length (proximal to distal) across DIVs. Intensity was analyzed using the line-trace tool of ImageJ. (B) Axonal length analysis across DIVs. > 35 neurons from 3 biological replicates for each segment and DIV were analysed. The data were analysed using the Kruskal-Wallis test with multiple comparison corrected by Dunn's test (**, $p \leq 0.01$; ****, $p \leq 0.0001$). (C) Average intensity across the percentage of axonal length: Proximal (0-25%), middle (25-75%), and distal (75-100%). > 35 neurons from 3 biological replicates for each segment and DIV were analysed. The data were analysed using the Kruskal-Wallis test with multiple comparison corrected by Dunn's test (ns, $p > 0.05$). (D) βII-spectrin intensity in the middle region of the axon is shown as corrected total cell fluorescence (CTCF). The data were analysed using Brown-Forsythe and Welch ANOVA test with multiple comparisons corrected by Dunnett's test (ns, $p > 0.05$). The data are derived from n=13 axons for all DIVs

Discussion

While the presence of MPS has been observed in multiple species and neuronal regions, this study demonstrates for the first time that MPS forms in peripheral nervous system neurons of *Gallus gallus*. Moreover, the results indicate that this formation initiates at DIV1, where the spectrin protein exhibits punctate and periodic characteristics at random regions along the axon, albeit with reduced autocorrelation amplitude. As developmental time progresses, MPS becomes more periodic (approximately 180-200 nm) and exhibits higher autocorrelation amplitude. These findings establish that MPS forms over time.

Multiple studies utilizing hippocampal neurons have demonstrated that MPS forms with a proximo-distal directionality or bias, which they attribute to the presence of the Axonal Initial Segment (AIS) (Zhong *et al.*, 2014; Han *et al.*, 2017; Lorenzo *et al.*, 2019; Hofmann *et al.*, 2022). MPS analysis of different axonal regions in chick DRG neurons indicates that MPS formation occurs across the entire axon, differing from the previous model.

A potential explanation for this discrepancy could be that the DRGs may lack a traditional or bona fide Axonal Initial Segment (AIS) (Nascimento *et al.*, 2018). In axons with AIS, such as hippocampal neurons, βII-spectrin expression exhibits a distinct profile characterized by elevated levels in the cell body, reduced levels in the proximal region, and increased levels in the middle-distal axonal compartment in stage five neurons (>DIV7) (Galiano *et al.*, 2012). This distribution pattern occurs because in the AIS (proximal region), βIV-spectrin forms a tetramer with αII-spectrin, and localization of βII-spectrin is strictly post-AIS region (Huang *et al.*, 2017c). In hippocampal neurons, as the AIS forms, βII-spectrin is displaced from the MPS in the proximal region and is observed to be periodically localized in the distal region of the axon (Zhong *et al.*, 2014). Since we did not observe any directionality in MPS formation, we quantified βII-spectrin expression across the axon from DIV1–DIV4; however, it did not demonstrate any such distribution pattern as observed in neurons harboring the capacity to form a distant AIS. This phenomenon could be attributed to the fact that AIS components are recruited later than the time frame utilized in this study.

Interestingly, researchers found minimal to no MPS in the proximal region of the axon of mouse DRG neurons, but high periodicity in the distal end (Wang *et al.*, 2019). This contrasts with hippocampal neurons, where the MPS has a proximo-distal bias. It is possible to examine the appropriate regions with more accuracy by using a microfluidic chamber to segregate axonal regions and quantify axonal

region with more confidence.

In conclusion, our findings suggest a fundamental difference in MPS assembly mechanisms between DRG and other neurons. The fact that the intensity of βII-spectrin was similar across the axon highlights that rather than just the quantity of the protein it is the re-organization that might be crucial during MPS formation. It needs to be noted that this intensity estimation is at longer lengths and at a gross level. This can be refined with imaging with higher magnification to observe finer or missing structures. Taken together, this would mean that the one of most important aspect for MPS to form would be recruitment of βII-spectrin to the cortex. This could be because of unknown protein interaction or due to its interaction with components like plasma-membrane, Ankyrin and F-actin via its domains. This will be discussed in detail in the later chapters.

Chapter 5

Role of actin and microtubule dynamics in MPS formation and stability

Relevance of actin and microtubules in maintenance of MPS

Previous research has conclusively demonstrated that disrupting microtubule and actin cytoskeleton components using nocodazole (Noco) and latrunculin-A (Lat-A), respectively, negatively impacts MPS maintenance (Zhong *et al.*, 2014; Han *et al.*, 2017; Qu *et al.*, 2017; Wang *et al.*, 2019). In parallel, studies have shown that reinforcing the actin cytoskeleton with jasplakinolide (Jasp) helps preserve MPS structure when NGF is withdrawn for trophic deprivation (Wang *et al.*, 2019). In 2020, we successfully replicated Lat-A-induced disruption of MPS at DIV2 (Dubey *et al.*, 2020). However, our objective was to systematically investigate the role of actin and microtubules throughout early development.

5.1 Microtubule and actin disruption affect MPS stability across DIVs

To achieve this objective, chick DRG neurons cultured for 1, 2, and 4 days were subjected to brief pharmacological treatments in different experiments. These treatments, including Lat-A, Nocodazole, Taxol, and Jasplakinolide, were designed to disrupt either microtubule or actin dynamics (see methods in chapter 2 and figure legends for details). After treatment, the neurons were fixed and immunostained with a βII-spectrin antibody. The prepared samples were then examined using STED-based super-resolution microscopy. It should be noted that all drug treatments were acute in nature, i.e., administered at high concentration and for a short duration.

Across DIVs, destabilizing agents - Latrunculin A and Nocodazole, disrupted MPS structure, as evidenced by a decrease in autocorrelation curves (dotted coloured lines) and first peak autocorrelation amplitude when compared to DMSO controls of respective DIVs (Fig.5.1 A, B, D, E, G, F). Periodicity analysis demonstrated increased mean and overall dispersion. Furthermore, the coefficient of variance exhibited an increase in both treatments across all DIVs when compared to the DMSO control (Fig. 5.1 C, F, I).

Across DIVs, stabilizing agents – Taxol and Jasplakinolide, did not affect MPS structure and did not enhance it at DIV 1, as evidenced by no change in autocorrelation curves (solid coloured lines) and first peak autocorrelation amplitude when compared to DMSO controls of respective DIVs (Fig.5.1 A, B, D, E, G, F).

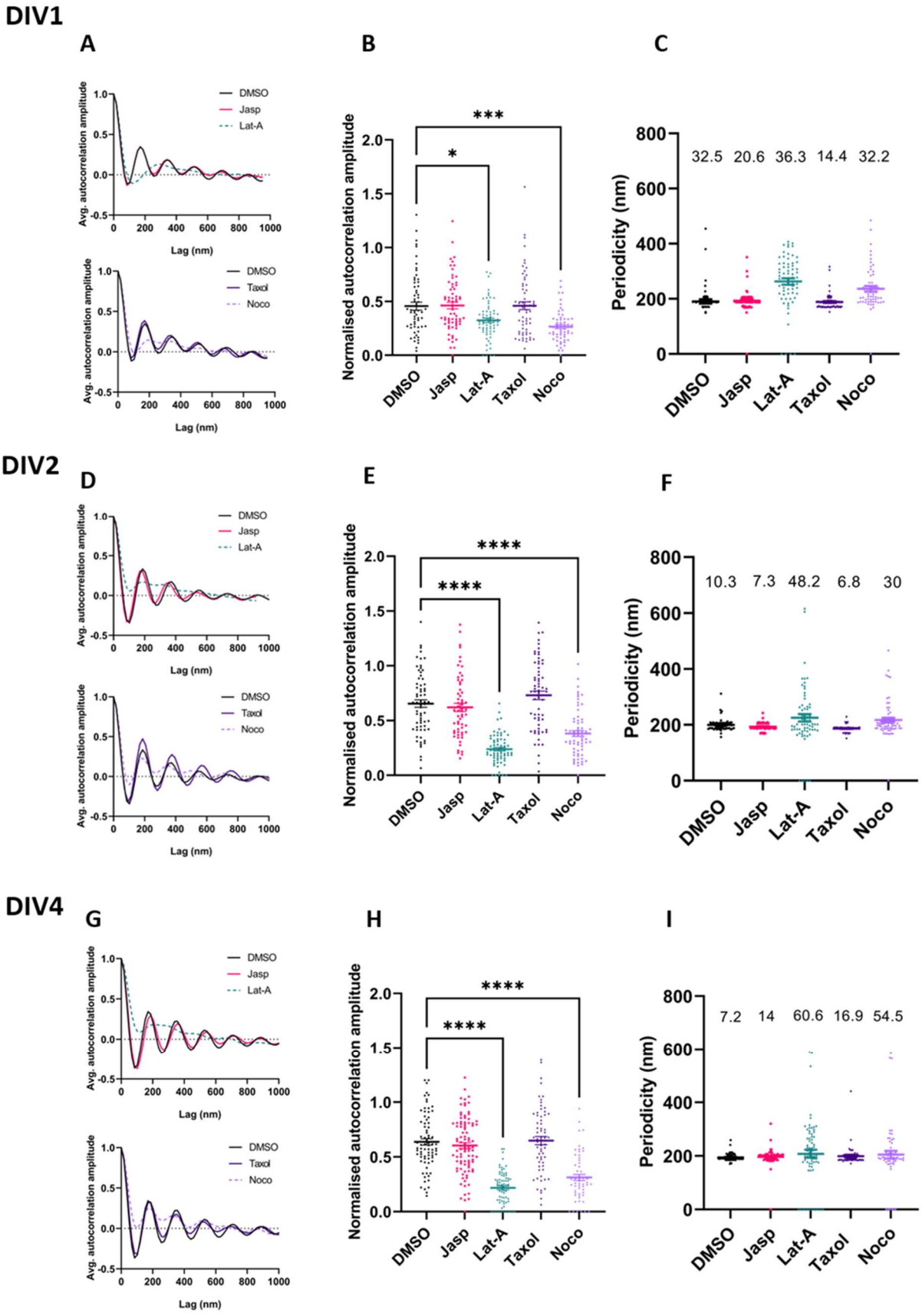

Figure 5.1. Destabilization of microtubules and actin affects MPS stability across development (A, D,G) Average autocorrelation curves of axonal segments across DIVs treated with DMSO (control), Jasplakinolide

(Jasp), latrunculin-A (Lat-A), Paclitaxel (Taxol) , and Nocodazole (Noco). (B, E,H) The autocorrelation amplitudes of the βII-spectrin rings across treatments and DIVs. The data were analysed using the Brown-Forsythe and Welch ANOVA test with multiple comparisons corrected by Games -Howell's test (ns, $p > 0.05$; *, $p \leq 0.05$; ***, $p \leq 0.001$; ****, $p \leq 0.0001$). (C,F,I) Periodicity (spacing) across DIVs treated with indicated drugs. The numbers below each data set indicate the coefficient of variation of the distribution. The numbers above each data set indicate the coefficient of variation of the distribution. For A-I, 60-90 axonal segments from 3 biological replicates for each DIV were analysed.

There appears to be a positive effect of both treatments, as indicated by an increase in autocorrelation amplitude; however, this effect is not statistically significant. Additionally, analysis of periodicity revealed a reduction in variance when actin and microtubules were stabilized at DIV1 as shown by drop in coefficient of variance, indicating a positive impact on MPS formation. However, this effect was less pronounced later on, possibly due to the scaffold having already been established (Fig.5.1 C, F, I). It is worth noting that Taxol treated DIV2 and DIV4 axons show increase in autocorrelation amplitude but it is statistically non-significant (Fig. 5.1 E,H). We hypothesise this could be because the MPS components are already at the cortex and MT stabilization aids this process of organisation. Comparison of individual autocorrelation amplitude and periodicities across all segments and treatments is shown in Figure 5.2 A.

Given that these treatments impact MPS, βII-spectrin spectrin diameter was measured as a proxy for axonal diameter across different DIVs. The disruption of MPS resulted in an enlarged axonal diameter throughout all DIVs when compared to the DMSO control (Fig.5.2 B). This observation aligns with previous findings that a reduction in MPS leads to increased axonal diameter (Zhou *et al.*, 2022). Stabilization did not alter axonal diameter across DIVs as seen in Fig. 5.2 B.

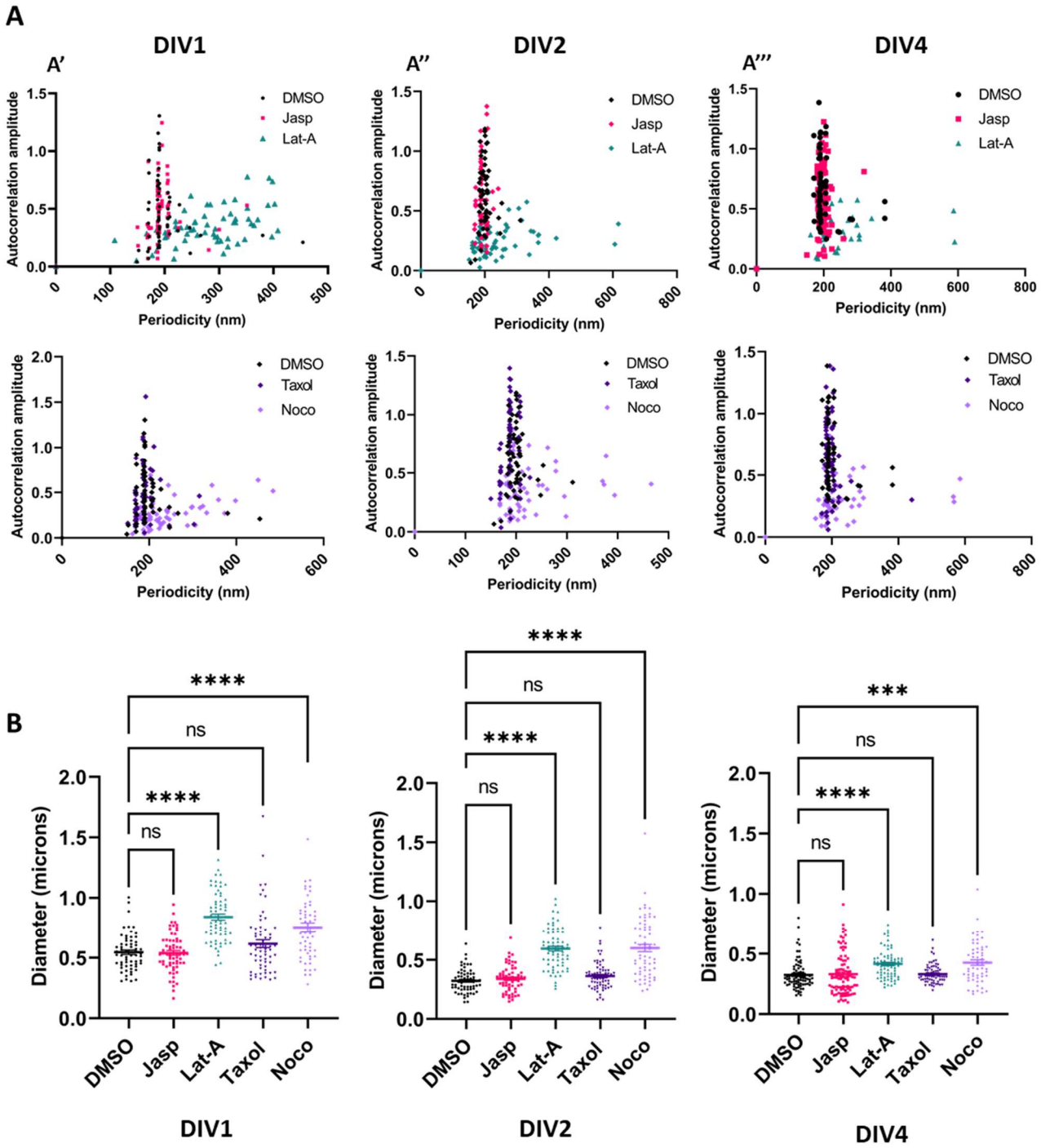

Figure 5.2. Destabilization of microtubules and actin affects axonal diameter and MPS autocorrelation (A) Quantification of autocorrelation amplitude versus periodicity for DIV1, DIV2, and DIV4 neurons treated with DMSO, Jasplakinolide (Jasp), latrunculin-A (Lat-A), Taxol, and Nocodazole (Noco). (B) Analysis of the diameter across DIVs and treatments. The data were analysed using the Kruskal-Wallis test with multiple comparison corrected by Dunn's test. 60-90 axonal segments from 3 biological replicates for each segment and DIV were analysed (ns, $p > 0.05$; *, $p \leq 0.05$ **, $p \leq 0.01$; ****, $p \leq 0.0001$).

5.2 Microtubule dynamics is essential for MPS formation

In the earlier section we show that microtubule disruption led to destabilisation of the early βII-spectrin MPS. This led us to investigate the role of microtubule dynamics in the process of MPS formation. We employed low concentrations of drugs to induce long-term alterations in microtubule dynamics. Chick DRG neurons were cultured, and following a 16-hour incubation period, we administered 1 nM Taxol and 10 nM Nocodazole to the culture medium. The treated cells were fixed at DIV2 (32 hr. post-treatment) and DIV4 (80 hr post-treatment), then subsequently immunostained with βII spectrin antibody (Fig 5.4A). Proximal, middle and distal regions of treated axons were imaged for both the DIVs.

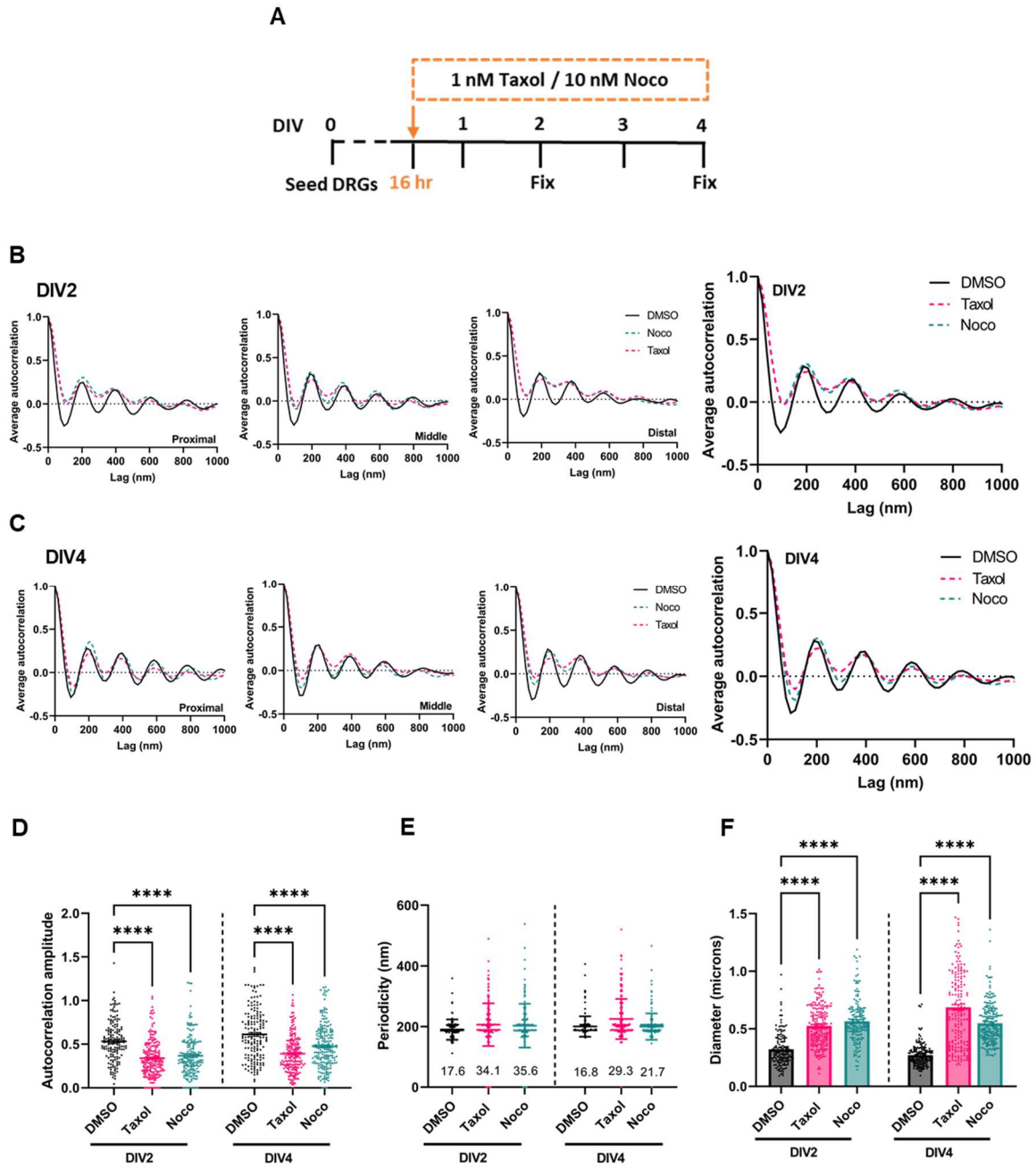

Figure 5.3. Perturbation of microtubule dynamics negatively affects MPS formation across the axon (A) Timeline of the experiment. 1 nM Taxol or 10 nM Nocodazole was added 16 hr after seeding the neurons and

fixed either after another 32 hrs (DIV2) or after 80 hrs (DIV4). (B, C) Individual and aggregated mean autocorrelation curves for the proximal (Pro), middle (Mid), and distal (Dis) regions of βII-spectrin -stained axons from cultures treated with 10 nM Nocodazole (green dotted line) and 1 nM Taxol (pink dotted line) for 32 (DIV2) and 80 h (DIV4), where the drug was introduced at 16 h post-seeding. Data for all regions were aggregated for the analysis. (D) Quantification of the aggregated autocorrelation amplitudes across DIVs and treatments. The data were analysed using the Brown-Forsythe and Welch ANOVA test with multiple comparisons corrected by Games -Howell's test E) Quantification of periodicity represented by the coefficient of variation across treatments and DIVs. (F) Quantification of the diameter. The data were analysed using the Kruskal-Wallis test with multiple comparison corrected by Dunn's test. 150-200 axonal segments from 3 biological replicates for each DIV were analysed. ****, $p \leq 0.0001$

Average autocorrelation curves show DIV2 neurons to be highly susceptible to these drugs across the entire axon (Fig. 5.3 B) but DIV4 axons show higher susceptibility in the distal region compared to other regions (Fig. 5.3 C). To understand over-all effect, all the data across segments were consolidated before analysis. The autocorrelation amplitude and periodicity were analyzed. Axons exposed to treatment showed a notable decrease in autocorrelation amplitude and greater variability in periodicities when compared to DMSO (Fig. 5.3 D, E). Additionally, the treated axons exhibited a larger diameter, supporting the findings presented in (Fig.5.3 F). This indicates involvement of microtubule dynamics in MPS formation.

Since majority of experiments were based on middle segment of the axon, separate analysis was made to compare disruption of MPS in those regions. For all middle segments, compared to the DMSO control, axonal segments exposed to both Taxol and Nocodazole at DIV2 exhibited impaired MPS formation, as evidenced by the mean autocorrelation curves of individual (Fig 5.4 C, D). Notably, at DIV4, while both Taxol and Nocodazole affected MPS formation, periodicity also showed increased dispersion with treatment as evidenced by increase in co-efficient of variance (Fig 5.4 F). Additionally, the treated axons exhibited a larger diameter, supporting the findings presented in (Fig.5.4 G).

To understand if this impairment in MPS assembly was because of transport defect or reduced abundance of βII-spectrin, we conducted intensity analysis of middle segments of the axons which we typically use for STED imaging. We found no difference in βII-spectrin levels across treatments (Fig. 5.4 H). This highlights that rather microtubule dynamics plays role in MPS organization rather than transport. While it is possible that there might be transport defects which we are not able to catch at least in these experiments and these low doses.

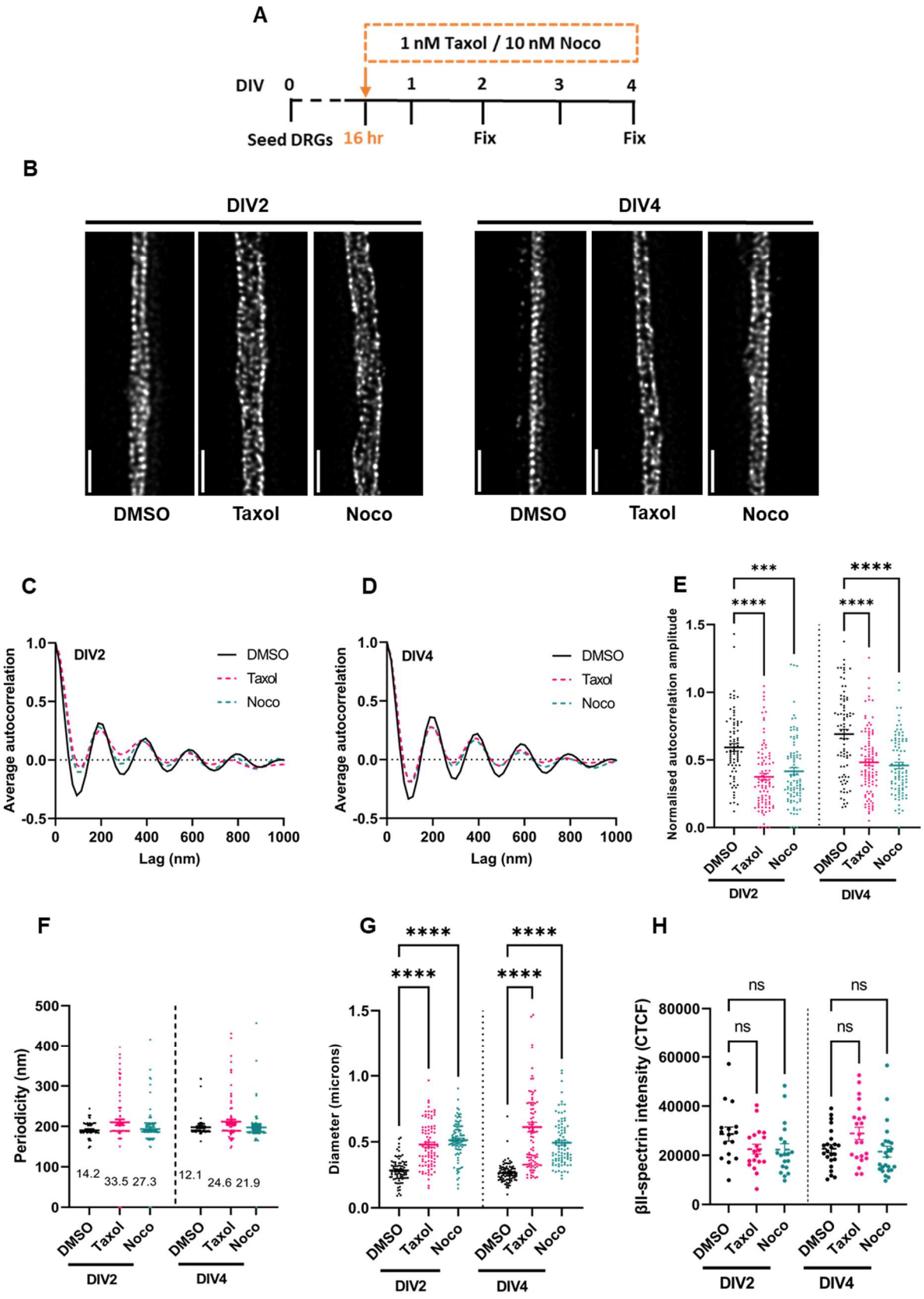

Figure 5.4. Microtubule dynamics is crucial for MPS formation in the middle segment of the axon (A) Timeline of the experiment. 1 nM Taxol or 10 nM Nocodazole was added 16 hr after seeding the neurons and

fixed either after another 32 hrs (DIV2) or after 80 hrs (DIV4). (B) Representative micrographs of treatments across all DIVs. (C,D) Average autocorrelation curves drop for βII-spectrin stained axons from cultures treated with 10 nM nocodazole (green dotted curve) and 1 nM Taxol (pink dotted curve) compared to DMSO (black curve) (E)The autocorrelation amplitudes of the βII-spectrin rings. The data were analysed using the Brown-Forsythe and Welch ANOVA test with multiple comparisons corrected by Games -Howell's test (*, $p \leq 0.05$; **, $p \leq 0.01$; ***, $p \leq 0.001$). (F) Periodicity across DIVs demonstrates an increase in variability between the βII-spectrin rings. (G) Diameter analysis treated axons across DIVs. Data was analysed using the Kruskal-Wallis test with Dunn's correction. 82-100 axonal segments from 3 biological replicates were analysed (*****, $p \leq 0.0001$). (H) βII-spectrin intensity in the middle region of the treated axons is shown as corrected total cell fluorescence (CTCF). The data were analysed using the Kruskal-Wallis test with multiple comparison corrected by Dunn's test. The data are derived from 16-24 axons for all DIVs (ns, $p > 0.05$). For B-G, 82-100 axonal segments from 3 biological replicates for each DIV were analysed.

5.3 Actin stabilisation or myosin contractility does not affect MPS formation

While myosin inhibition leads to increase in axonal diameter (Costa *et al.*, 2020) there is no information regarding role of contractility during MPS formation. A recent investigation into fibroblasts has indicated that acto-myosin contractility may facilitate spectrin clustering and the periodic distribution of βII-spectrin (Ghisleni *et al.*, 2024). The suppression of actin dynamics through jasplakinolide treatment resulted in increased periodic βII-spectrin clusters via myosin activity, whereas the inhibition of non-muscle myosin II with blebbistatin led to the dissipation of βII-spectrin clusters (Ghisleni *et al.*, 2024). However as seen earlier (Fig. 5.1), an acute reduction in F-actin turnover by jasplakinolide (Jasp) did not influence the MPS across development.

In order to understand the role of suppression of actin dynamics and acto-myosin contractility, we wondered if a chronic, low-dose stabilization of F-action would impact MPS development. To this end, 10 nM Jasp was administered to DRG cultures 16 hours post-seeding, and neurons were fixed at DIV2 and DIV4. We found Jasp treated axons to be shorter which is consistent with previous findings, (Gallo *et al.*, 2002), yet the development of the βII-spectrin MPS remained unaffected at both DIV2 and DIV4 compared to DMSO treatment (Fig.5.5 C-F) These axons were not just shorter but substantially thicker than control set as seen in the diameter quantification (Fig. 5.5 G). Since both acute and chronic treatment had no difference in MPS status this suggest that this effect is specific to long-term exposure of Jasplakinolide and not contingent upon the absence of the βII-spectrin MPS.

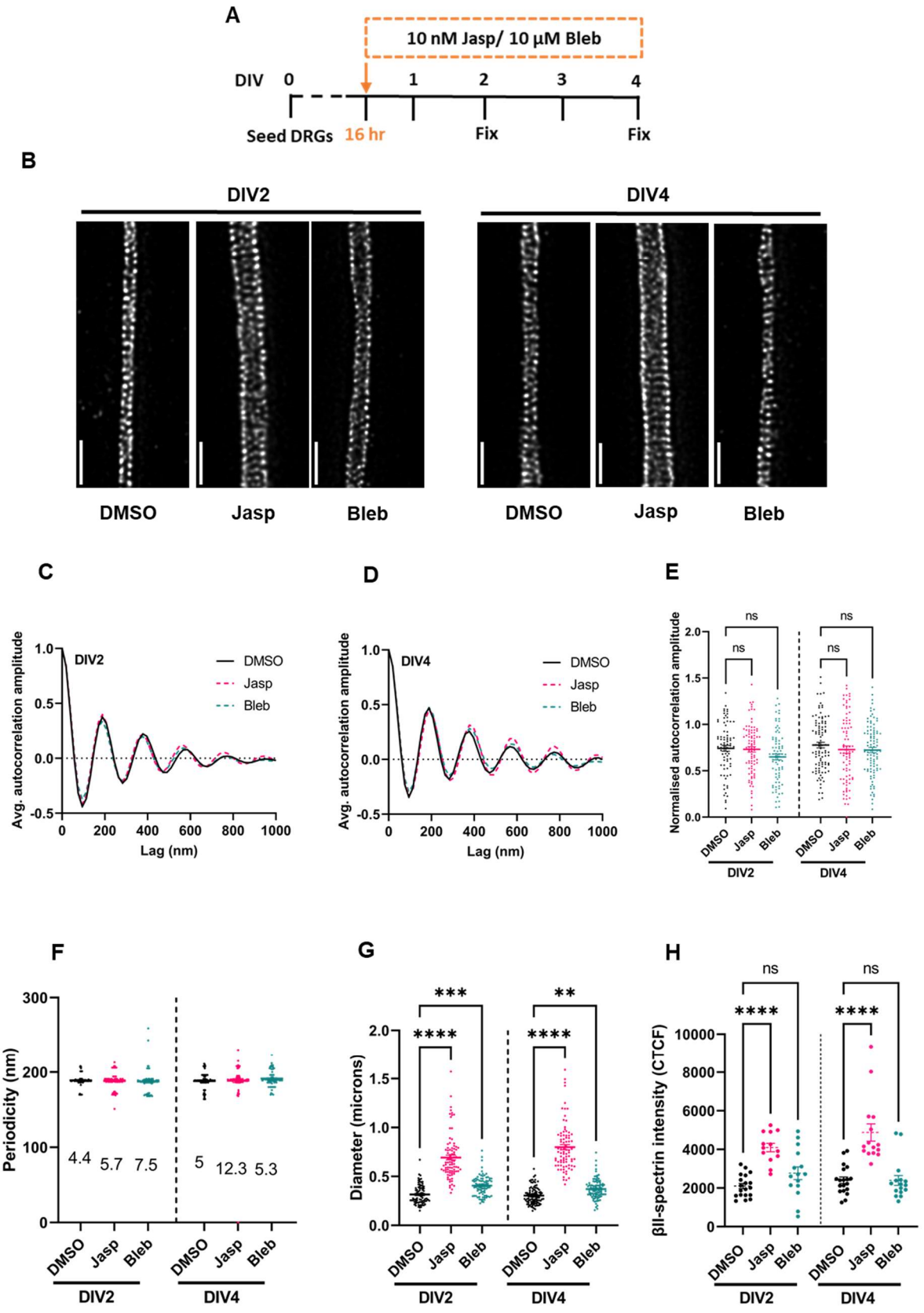

Figure 5.5: Actin stabilization and myosin contractility does not affect MPS formation. (A) Timeline of the experiment. 10 nM Jasplakinolide or 10 µM Blebbistatin was added 16 hr after seeding the neurons and fixed either after another 32 hrs (DIV2) or after 80 hrs (DIV4). (B) Representative micrographs of treatments

across all DIVs. (C, D) Average autocorrelation curves show no difference for βII- spectrin stained axons from cultures treated with 10 μM Blebbistatin (green dotted curve) and 10 nM Jasplakinolide (pink dotted curve) compared to DMSO (black curve) (E)The normalised autocorrelation amplitudes of the βII-spectrin rings. The data were analysed using the Brown-Forsythe and Welch ANOVA test with multiple comparisons corrected by Games -Howell's test (ns, $p > 0.05$). (F) Periodicity across DIVs demonstrates variability between the βII-spectrin rings. The numbers below each data set indicate the coefficient of variation of the distribution. (G) Diameter analysis treated axons across DIVs. Data was analysed using the Kruskal-Wallis test with Dunn's correction (**, $p \leq 0.01$; ***, $p \leq 0.001$; *****, $p \leq 0.0001$)**.** (H) βII-spectrin intensity in the middle region of the treated axons is shown as corrected total cell fluorescence (CTCF). The data were analysed using the Kruskal-Wallis test with multiple comparison corrected by Dunn's test. The data are derived from 13-19 axons for all DIVs (ns, $p > 0.05$; *****, $p \leq 0.0001$)**.** For B-G, 79-98 axonal segments from 3 biological replicates for each DIV were analysed.

Levels of spectrin also changed with Jasp treatment, something extremely interesting and novel. This could be thought in different ways, first being that Jasplakinolide can not only supress dynamic F-actin pool but also nucleate. Chronic exposure to Jasp may result in excessive, hyper stabilized axonal F-actin, leading to short and thick axons. The stronger spectrin signal observed in Jasp-treated axons compared to controls could just be recruitment of more spectrin (Fig. 5.5 H). The other possibility is that Jasplakinolide might trigger increased expression of spectrin which is unknown and needs to be figured out.

Next, we inhibited myosin activity by using 10 μM Blebbistatin to DRGs at 16 hours post-seeding. These were fixed for analysis at DIV2 and DIV4. Low-dose, prolonged inhibition of non-muscle myosin II did affect the development of the βII-spectrin MPS (Fig. 5.5). As expected low concentration of Bleb increased the average diameter of βII-spectrin rings compared to controls (Fig. 5.5 G) while the levels of spectrin remained comparable to the DMSO treated axons. These finding suggests that in neurons the assembly is independent of decreased F-actin dynamics or myosin driven contractility,

Discussion

Our investigation into the microtubule-dependent formation of MPS revealed that both stabilization and destabilization of microtubules during early neuronal development disrupted MPS formation. This finding suggests that a delicate balance in microtubule dynamics is necessary for proper MPS assembly. The observed regional differences in MPS disruption, with distal axonal regions showing increased susceptibility to treatment could potentially be because microtubules are more dynamic at

the distal end of the axon (Ahmad *et al.*, 1993) and a chronic treatment can cause severe effect at the distal end where it is already quite dynamic.

Apart from stabilizing microtubule, taxol can also promote microtubule growth and nucleation while altering axonal transport, these changes may influence MPS development (Theiss and Meller, 2000; Witte *et al.*, 2008; Verma *et al.*, 2016). Interestingly, Taxol and Lat-A can bind to spectrin at the ABD domain of βII-spectrin with varying affinity, and Taxol can also bind to the rest of the βII-spectrin (Dutta *et al.*, 2023). Even though It's not clear what this binding would affect but this needs to be considered as a potential caveat while using taxol as a microtubule stabilizing drug. Even though microtubules and the MPS scaffold have been found to interact indirectly (He *et al.*, 2020), its destabilization has been found to be detrimental for MPS stability (Zhong *et al.*, 2014). We hypothesize that early on, microtubule dynamics is important to maintain structural stability and perturbing it chronically affects the over-all transport, structure and molecular mechanisms that include formation of MPS.

We also show that F-actin stabilization and actomyosin contractility is dispensable in the case of MPS assembly and might be driven by other factors/proteins. This deviates from the model proposed in fibroblasts which might mean that the scaffold of a cylindrical tube (axon) might be equally relevant for the ring assembly.

We also want to highlight that the spectrin levels across chronic treatments in DMSO controls do not vary across DIVs, this gives us confidence across multiple experiment that it is the re-organisation of cortically present spectrin that forms the MPS (becomes relevant for the upcoming chapter).

The intricate interdependence of microtubules, actin, and spectrin in maintaining axonal integrity and withstanding mechanical stress, as previously demonstrated in various model organisms (Krieg *et al.*, 2017b; Qu *et al.*, 2017; Lorenzo *et al.*, 2019), is further supported by our findings. These results expand our understanding of the intricate relationship between cytoskeletal dynamics and MPS formation in developing neurons. In summary, this study underscores the crucial role of both microtubule and actin dynamics in the formation and maintenance of the MPS, a key structural component of neuronal axons. These insights contribute to our understanding of neuronal development and may have implications for neurological disorders associated with cytoskeletal abnormalities. Future research should focus on elucidating the molecular mechanisms governing the interplay between microtubule and MPS assembly.

Chapter 6

Role of Arp2/3 complex and Formin in maintenance of MPS

6.1 MPS is under constant actin turnover during early development

The MPS stands out as the sole known enduring actin network extending throughout axon. Other actin structures, such as actin waves, dense actin, longitudinal actin filaments, and actin hotspots, are either temporary, confined to specific areas, or short-lived across various neuronal regions (Watanabe *et al.*, 2012; Kalil and Dent, 2014; Ganguly *et al.*, 2015; Flynn *et al.*, 2009). A study in *Drosophila* neurons has shown Mutants of Arp2/3 and formin DAAM to negatively affect MPS abundance (Qu *et al.*, 2017). Unpublished research on mouse hippocampal neurons has demonstrated that the Arp2/3 complex and formin are relevant for MPS abundance; however, their role appears to be significant primarily in the early phases (Moura, 2023). Nonetheless, a comprehensive time-dependent analysis of Arp2/3 and Formin during MPS maintenance is not yet known.

Chick DRG neurons from DIV2,4 and 6 were subjected to Arp2/3 complex and formin inhibitors (20 µM CK666 and 20 µM SMIFH2) for 30 min at various culture stages. Post treatment, MPS periodicity, autocorrelation amplitude, and axon diameter were evaluated. Fig 6.1 A displays representative micrographs for all treatments and DIVs. The mean autocorrelation curves indicated a progressive reduction in inhibitor treated group, as shown by pink and green dotted lines, in comparison to the DMSO control (black line) for DIV2 and DIV4. Interestingly, DIV6 neurons showed resistance against disruption (Fig. 6.1 A).

When quantified, autocorrelation amplitude showed significant reduction for DIV2 and DIV4, but not at DIV6 (Fig.6.1 B). Similarly, periodicity was only affected in DIV2 and DIV4 neurons but had no effect on DIV6 (Fig. 6.1 C). A comparison of autocorrelation and periodicity is shown in Fig. 6.2 A where the effect of the inhibitors is clearly understandable. Since MPS was disrupted, we analysed axon diameter which turned out to be larger for DIV2 and DIV4 but comparable to DMSO control in DIV6 (Fig.6.1 D).

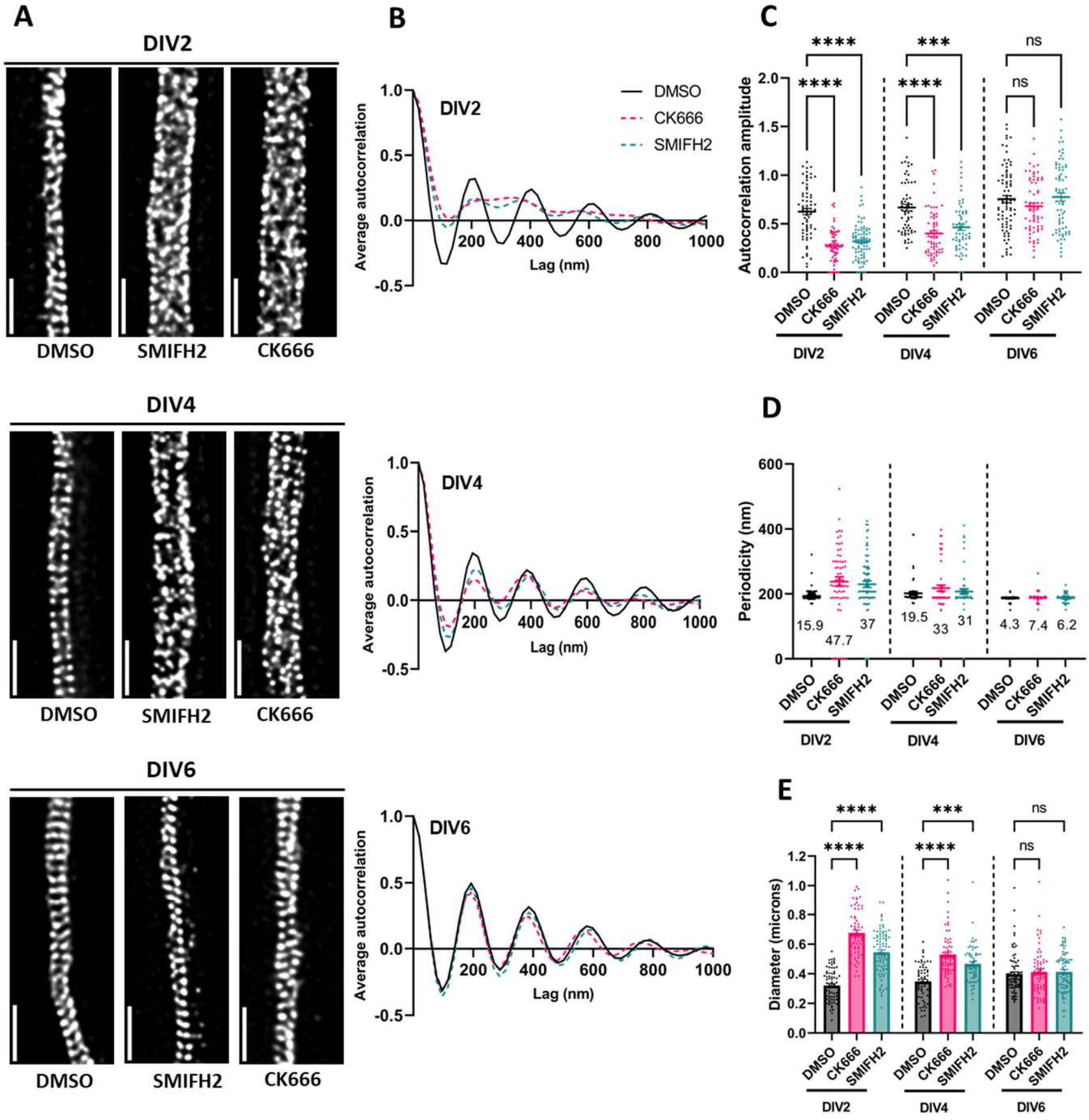

Figure 6.1. Role of Formins and Arp2/3 in MPS formation and maintenance (A) Average autocorrelation curves of DIV2, DIV4, and DIV6 axonal regions from cultures treated with 20 µM CK666 (Arp2/3 inhibitor, indicated by a pink dotted line) and 20 µM SMIFH2 (formin inhibitor, indicated by a green dotted line) for 30 min, along with a DMSO control (indicated by a solid black line). (B) Quantification of autocorrelation amplitudes across DIVs and treatments. The data were analysed using the Brown-Forsythe and Welch ANOVA test with multiple comparisons corrected by Games -Howell's test. (C) Periodicity of inhibitor-treated axons along with the coefficient of variation show increased dispersion. (D) Quantification of the diameter across DIVs and treatments. The data were analysed using the Kruskal-Wallis test with multiple comparison corrected

by Dunn's test. 60-70 axonal segments from 3 biological replicates for each DIV were analysed. (***, $p \leq 0.001$; ****, $p \leq 0.0001$)

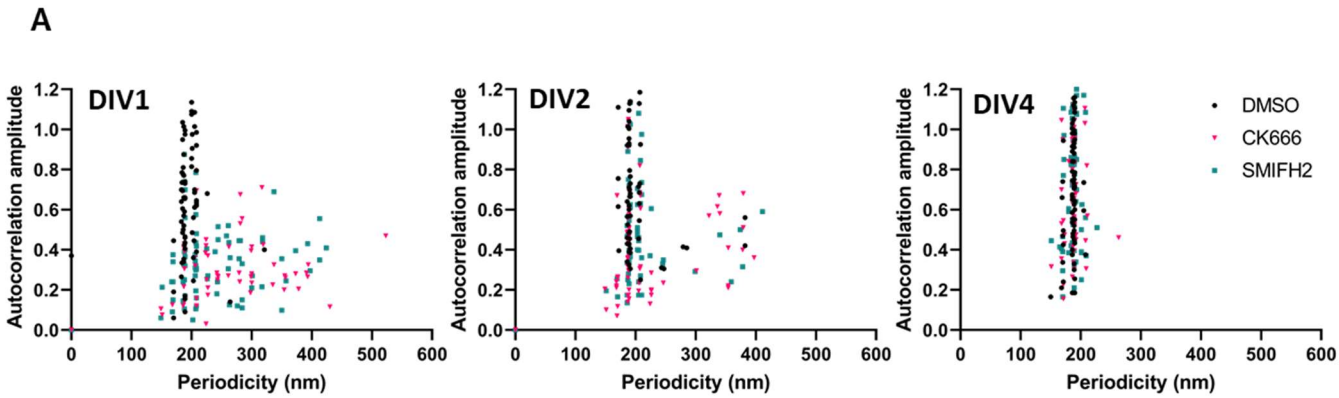

Figure 6.2. Autocorrelation vs periodicity analysis of SMIFH2 and CK666 treated neurons across DIVs
(A) Representative micrographs of βII-spectrin -stained axons following treatment with CK666, SMIFH2, and DMSO at DIV2, DIV4, and DIV6, respectively. Additionally, an analysis of autocorrelation and periodicity for the individual conditions is presented. 60-70 axonal segments from 3 biological replicates for each DIV were analysed.

Discussion

When the developing MPS was treated with the same concentration of Arp2/3 complex and formin inhibitors over DIVs, we observed that although DIV2 and DIV4 exhibited satisfactory autocorrelation (DMSO controls) and thus successfully formed the MPS, they were susceptible to the availability of functioning actin nucleation by both Arp2/3 and formin inhibitors. This observation not only underscores the critical role of these nucleators but also suggests that the already formed or forming MPS is in constant need of them, pointing to the fact that it is likely undergoing continuous turnover. Two days later, at DIV6, MPS demonstrated resistance to disruption by both inhibitors at the same concentration. This outcome indicates that even after the scaffold is formed, we observe varying dependence on F-actin turnover facilitated by these nucleators. This is in line with the fact that MPS becomes stable over time as spectrin has previously been shown to have reduced mobility at DIV10 (Zhong *et al.*, 2014). Interestingly, actin in rings is thought to be either made up of short bundled F-actin filaments (Qu *et al.*, 2017) or by braided F-actin filaments (Vassilopoulos *et al.*, 2019). Role of formin aligns well with both the models as it forms filamentous actin but the role of Arp2/3 which forms branched actin network is intriguing. This highlights the role of branched pool of actin in MPS formation and maintenance. We think that this network of F-actin formed by Arp2/4 complex could be pool of F-actin that aids in recruitment and anchoring of spectrin.

Chapter 7

Role of βII-spectrin domains in recruitment and stability in the MPS

7.1 Dynamics of βII-spectrin during MPS formation

We hypothesized that if βII-spectrin is incorporated into the MPS as a tetramer, we would observe decreased mobility as the MPS develops. To investigate this hypothesis, we transfected βII-spectrin - GFP in DRGs and conducted FRAP at DIV1, DIV2, and DIV4 (Fig.7.1 A, B).

To minimize the impact of the soluble fraction, axons exhibiting low expression were chosen for analysis. The mean normalized recovery curves and mobile fraction revealed a progressive decline in overall mobility, with notable decreases observed at DIV 2 and DIV4 (Fig. 7.1 B, C). Significant differences between all curves were confirmed through F-test comparisons of their plateaus. Half-lives remained consistent across DIVs (Fig.7.1 D). This observation supports the increase in autocorrelation amplitude from DIV1 to DIV4 (Fig. 4), suggesting that the periodic membrane skeleton becomes increasingly stable during development. These findings are consistent with previous studies on hippocampal DIV10 neurons, which showed that spectrin is immobile and firmly integrated into the MPS scaffold (Zhong *et al.*, 2014).

Mobility of βII-spectrin during MPS formation is dependent on F-actin pool

Given that MPS is dependent on F-actin interaction (Fig. 5.1 and Fig. 6.1), we sought to investigate whether spectrin mobility is dependent on F-actin stability. To this end, we treated βII-spectrin-GFP transfected DIV1, 2, and 4 DRG neurons with 5 μM Latrunculin-A for 15 minutes. This concentration was previously demonstrated to disrupt the MPS (Fig.5.1), thus ensuring its efficacy prior to conducting the FRAP experiment. All experiments were performed after drug removal, and FRAP was restricted to 1-hour post-treatment.

Unlike the DMSO control recovery curves for DIV1 and DIV2 neurons, axons treated with Lat-A showed enhanced βII-spectrin mobility (Fig. 7.1 E, F). However, DIV4 axons subjected to Lat-A treatment did not deviate from the DMSO recovery curve. Analysis of the mobile fraction indicated

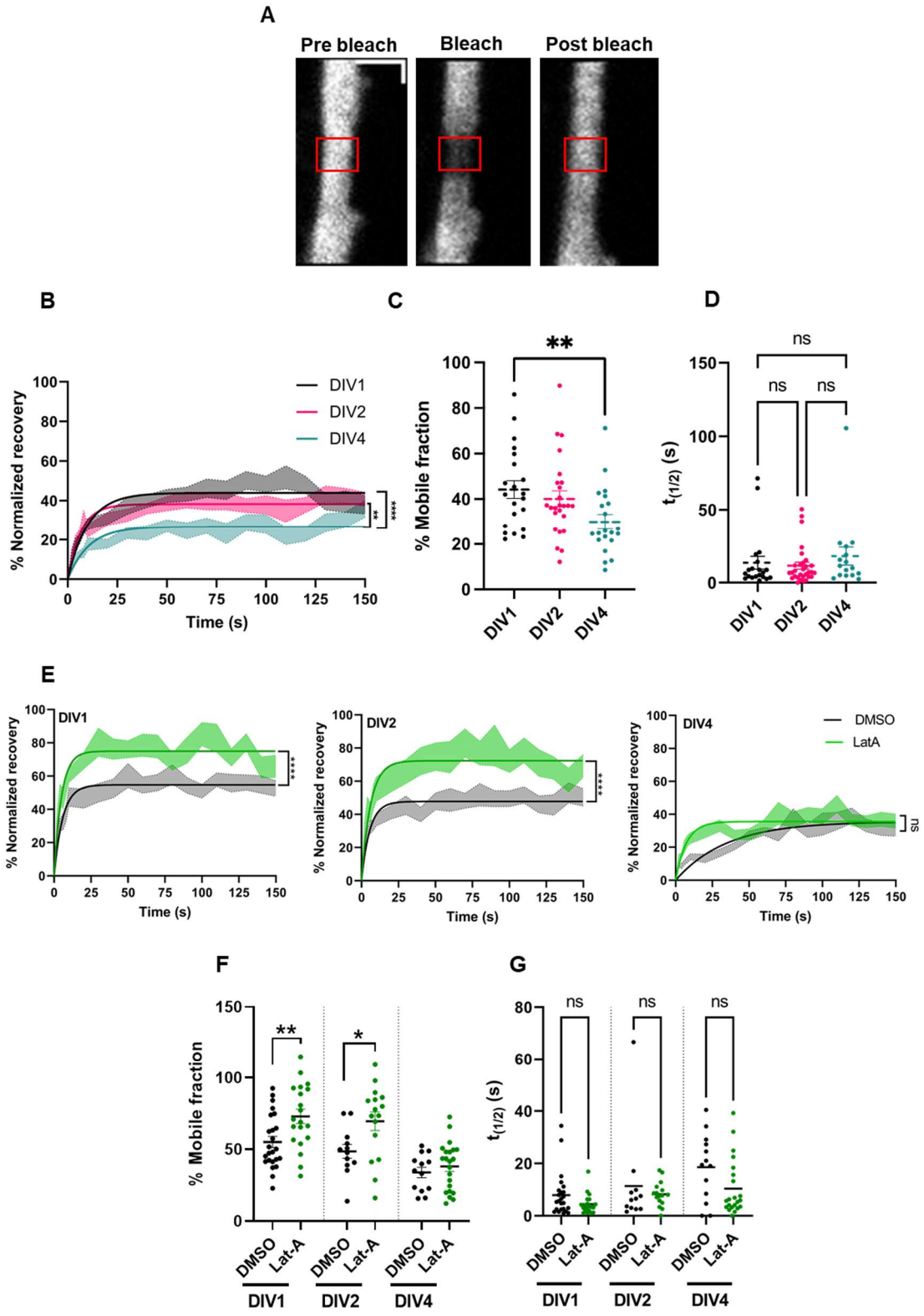

Figure 7.1 Spectrin mobility is dependent on MPS formation and F-actin interaction (A) Representative micrograph of an axonal region transfected with βII-spectrin-GFP, followed by FRAP experiment. Red box highlights region that was bleached and later analysed for recovery. Scale bar: 1micron (B) βII-spectrin-GFP FRAP recovery curves for the DIV1, DIV2, and DIV4 axons. The recovery curves are represented as a one-phase fit of the means (± SEM). Plateau of curves were compared using the extra sum-of-squares F-test (C)

Quantification of the % mobile fraction. The data were analysed using the Mann-Whitney test. (D) *t1/2* values of recovery curves obtained from one phase fit of Latrunculin A and DMSO-treated DRG neurons. Data were analysed using the Kruskal-Wallis test. For A-C, 16-30 neurons for all DIVs from 3 biological replicates were analysed (E) βII-spectrin-GFP FRAP recovery curves for DRG axons treated with Lat- A across DIV1 DIV2 and DIV4. The green and black traces represent the average one-phase fit for Lat-A- and DMSO-treated neurons, respectively. The recovery curves are represented as a one- phase fit of the means (± SEM). Plateau of curves were compared using the extra sum-of-squares F- test (F) Quantification of the % mobile fraction. The data were analysed using the Mann-Whitney test. In this experiment, 12-24 neurons for all DIVs from 3 biological replicates were analysed. (G) *t1/2* values of recovery curves obtained from one phase fit of Latrunculin A and DMSO-treated DRG neurons. Data were analysed using the Kruskal-Wallis test. 12-24 neurons for all DIVs from 3 biological replicates were analysed. (ns, $p > 0.05$; *, $p \leq 0.05$; **, $p \leq 0.01$).

that Lat-A-treated DIV1 and DIV2 axons exhibited a significantly higher mobile fraction, while DIV4 axons remained unchanged compared to DMSO. This finding was further supported by significant differences observed when comparing the plateaus of treated and DMSO curves using an F-test (Fig. 7.1 E). Despite observing a trend in DIV4, half-lives remained consistent across DIVs (Fig.7.1 G)

MPS having showing strong autocorrelation were relatively less abundant at DIV1 (Fig. 4.1). The application of Lat-A further reduced autocorrelation, suggesting interaction with filamentous actin despite the absence of a periodic scaffold (Fig.5.1). FRAP analysis of Lat-A-treated neurons revealed enhanced spectrin mobility and a significant dependence on F-actin cytoskeleton interactions, particularly emphasizing spectrin's association with a cortical F-actin pool, even though MPS was not detected. By DIV2, the MPS scaffold had become more established and was interacting with actin rings, demonstrating an ongoing and anticipated reliance on F-actin. Notably, at DIV4, even when the MPS scaffold was disrupted, the spectrin protein remained immobile, unlike at DIV2, indicating the presence of additional supporting interactions maintaining its stability. These findings offered insights into the characteristics of the βII-spectrin mobility and its dependence on the F-actin cortical pool during these developmental phases.

7.2 SH-SY5Y cells form MPS post differentiation

Subsequently, our objective was to elucidate the importance of various domains of βII-spectrin, as these may contribute to its recruitment in the MPS scaffold and potentially influence stability or turnover. To achieve this, we generated spectrin mutants and aimed to transfect them to conduct FRAP-based mobility assays and determine whether the mutants could form the MPS scaffold.

To determine whether MPS forms in differentiated SH-SY5Y cells, we employed the RA+ BDNF-based differentiation protocol described in the materials and methods section (Chapter 2). Cells were stained with βII-spectrin on Day 4, Day 6, and Day 8 following the addition of BDNF/B27. The middle region of axons was imaged using STED, followed by quantification of autocorrelation amplitude and periodicity (Fig.7.2)

Representative micrographs demonstrate the presence of periodic structures from days 4 to 8 post BDNF addition (Fig. 7.2 B) The average autocorrelation curves and the quantification of autocorrelation amplitude both increased during this time period (Fig. 7.2 C, D). Periodicity measurements demonstrated a decrease in variability (Fig. 7.2 E). These findings exhibited a pattern comparable to that of the chick DRG neurons (Chapter 4) but it is important to note that the autocorrelation amplitude wasn't as high as DIV4 Chick DRG neurons. These differentiated cells have a lot of variability in their morphology and it is possible that at a later time point in differentiation, we might see higher autocorrelation amplitude. For this work and due to technical limitation, we decided to conduct later experiments at Day 6 post BDNF.

We wanted to express βII-spectrin mutant variants in a protein null background to avoid any interference of the endogenous βII-spectrin as it not only will interact with mutant protein but can also form a mixed tetramer. In this dissertation, CRISPR-Cas9 genome editing was employed to generate a substantial deletion with the aim of creating an immediate stop codon in the coding sequence of βII-spectrin.

7.3 Generation and validation of βII-spectrin KO in SH-SY5Y

The highly modular structure of βII-spectrin, characterized by numerous structural motifs, includes 16 spectrin repeats (SRs, consisting of 106 contiguous amino acid sequence motifs), Actin-Binding Domains (ABDs) (Calponin Homology (CH) domains), EF-hands, Pleckstrin Homology (PH) domains, Src Homology 3 (SH3) domains, and various other signaling domains and motifs. This structural complexity contributes to the multiple functions of spectrin (Yang *et al.*, 2021).

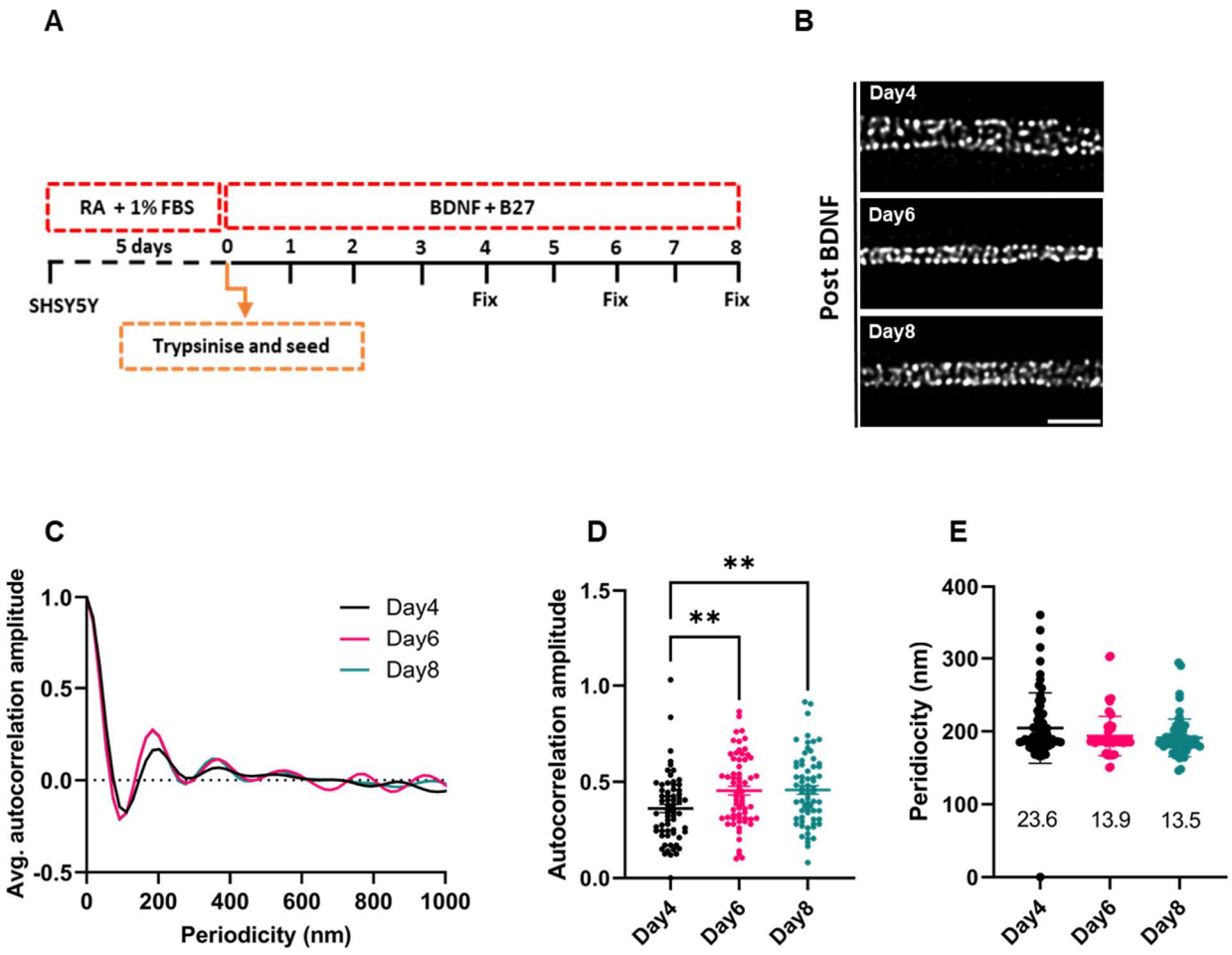

Figure 7.2 MPS in differentiated SH-SY5Y neurons A) Timeline indicating the differentiation protocol of SH-SY5Y cells. (B) Representative STED micrographs of βII-spectrin stained differentiating neurons (4, 6, and 8 days post-BDNF). Scale bar: 1 µm. (C, D) Average autocorrelation curves and quantification of autocorrelation amplitudes across time points. The data were analyzed using the Brown-Forsythe and Welch ANOVA test with multiple comparisons corrected by Games -Howell's test. (**, $p \leq 0.01$). (E) Periodicity across days demonstrates a reduction in variability. The numbers below each data set indicate the coefficient of variation of the distribution. For B-E, 65 axonal segments from 3 biological replicates for each time-point were analysed.

Our strategy involved selecting the actin-binding domain in exon 2, middle region of spectrin repeats in exon 16, and plasma-membrane binding in exon 34 as targets. The rationale for choosing these specific exons was to address multiple sites and ensure that these functions were targeted, even in cases where truncated proteins might form. To this end, we designed two single-guide RNAs (sgRNAs) for each exon to increase the chances of deletion and immediate stop codon formation. We followed the procedure described by Ran FA and Co. to build reagents for knockout generation (Ran *et al.*, 2013).

Multiple tools, such as benchling and chop-chop, were used to determine the off-target effects of the designed sgRNAs. The following table describes the details of all the sgRNAs:

Gene	sgRNA name	sgRNA sequence (PAM)	On target score	Off target score	sgRNA location
SPTBN1 (βII-spectrin)	hSptbn1_sg1	cagtgatgtcaacaaccgctGGG	64.3	46.3	exon 2
	hSptbn1_sg2	gctctgcgcggctttttgagCGG	60.4	46.4	exon 2
	hSptbn1_sg3	ccagacagcgatcgcctcggAGG	61.3	48.5	exon 16
	hSptbn1_sg4	gaacgagatcgacaactacgAGG	76.3	47.8	exon 16
	hSptbn1_sg5	tggaattccctaccacagcgAGG	70.2	44.5	exon 34
	hSptbn1_sg6	gaaagaagctgtctgcgaagTGG	65.9	40.9	exon 34

Complementary oligonucleotides representing the top and bottom strands of these sgRNAs, containing BbsI restriction sites, were utilized for cloning into the pSpCas9(BB)-2A-GFP (PX458) plasmid (Addgene #48138) using restriction digestion and ligation methodology. These plasmids contained a Cas9 expression cassette in conjunction with GFP. All six clones were subsequently verified through sequencing.

Transfection and sorting

The plasmids containing sgRNAs and Cas9 were co-transfected into SH-SY5Y cells to target either exon 2, 16, or 34, respectively, using electroporation. After 48 hours, the GFP-expressing cells were sorted into a 96-well plate. These sorted cells were maintained and subsequently transferred to a 24-well plate for expansion. Upon reaching confluency, they were transferred to 35 mm plates.

Knockout validation by western blotting and genotyping

Initially, the samples were screened by western blotting of more than 50 expanded clonal cell populations using βII-spectrin 1:1000 (BD Bioscience; 612563) and GAPDH 1:10000 (Santa Cruz; sc-365062). It is to be noted that βII-spectrin antibody binds at the C- terminal of the protein and won't be able to show any truncated protein, if any. Among all the screened samples, five clones demonstrated the absence of a band for the βII-spectrin antibody when compared to wild-type SH-SY5Y. (Fig. 7.3 as highlighted in red). Loss of protein was only observed with sgRNA targeting exon 16. The five selected clones were subsequently processed for genomic analysis through genomic DNA extraction and PCR of regions surrounding the guide RNA region flanking the exon-intron region, using the following primers: forward 5' CCCTGAAAAACCGAGAGGCC 3' and reverse

5'GCTCGTTCCATCCAGTGTCC3'. Figure 7.4 illustrates deletions of 80 base pairs (bp) (in clones 5, 20, and 29) and 68 bp (in clones 26 and 27), which would result in the generation of a stop codon prior to the termination of exon 16. If protein translation occurs, the resulting polypeptide would consist of 1084 or 1158 amino acids, respectively (Fig. 7.4).

βII-spectrin KO clones exhibit axonal length deficit post differentiation

Neurons derived from βII-Spectrin knockout mouse were shown to have reduced axonal length when cultured (Lorenzo *et al.*, 2019). We wanted to verify if SH-SY5Y when differentiated also show axonal length deficit. To this end, we differentiated WT and βII-Spectrin knockout (clone 29) till day 4 post BDNF addition (detailed differentiation illustrated in material and methods section). These differentiated cells were stained for βIII-tubulin antibody which is a marker of neuronal processes. The length of these neuronal processes were quantified and analysed (Fig 7.5). KO axons demonstrate an increase in length over time; however, they fail to attain the growth level of WT axons, as illustrated in Fig 7.5

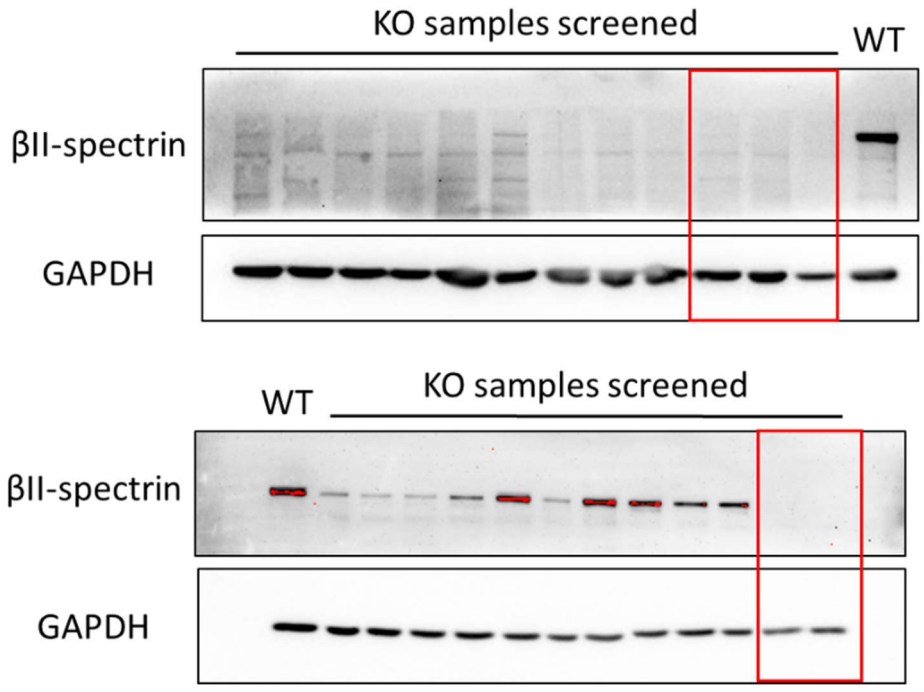

Figure 7.3: βII-spectrin KO screening in SH-SY5Y with western-blotting: Samples highlighted in red boxes showed minimal to no signal post anti-body staining confirming loss of protein. These 5 clones were further selected for genomic analysis.

To summarize, CRISPR-Cas9 gene-editing technique was employed to generate multiple βII-Spectrin knockout clones. Although recent advancements have improved Cas9 nuclease accuracy, there remains

a significant risk of unintended genetic alterations in organisms modified using CRISPR-Cas9. To confirm the specificity of the mutation's effect on gene function, we evaluate various clones. However, this approach does not eliminate the potential for off-target effects. As anticipated with other βII-Spectrin knockout models, differentiated SH-SY5Y cells exhibited reduced axon length, supporting the reliability of this knockout system. For all subsequent experiments, Clone 29 was chosen due to its minimal non-specific labelling, negligible truncated product (if any), and demonstrated axonal length deficit.

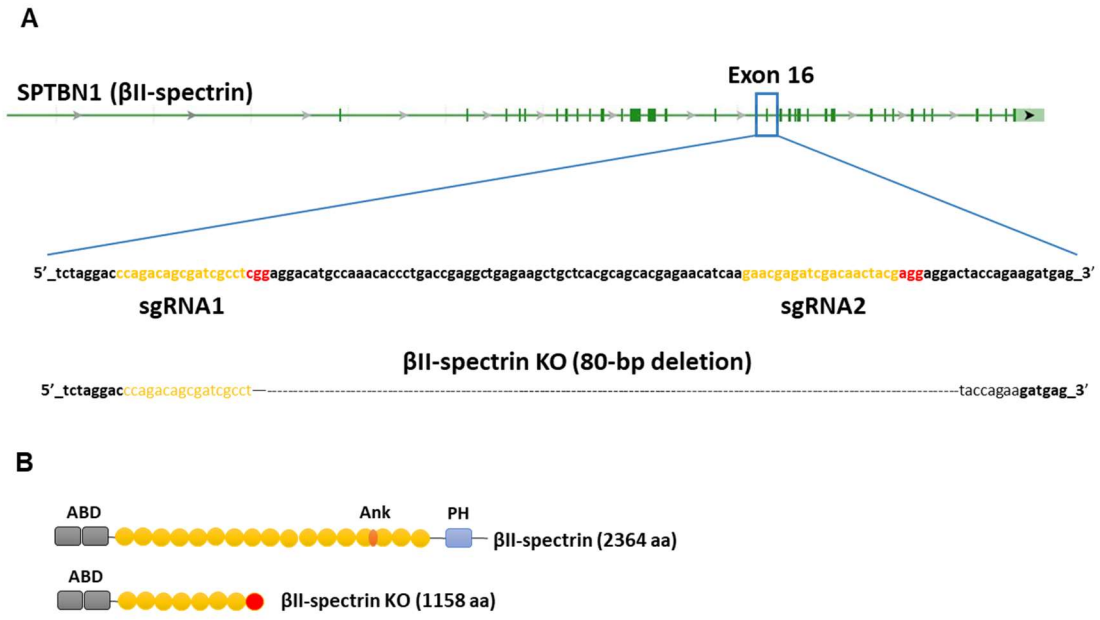

Figure 7.4: βII-spectrin knockout screening in SH-SY5Y cells utilizing genomic sequencing: (A) Sequencing analysis of indel SH-SY5Y βII-spectrin knockout cells. Sequences targeted by gRNA 3 and 4 are highlighted in yellow, and the PAM sequences are indicated in red. Translation products are denoted in red for each genotype. (B) Schematic of βII-spectrin protein in WT in comparison with βII-spectrin KO cells in case of truncation product forms.

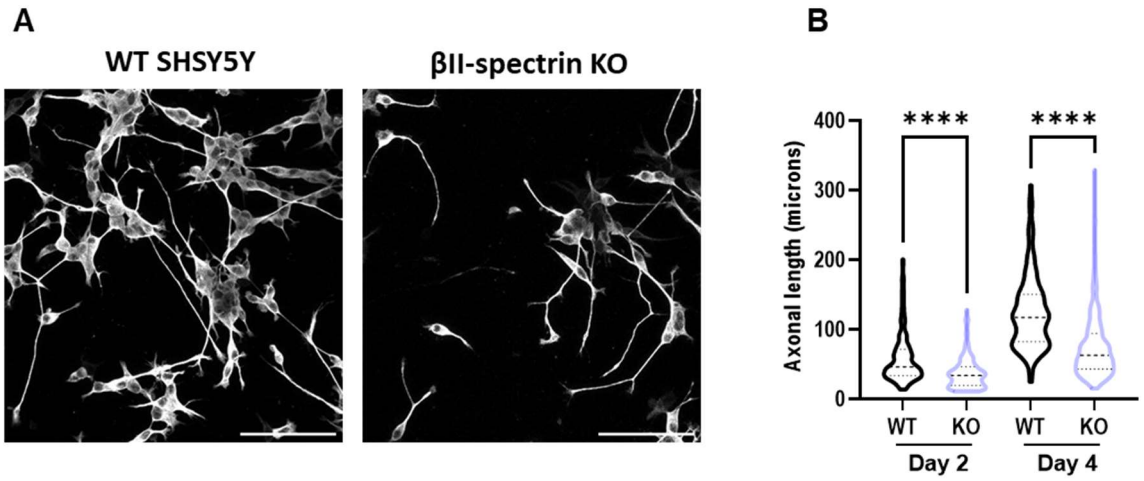

Figure 7.5 βII-Spectrin knockout axons exhibit axonal length deficit (A) Representative micrographs of differentiating WT and βII-Spectrin KO (clone 29) cells stained with βIII-tubulin. Scale bar 50 µM (B) Quantification of axonal length across Day 2 and Day 4 cells post BDNF addition. ****p < 0.0001 (One-way ANOVA) from N=3 and n>100

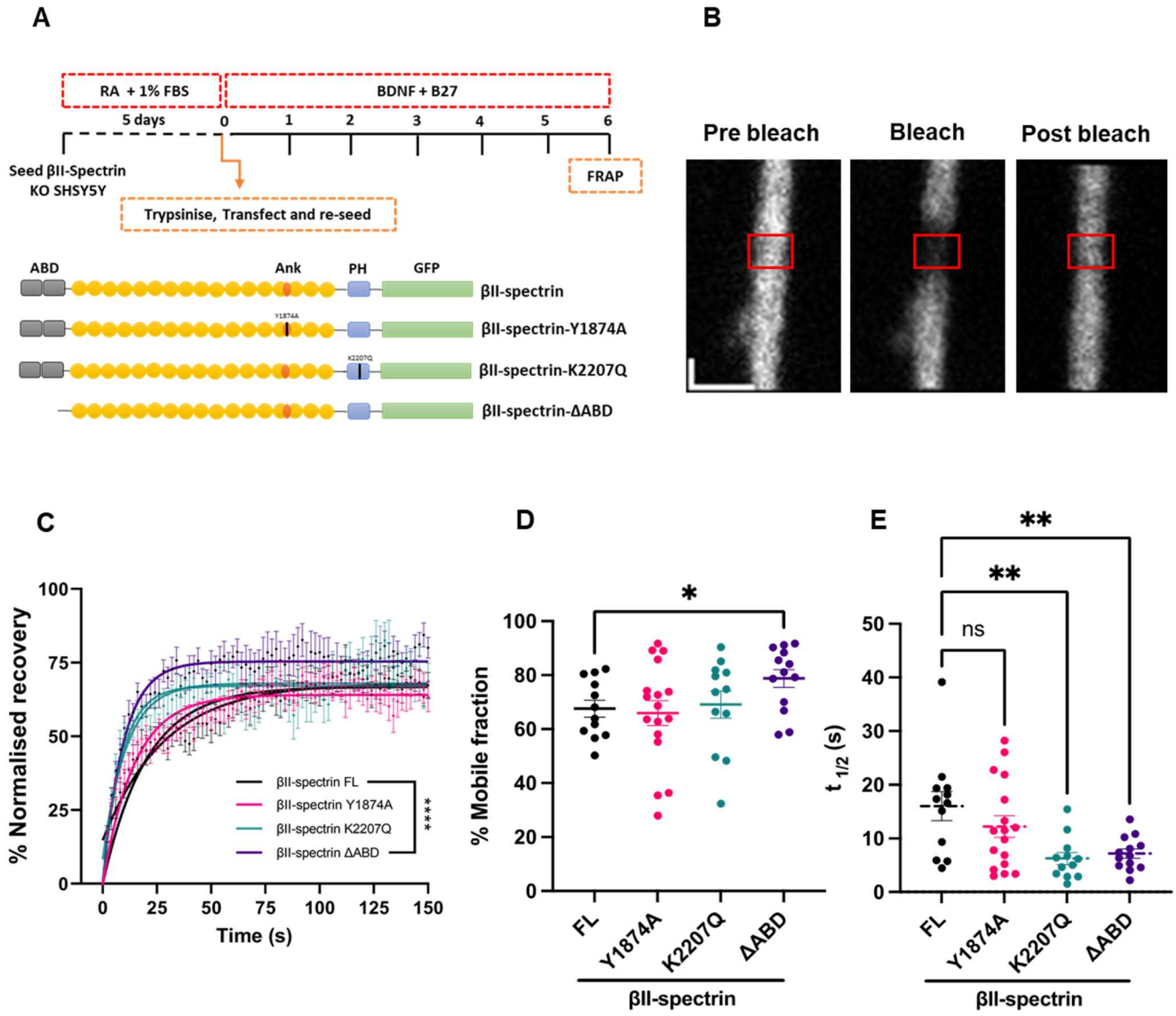

Figure 7.6 Plasma membrane and actin-binding domains are crucial for βII-spectrin mobility (A) Timeline indicating the differentiation protocol of βII-Spectrin KO cells and experimental procedures. βII-spectrin KO were transfected mid-differentiation with βII-spectrin variants indicated. The domains are denoted as follows: GFP-tag in green, actin-binding domain (ABD) in grey, ankyrin domain-binding domain in orange, and plasma membrane-binding domain in blue. (B) Representative micrograph of an KO neuron transfected with βII-spectrin-FL-GFP, followed by FRAP experiment. Red box highlights region that was bleached and later analysed for recovery. Scale bar: 1micron (C) FRAP recovery curves of mutant and βII-FL-spectrin expressing βII-Spectrin KO cells 6 days after transfection and BDNF treatment. The recovery curves are

represented as a one-phase fit of the means (± SEM). Plateau of curves were compared using the extra sum-of-squares F-test. (D) Quantification of the % mobile fraction. The data were analysed using the Mann-Whitney test. (E) $t_{1/2}$ values extracted from the fit were analysed using the one-way ANOVA test. In this experiment, 12-24 neurons for all DIVs from 3 biological replicates were analysed. ns, $p > 0.05$; *, $p \leq 0.05$; **, $p \leq 0.01$; ****, $p \leq 0.0001$.

7.4 βII-spectrin mobility depends on plasma membrane and actin binding activity

We created βII-spectrin variants with a green fluorescent protein (GFP) tag. These variants included the complete protein and mutants lacking ankyrin domain-binding activity (Y1874A), plasma membrane activity (K2207Q), and actin- binding domain (ΔABD) (Fig.7.6 A). We transfected these variants into differentiating βII-Spectrin KO SH-SY5Y cells and conducted FRAP analysis 6 days after transfection (Fig.7.6 A). It is also crucial to note here that ΔABD mutant formed aggregates and experiments were conducted on axons that had no such phenotype. This is in line with work published by Lorenzo and group where they see pathogenic variants on ABD mutants to aggregate at variable severity (Cousin *et al.*, 2021).

The recovery curves showed patterns similar to FL (Fig.7.6 C), but mobile fraction quantification revealed increased mobility in the ΔABD variant (Fig.7.6 D). The PH and ΔABD mutants showed a shorter half-life, indicating quicker recovery compared to the full-length βII-Spectrin (Fig.7.6 E). In contrast, the Y1874A Ankyrin mutant showed no significant difference from the FL protein. These findings emphasize the crucial role of both plasma membrane and actin-binding activity in βII-spectrin mobility.

7.5 Plasma membrane and actin binding activity is crucial for recruitment of βII-spectrin in the MPS

Given the reduced half-life of PH and ΔABD mutants, we explored whether MPS could be restored in βII-spectrin KO neurons through overexpression of these mutant proteins. We used STED microscopy to image GFP-labeled axons at day6 post BDNF and transfection (Fig 7.7 A) and discovered that K2207Q and ΔABD mutants failed to form a periodic MPS structure, as evidenced by the average autocorrelation curves and amplitude (Fig.7.7 B, C). Furthermore, periodicity analysis revealed higher variance for both mutants compared to the full-length control (Fig.7.7 C). These results demonstrate that βII-spectrin relies on its ability to bind to the plasma membrane and actin for proper recruitment and function.

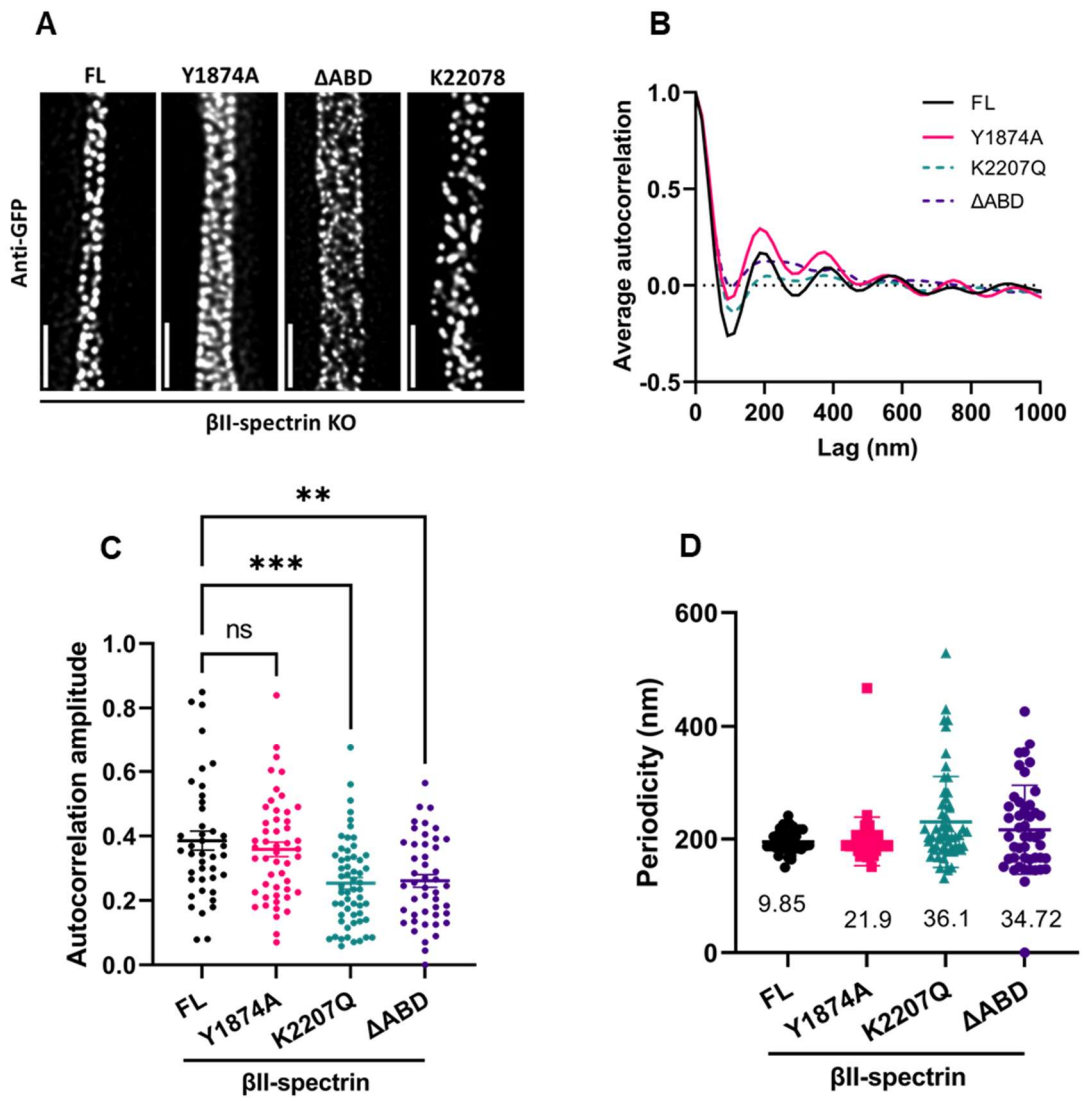

Figure 7.7 Plasma membrane and actin-binding domains are crucial for recruitment of βII-spectrin in the MPS (A) Representative STED micrographs of anti-GFP stained differentiated neurites (day 6 post-BDNF) transfected with βII-spectrin variants. (B, C) Average autocorrelation curves and quantification of autocorrelation amplitudes for all βII-spectrin variants. The data were analysed using the Brown-Forsythe and Welch ANOVA test with multiple comparisons corrected by Games -Howell's test (ns, $p > 0.05$; **, $p \leq 0.01$; ***, $p \leq 0.001$). (D) Periodicity demonstrates high variation in the spacing between the βII-spectrin rings in K227Q and ΔABD variants. The numbers below each data set indicate the coefficient of variation of the distribution. In this experiment, 40–60 axonal regions were examined for each condition across 3 biological replicates.

Discussion

Previous work has shown βII-spectrin to be extremely immobile in DIV10 hippocampal neurons (Zhong *et al.*, 2014). We found that as the MPS scaffold forms the mobility of βII-spectrin decreased. We had initially theorized that this reduced mobility would be due to its integration into the scaffold structure. Intriguingly, we observed low mobility even at a time-point (DIV1) where the MPS is not highly periodic. We hypothesised that there must be some interaction that regulates the mobility. To investigate this, we disrupted F-actin using Lat-A since it is a known interactor and the most crucial one to form the structure. We observed that βII-spectrin mobility increased after actin disruption at DIV1 and DIV2, but showed no change at DIV4. This demonstrates that F-actin interaction influences βII-spectrin mobility; however, by DIV4, the protein becomes more stable, even when the MPS structure is compromised. This could be explained by interactions with other structures and proteins as the structure matures with increase in DIV. Our findings highlight the interaction between F-actin and βII-spectrin since DIV1 even when there is no proper MPS structure found. This also corroborates and possibly explains the presence/need of branched actin (as seen and explained in chapter 6) that might aid in this process of early anchoring of βII-spectrin to the cortex which eventually might re-organise with developmental time.

Previous studies have shown the plasma membrane domain of βII-spectrin to be crucial for sustaining axonal transport and elongation (Lorenzo *et al.*, 2019). Furthermore, studies have revealed that βII-spectrin mutants lacking actin-binding and PH domains are unable to assemble the periodic MPS when expressed in βII-spectrin knockout mouse hippocampal neurons (Zhou *et al.*, 2022). We wanted to understand the role of βII-spectrin domains in aiding the process of recruitment and assembly of MPS. In order to conduct the FRAP analysis and to see if these mutants form periodic structures, we established SH-SY5Y as a model while demonstrating that these differentiated neurons form MPS and also show a developmental timeline with increasing autocorrelation amplitude similar to DRGs. Next, we generated a βII-spectrin KO SH-SY5Y and conducted the experiments on differentiating cells.

Analysing FRAP of βII-spectrin mutants in KO background, we found that PH and ABD domain mutant had faster recovery (lower $t_{1/2}$) than FL-βII-spectrin protein and hence less stability. From this, we understood that both these domains were crucial for maintaining βII-spectrin anchoring and stability. Next, we imaged all the mutants via STED to confer if they are able to form periodic scaffold. Our findings not only corroborates with previous finding of spectrin actin-binding (ΔABD) and PH (K2207Q) binding mutant being unable to assemble the periodic MPS (Zhou *et al.*, 2022) but also adds

the potential reason behind K2207Q and ΔABD mutant not being able to form the MPS as they exhibit increased dynamics (reduced stability) as seen with the FRAP analysis. The finding of ΔABD exhibiting increased mobility and lower $t_{1/2}$ also aligns with FRAP experiments in DRGs where F-actin-disruption led to increased βII-spectrin mobility.

Chapter 8

Role of βII-Spectrin and MPS in maintaining axonal tension

Work mentioned in this chapter was done in collaboration with Prof. Pramod Pullarkat's lab. Ashish Mishra developed the ablation setup and we performed the ablation experiments at RRI, Bangalore.

8.1 Probing the role of developing MPS in maintaining axonal tension

Computational models emphasize the role of MPS in protecting axons during traumatic brain injuries (Kant *et al.*, 2021) whereas atomic force microscopy and simulations indicate that the spectrin scaffold influences membrane mechanics, and its disruption compromises axonal integrity under stress (Zhang *et al.*,2017). Research using atomic force microscopy (AFM) revealed that spectrin tetramers from red blood cells (RBCs) unfold when subjected to tension (Rief *et al.*, 1999). In neuronal cells, the absence of spectrin leads to axon breakage and reduced structural stability (Hammarlund *et al.*, 2007). Additionally, laser ablation experiments on spectrin mutants in C. elegans neurons indicate that spectrin is under tension and contributes to axonal pre-stress (Krieg *et al.*, 2014). Recently with in-vitro experiments and theoretical modelling we have found how spectrin tetramers may act as tension buffers through the folding and unfolding of spectrin repeats, allowing axons to deform without experiencing excessive tension (Dubey *et al.*, 2020). Interestingly, the MPS, known for its 190 nm periodicity, is believed to exist in a fully stretched state under minimal tension. The mechanism behind this configuration, whether it occurs during formation or through subsequent stretching, remains uncertain. Based on these prior studies, our aim was to investigate the potential connection between MPS formation and axonal tension.

Using a custom-built laser ablation setup, we ablated DIV1, DIV2, and DIV4 axons and recorded the retraction event at 2000 fps for ~ 0.8s (Fig. 8.1 A). (Details of the experimental procedure is written chapter 2) These neurons were grown on glass-bottom dishes without any coating to obtain detached axons. We measured the evolving gap between the two cut ends because the retraction of a prestressed system following laser axotomy occurs at a rate consistent with its pre-existing tensile state (Kumar *et al.*, 2006; Krieg *et al.*, 2014) .

Quantification was performed using a custom-built code. The average curves demonstrate a gradual but modest increase in gap size across advancing DIVs, while quantitative analysis of maximum gap revealed a significant size effect compared to DIV1 (Fig. 8.1 B, C). F-test that compares plateaus also showed significant difference between developing DIVs. This correlates with the observed increase in the amplitude of the MPS autocorrelation across the DIVs (Fig 4.1).

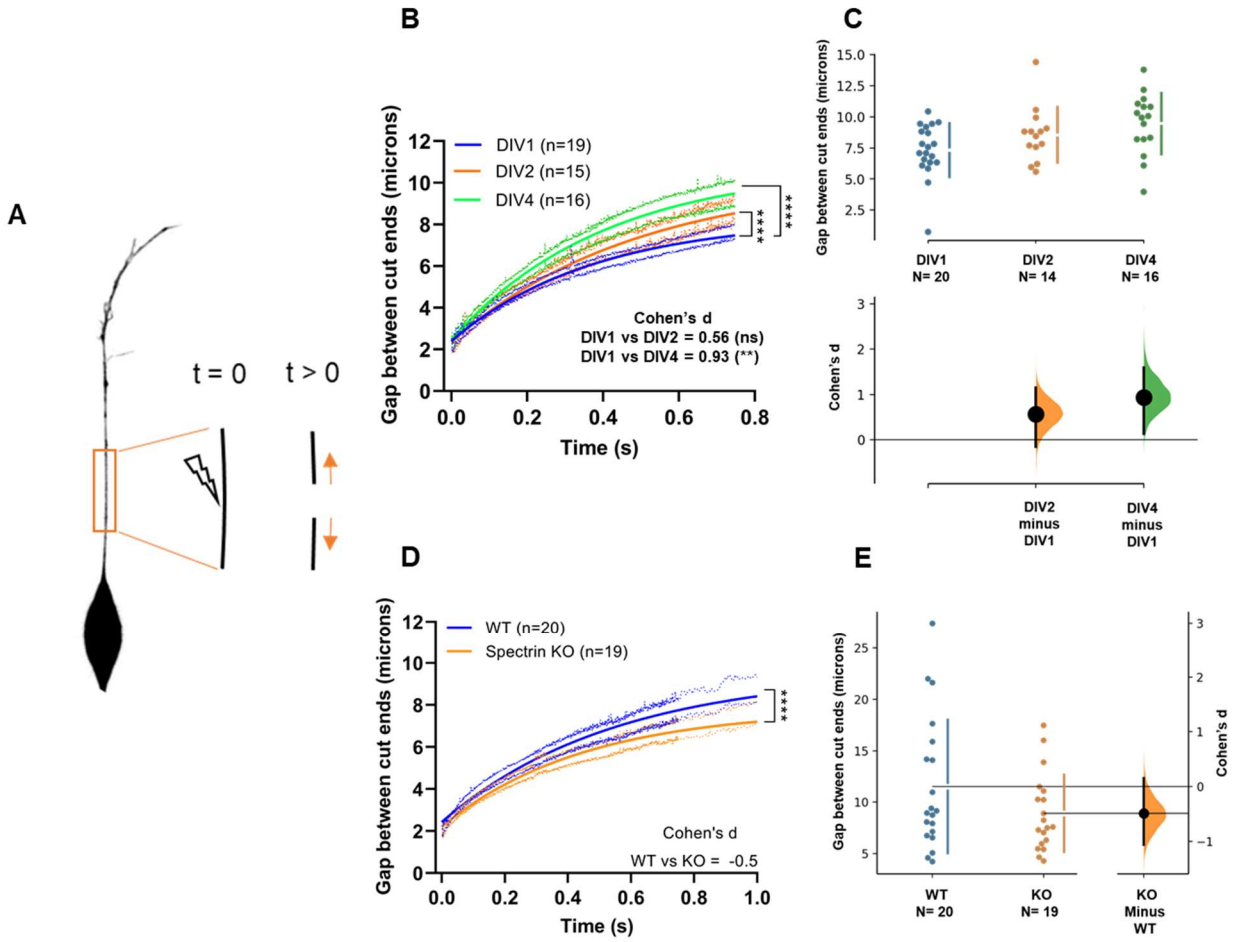

Figure 8.1 Contribution of MPS in the maintenance of axonal tension (A) Schematic representation of neuronal ablation demonstrating an evolving gap between cut ends as time progresses; (B) Evolving gap between cut ends post-ablation with one-phase fit for DIV1 (in blue), DIV2 (in orange), and DIV4 (in green) neurons. F test comparing difference in plateau showed significant difference across DIVs; **** $p<0.0001$ (C) Quantification of the size effect of the gap length utilizing estimation statistics. The unpaired Cohen's d between DIV1 and DIV2 is 0.564 [95.0%CI -0.151, 1.15] with $p = 0.123$ (ns) and between DIV1 and DIV4 is 0.934 95.0%CI 0.136, 1.59] with $p = 0.0078$ (**). (ns, $p > 0.05$; *, $p \leq 0.05$; **, $p \leq 0.01$; ****, $p \leq 0.0001$). The data are derived from n=20 (DIV1), n=14 (DIV2) and n=16 (DIV4) axons from three independent biological replicates. (D) Evolving gap between differentiated day 8 (post-BDNF) SH-SY5Y axons of both spectrin KO and WT genotypes. F test comparing difference in plateau for both genotypes showed significant difference; **** $p<0.0001$ (E) Quantification of the size effect of gap length utilizing estimation statistics. The unpaired Cohen's d between the WT and KO was -0.444 [95.0%CI -1.09, 0.247] with $p= 0.175$.

To understand if there is any causal link between formation of MPS and maintenance of rest tension, we ablated differentiated WT and spectrin KO SH-SY5Y axons at day 8 post BDNF addition, where MPS was observed. KO axons exhibited a reduced gap distance compared to WT axons (Fig. 8.1 D), whereas quantification of the maximum gap showed a considerable size effect compared with WT

axons (Fig. 8.1 E). These results suggest that spectrin is one of the components that maintains axonal tension.

Discussion

Our observations revealed a gradual rise in axonal tension over increasing DIVs, which showed a strong correlation with the increasing MPS. Axons lacking spectrin exhibited lower tension compared to their wild-type counterpart, indicating that spectrin-based MPS plays a role in contributing to axonal tension. It's worth noting that despite substantial MPS formation by DIV4, we didn't observe a huge increase in tension compared to DIV1. This suggests that the axon is already under tension (at DIV1) before the MPS scaffold forms.

The decrease in tension in the spectrin knockout system was relatively modest when compared to the reduction observed in spectrin tetramerization mutant-unc-70(e524) (E2008K) TRN neurons in C. elegans (Krieg *et al.*, 2014). In their experiment when they ablated unc-70(e524) axons, they did not see an extremely stark loss of retraction (tension) where as their control also did not show much retraction. They hypothesised that it could be because of extra-cellular attachment and hence used whole body him-4(e1267); unc-70(e524) double mutant where the mutants had defects in TRN attachment. In these experiment they observed a starkly high retraction in their him-4(e1267) control axons while him-4(e1267); unc-70(e524) double mutant should similar retraction as unc-70(e524). It seems as if the change was in retraction of the control group him-4(e1267) rather than the double mutant. Notably, unc-70(e524) TRN neurons display a periodic MPS despite being a tetramerization mutant (Krieg *et al.*, 2017).This means that the mutation did not lead to any defect in tetramerization and is not only forming the MPS structure but is also (in contrast) showing changes in axial tension. These findings indicate that the presence of spectrin in the MPS scaffold is not the sole factor responsible for maintaining systemic tension.

On the other hand, FRET experiments have shown that the spectrin-tetramer may be under constant tension (Krieg, Dunn and Goodman, 2014), which could be more significant at a localized molecular level. While βII-Spectrin is thought to buffer tension (Dubey *et al.*, 2020) and might be already pre-stressed, it is possible that the systemic rest-tension might be maintained and influenced by multiple components, like the underlying microtubule network, contractile actomyosin forces, extracellular adhesion and integrin signalling and intracellular transport forces which needs to be studied. This needs to be further studied in detail by systematically ablating detached axons of WT and KO animals across development after disruption microtubules, F-actin and myosin activity.

Chapter 9

Discussion and perspectives

The Membrane-associated Periodic Skeleton (MPS) forms and spreads within axons during various phases of neuronal growth, starting as early as DIV2, and shows significant autocorrelation in later stages (Zhong *et al.*, 2014). Although many studies have examined later developmental periods, these have been conducted across different species and neuronal type (Leterrier *et al.*, 2015; Han *et al.*, 2017; Zhou *et al.*, 2022). However, a thorough examination of the MPS's developmental sequence during early axonal growth and extension was missing, particularly in neuron subtypes like Dorsal Root Ganglia (DRG), which may lack a conventional Axonal Initial Segment (AIS) (Nascimento *et al.*, 2018).

We aimed to explore the time-line of MPS formation and key components that regulate this process in embryonic chick DRG neurons. Our findings suggest that MPS development begins as early as DIV1 and gradually matures, showing increased regularity and autocorrelation strength. The formation of MPS is associated with a decrease in axon diameter, a phenomenon noted in several neuron types. A systematic analysis of the proximal, middle, and distal regions revealed that the MPS emerges concurrently along the axon during early developmental stages. This finding aligns with the proposed formation of rings through spectrin patches (Hofmann *et al.*, 2022) but diverges from the proximo-distal directional bias reported in multiple studies utilizing hippocampal neurons (Zhong *et al.*, 2014; Han *et al.*, 2017; Lorenzo *et al.*, 2019; Hofmann *et al.*, 2022).Developing probes and imaging technique that is capable of live imaging which can tracks periodic assembly of βII-Spectrin in early stages of development will be crucial and extremely relevant for a lot of future research.

Studies have consistently shown that interfering with microtubule and actin cytoskeleton negatively impacts MPS maintenance (Zhong *et al.*, 2014; Han *et al.*, 2017; Qu *et al.*, 2017; Wang *et al.*, 2019). Our findings indicate that both microtubule and actin cytoskeleton elements are essential for MPS maintenance and formation during early development. Destabilizing these structures leads to MPS instability, while reinforcing them may enhance MPS, especially in early developmental phases.

Notably, when microtubule dynamics is disrupted during early development using low concentrations of taxol and nocodazole. MPS formation was impaired. The distal end was more susceptible to the perturbation potentially because distal end of the axon has more dynamic pool of microtubule and the MPS in that region could be more susceptible to perturbation. It could also be possible that MPS in the distal region is more labile and can undergo turnover quickly compared to other regions. This highlighted the importance of microtubule dynamics in MPS formation, possibly due to its role in preserving neuronal structural integrity. Perturbation of the microtubule via destabilization is expected

to perturb MPS formation (Zhong *et al.*, 2014) but delay in MPS formation because of stabilization was novel. We also found levels of spectrin to remain similar across treatments and time-points in the middle region of the axon. This potentially highlights that the concentration used for perturbing microtubule dynamics did not affect the transport of spectrin but rather the arrangement. This finding needs to be expanded and thoroughly studied to figure out if there is any direct cross talk between microtubule and MPS architecture or is the dependence because of overall loss of axonal structural integrity. It is also possible that chronic taxol treatment can trigger calpain mediated proteolytic lysis (Wang *et al.*, 2004) and spectrin is a known target of calpain (Czogalla and Sikorski, 2005). Moreover, blocking the calcium-activated calpain enzymes provides protection against taxol-induced sensory nerve damage in living organisms. Additionally, Taxol triggers the activation of both calpain and caspase enzymes in PC12 cells (Wang *et al.*, 2004). It is crucial to understand how exactly is dynamics of microtubule affecting MPS formation and maintenance since there is no direction interaction known.

We for the first time show that F-actin stabilization and actomyosin contractility is dispensable in the case of MPS assembly and might be driven by other factors/proteins. This deviates from the model proposed in fibroblasts which might mean that the scaffold of a cylindrical tube (axon) might be equally relevant for the ring assembly

The Arp2/3 complex and formin inhibitors significantly hindered MPS development at DIV2 and DIV4, highlighting their crucial importance in the initial formation of structures. Nevertheless, by DIV6, MPS showed resilience against disruption, suggesting a decreased dependence on these regulators. Research has previously demonstrated that MPS levels decline in *Drosophila* mutants lacking these regulatory proteins (Qu *et al.*, 2017). Recently, Daam1 a formin family protein has been shown to regulate AIS plasticity while being found to occasionally co-localise with F-actin rings (Micinski and Hotulainen, 2024). Notably, the Arp2/3 complex, which generates branched F-actin, plays a role in MPS regulation, despite the prevailing notion that actin rings are composed of filamentous or braided actin.(Qu *et al.*, 2017; Vassilopoulos *et al.*, 2019; Moura, 2023). Further experiments need to be conducted to figure out the reason behind requirement of branched-actin and to also show localisation of Arp complex in around MPS scaffold.

MPS undergoes turnover in early stages, as evidenced by regulator experiments and other studies showing increased stability of the MPS scaffold (Zhong *et al.*, 2014). Using Fluorescence Recovery After Photobleaching (FRAP), we assessed the mobility of βII-spectrin over development of MPS.

Our analysis showed a gradual reduction in overall mobility as the MPS formed, indicating increased stability of the structure over time. We found that βII-spectrin mobility was influenced by interactions with F-actin, particularly during early developmental stages, regardless of proper MPS formation (at DIV1). Based on these observations, we suggest the presence of a pool of branched and filamentous actin that interacts with spectrin tetramers prior to their assembly into a scaffold that affects mobility. This also corroborated well with how inhibition of actin regulator caused disruption of MPS with reducing effect as DIVs progressed.

Following this, we established differentiated SH-SY5Y cells do form MPS. We then proceeded to create βII-Spectrin knockout in the a SH-SY5Y cell line. This gene knockout was employed to investigate the functions of various spectrin domains as they can also determine mobility and recruitment. The findings underscored the importance of βII-Spectrin's ability to bind to both the plasma membrane and actin in restricting its movement and ability to create the periodic MPS structure.

These findings expand our understanding of the developmental sequence and molecular mechanisms involved in the establishment and preservation of MPS in neuronal cells. There remains significant potential for a more in-depth examination of the transition between DIV1-2 to identify the key molecular components and regulators that may be constructing this framework. Additionally, it is crucial to definitively demonstrate whether MPS formation in DRG neurons occurs in a non-directional manner when compared to CNS neurons.

Over the past ten years, numerous publications have explored the functional significance of MPS. Our previous work demonstrated that MPS can serve as a tension buffer by absorbing mechanical stress through the folding and unfolding of spectrin repeats (Dubey *et al.*, 2020). Leveraging the well-established timeline of MPS development, we conducted experiments involving axon ablation and tension measurement. Our findings revealed a gradual increase in axonal tension from DIV1 to DIV4, which aligned with the stages of MPS formation. When we ablated βII-Spectrin knockout SH-SY5Y axons, we observed a minor decrease in axonal tension compared to wild-type axons. Reduction in tension was not was stark as what was previously shown in *C.elegans* (Krieg *et al.*, 2014). Their observation was unexpected, as these *C.elegan* neurons with mutant spectrin tetramerization still displayed periodic MPS (Krieg *et al.*, 2017). The reduction in tension they observed appears to be caused by factors other than the absence of spectrin or MPS. In-depth analysis needs to be done to dissect the relevance of spectrin and MPS in regulation of axonal axial tension. Since DIV1 neurons

also show some tension and the difference between DIV1 and DIV4 isn't very large, we think there must be other regulators of axonal tension apart from MPS or spectrin. This corroborates with minimal reduction in axonal tension in βII-Spectrin KO axons. It will be interesting to see how circumferential contractility and axial axonal tension are coupled by MPS scaffold. Systematic ablation experiments after perturbation of MPS and other cytoskeletal structure can inform us about how axonal tension is regulated.

Based on the findings of this thesis and information known from findings in the field, we propose a working model of MPS formation during early development:

Initiation and early assembly (DIV1-2):

Right when neurites form, βII-spectrin is transported along the growing axon by bimodal transport where it interacts with a pool of branched and filamentous actin regulated by Arp2/3 complex and Formins. This interaction leads to stabilization of βII-spectrin at the cortex hence decreasing mobility despite not being yet periodically arranged in a scaffold.

Recruitment of βII-spectrin is not just dependent on its interaction with F-actin but also on plasma-membrane binding activity. These interactions lead to formation of periodic βII-spectrin with increasing autocorrelation amplitude. At this early stage when the F-actin and βII-spectrin are getting localised cortically, they are sensitive to disruption in F-actin and microtubule dynamics.

Axons which exhibit this assembling periodic scaffold are under tension. This Initial tension at DIV1 could be because of other cytoskeletal components as MPS is not completely established.

Maturation and stabilization (DIV2-4):

In this phase, MPS exhibits increased regularity and autocorrelation amplitude which corroborates with gradual decrease in βII-spectrin mobility and increase in axonal tension. This is potentially because of increased incorporation βII-spectrin in the existing scaffold (stoichiometrically). With time dependency of βII-spectrin mobility on F-actin drops as MPS matures. This corroborates with how inhibition of Arp2/3 complex and Formin activity has more effect on DIV2 compared to DIV4. As the system matures from DIV2 to DIV4, it not only shows reduction in βII-spectrin mobility but also continued increase in axonal tension. This scaffold formation is not dependent on level of spectrin as intensity per unity area of the protein remains constant highlighting that the formation of MPS happens via re-organisation of already recruited spectrin in that particular region.

Formation of MPS is dependent on microtubule dynamics. Chronic perturbation of microtubule dynamics in either direction (stabilization and destabilization) causes disruption in MPS assembly process. This needs to be inquired in depth as from this there is no direct interaction of MPS and neither did levels of spectrin change removing role of delayed or aberrant transport.

In neurons, chronic increase of F-actin stabilisation, doesn't promote more MPS formation and neither does MPS depend of myosin dependent contractility for assembly unlike fibroblasts.

Maintenance (DIV6 and above)

The structure is established and it becomes difficult to perturb it. It becomes insensitive to inhibition of Arp2/3 complex and Formin and does not require frequent F-actin turnover in comparison to DIV2 and DIV4. Axonal tension is hypothesized to increase whereas mobility of βII-spectrin would decrease even more than DIV4 axons. This phase also leads to recruitment of adducin and Ankyrin in the scaffold. Axons (hippocampal) at these stage show patchy spectrin accumulation at the distal end while it is intriguingly absent in early stages. This could potentially be how spectrins are deposited but at earlier stages due to shorter lengths the accumulation seems continuous. This can be corroborated by how kinesin 1 and adaptor proteins perturb spectrin transport and localization in the distal end of the neuron.

A short summary:

βII-spectrin is transported at a slower bimodal rate and recruited to the plasma-membrane cortex along the entire axon. This recruitment to the plasma-membrane cortex is contingent upon F-actin and plasma-membrane binding activity. At subsequent developmental stages, this previously recruited βII-spectrin undergoes reorganization, which is independent of an increase in protein concentration but is dependent on the equilibrium between the dynamic nature of microtubules and is independent of myosin contractility. Given that DIV1 neurons are already under tension and myosin doesn't affect MPS formation, the systemic axonal tension must be getting stored or contributed by other cytoskeletal elements. While few studies show increased patchy appearance of spectrin at the distal/middle region of the axon in the later stages (DIV6 onwards), the question remains whether it is because of spectrin transport lagging compared to the increase in axonal length (growth rate) or is this specific to later stage axons.

Open questions:

Spatiotemporal Assembly and Dynamics of the MPS

Quantitative Intensity Profiling Across Development:

Analyze βII-spectrin and F-actin intensity along the axon at different developmental stages (e.g., DIV1, DIV2, DIV4, etc.) using a microfluidic compartmentalization system to distinguish axonal segments.

Longitudinal Spectrin Imaging:

Develop and use endogenously tagged βII-spectrin lines to track its transport and deposition over time in the same axon. Estimate spectrin half-life using pulse-chase or photo-conversion techniques.

FRAP Dynamics & MPS Assembly:

Perform FRAP on βII-spectrin under control and perturbed conditions (e.g., after Latrunculin A, Jasplakinolide, Taxol treatment) to assess dynamic exchange and membrane-association of the protein during and after MPS disruption.

MPS Reassembly Post-Disruption:

Induce MPS disassembly at DIV4 using Lat-A, then allow recovery for defined time points (e.g., 6h, 10h, 24h) to model MPS regeneration and study potential re-assembly trajectories.

Cytoskeletal Regulation of MPS Formation

Actin Nucleator Inhibition:

Chronically inhibit Arp2/3 and Formins at DIV1 and assess MPS assembly at DIV2 and DIV4 using βII-spectrin staining and live SiR-actin imaging.

Role of Microtubules in MPS Assembly:

Perturb microtubules using Taxol (stabilization) or Nocodazole (depolymerization); assess effects on MPS formation and correlate with microtubule post-translational modifications (PTMs) and structure using super-resolution microscopy or EM.

Cytoskeletal Crosstalk via Combinatorial Drug Perturbation:

Conduct dual drug treatments (e.g., stabilize microtubules and depolymerize actin, and vice versa) at various DIVs to delineate cytoskeletal interdependencies in MPS assembly.

Mechanical and Biophysical Aspects of the MPS

Spectrin Tension Sensing in Early Development:

Use FRET-based spectrin tension sensors to quantify force on spectrin at early stages (e.g., DIV1), before mature MPS rings form.

Recoil and Tension Buffering Capacity:

Perform laser ablation experiments to measure axonal recoil in the presence/absence of cytoskeletal perturbations, assessing MPS contributions to axonal tension buffering.

Stretching and Periodicity Modulation:

Investigate whether mechanical stretching (applied at different rates) affects the spacing between spectrin rings, mimicking physiological nerve stretching during body movements.

MPS Reconstitution and Geometry-Driven Assembly:

Explore in vitro reconstitution of spectrin-F-actin assemblies in micro tubes mimicking axonal geometry to test whether geometry/constraints alone can drive periodicity.

Spectrin mutant tension in Null Background:

Express βII-spectrin mutants in spectrin-null neurons and assess mechanics (via rheology or ablation), probing functional domains in mechanical load-bearing.

Contextual and Comparative Insights

Influence of Surface Adhesion & Substrate Cues:

Assess whether contact with other cells or ECM substrates affects MPS formation—relevant to understanding axon-environment interactions during development or regeneration.

Comparative MPS Dynamics in CNS vs. PNS:

Compare MPS assembly rates, stability, and periodicity in peripheral vs. central neurons, to test whether cytoskeletal regulation differs between systems.

Intrinsic vs. Cue-Driven Assembly:

Test whether MPS assembly is intrinsically programmed or externally cued by examining spontaneous formation under varied chemical and geometrical constraints.

Publications

- Sushil Dubey, Nishita Bhembre, Shivani Bodas, Sukh Veer, Aurnab Ghose, Andrew Callan-Jones, Pramod Pullarkat (2020) The axonal actin-spectrin lattice acts as a tension buffering shock absorber eLife 9:e51772 https://doi.org/10.7554/eLife.51772

- Shivani Bodas, Ashish Mishra, Pramod Pullarkat, Aurnab Ghose (2025) Development of the axonal βII-spectrin periodic skeleton requires active cytoskeletal remodeling. doi: https://doi.org/10.1101/2025.02.19.639207 (in review)

References

Adli, M (2018). The CRISPR tool kit for genome editing and beyond. Nat Commun 9, 1911.

Ahmad, FJ, Pienkowski, TP, and Baas, PW (1993). Regional differences in microtubule dynamics in the axon. J Neurosci 13, 856–866.

Arbuthnott, ER, Boyd, IA, and Kalu, KU (1980). Ultrastructural dimensions of myelinated peripheral nerve fibres in the cat and their relation to conduction velocity. J Physiol 308, 125–157.

Bear, JE, and Gertler, FB (2009). Ena/VASP: towards resolving a pointed controversy at the barbed end. J Cell Sci 122, 1947–1953.

Bennett, V, and Healy, J (2008). Organizing the fluid membrane bilayer: diseases linked to spectrin and ankyrin. Trends Mol Med 14, 28–36.

Bennett, V, and Healy, J (2009). Membrane Domains Based on Ankyrin and Spectrin Associated with Cell–Cell Interactions. Cold Spring Harb Perspect Biol 1, a003012.

Bennett, V, and Lorenzo, DN (2013). Chapter One - Spectrin- and Ankyrin-Based Membrane Domains and the Evolution of Vertebrates. In: Current Topics in Membranes, ed. V Bennett, Academic Press, 1–37.

Blanchoin, L, Pollard, TD, and Mullins, RD (2000). Interactions of ADF/cofilin, Arp2/3 complex, capping protein and profilin in remodeling of branched actin filament networks. Curr Biol 10, 1273–1282.

Boyer, NP, Sharma, R, Wiesner, T, Delamare, A, Pelletier, F, Leterrier, C, and Roy, S (2024). Spectrin condensates provide a nidus for assembling the periodic axonal structure. 2024.06.05.597638.

Bronner, ME, and LeDouarin, NM (2012). Development and evolution of the neural crest: An overview. Dev Biol 366, 2–9.

Chakrabarti, R, Lee, M, and Higgs, HN (2021). Multiple roles for actin in secretory and endocytic pathways. Curr Biol 31, R603–R618.

Coles, CH, and Bradke, F (2015). Coordinating Neuronal Actin–Microtubule Dynamics. Curr Biol 25, R677–R691.

Cooper, GM (2000). Microtubule Motors and Movements. Sinauer Associates.

Costa, AR, Pinto-Costa, R, Sousa, SC, and Sousa, MM (2018). The Regulation of Axon Diameter: From Axonal Circumferential Contractility to Activity-Dependent Axon Swelling. Front Mol Neurosci 11.

Costa, AR, Sousa, SC, Pinto-Costa, R, Mateus, JC, Lopes, CD, Costa, AC, Rosa, D, Machado, D, Pajuelo, L, Wang, X, *et al.* (2020). The membrane periodic skeleton is an actomyosin network that regulates axonal diameter and conduction. eLife 9, e55471.

Cousin, MA, Creighton, BA, Breau, KA, Spillmann, RC, Torti, E, Dontu, S, Tripathi, S, Ajit, D, Edwards, RJ, Afriyie, S, *et al.* (2021). Pathogenic SPTBN1 variants cause an autosomal dominant neurodevelopmental syndrome. Nat Genet 53, 1006–1021.

Czogalla, A, and Sikorski, AF (2005). Spectrin and calpain: a “target” and a “sniper” in the pathology of neuronal cells. Cell Mol Life Sci CMLS 62, 1913–1924.

D’Este, E, Kamin, D, Balzarotti, F, and Hell, SW (2017). Ultrastructural anatomy of nodes of Ranvier in the peripheral nervous system as revealed by STED microscopy. Proc Natl Acad Sci.

D’Este, E, Kamin, D, Göttfert, F, El-Hady, A, and Hell, SW (2015). STED Nanoscopy Reveals the Ubiquity of Subcortical Cytoskeleton Periodicity in Living Neurons. Cell Rep.

D’Este, E, Kamin, D, Velte, C, Göttfert, F, Simons, M, and Hell, SW (2016). Subcortical cytoskeleton periodicity throughout the nervous system. Sci Rep 6, 22741.

Dubey, S, Bhembre, N, Bodas, S, Veer, S, Ghose, A, Callan-Jones, A, and Pullarkat, P (2020). The axonal actin-spectrin lattice acts as a tension buffering shock absorber. eLife 9, e51772.

Dutta, S, Bose, D, Ghosh, S, and Chakrabarti, A (2023). Spectrin: an alternate target for cytoskeletal drugs. J Biomol Struct Dyn 41, 6534–6545.

Encinas, M, Iglesias, M, Liu, Y, Wang, H, Muhaisen, A, Ceña, V, Gallego, C, and Comella, JX (2000). Sequential Treatment of SH-SY5Y Cells with Retinoic Acid and Brain-Derived Neurotrophic Factor Gives Rise to Fully Differentiated, Neurotrophic Factor-Dependent, Human Neuron-Like Cells. J Neurochem 75, 991–1003.

Fletcher, DA, and Mullins, RD (2010). Cell mechanics and the cytoskeleton. Nature 463, 485–492.

Flynn, KC, Pak, CW, Shaw, AE, Bradke, F, and Bamburg, JR Growth cone-like waves transport actin and promote axonogenesis and neurite branching.

Fuchs, E, and Cleveland, DW (1998). A Structural Scaffolding of Intermediate Filaments in Health and Disease. Science 279, 514–519.

Galiano, MR, Jha, S, Ho, TS-Y, Zhang, C, Ogawa, Y, Chang, K-J, Stankewich, MC, Mohler, PJ, and Rasband, MN (2012). A Distal Axonal Cytoskeleton Forms an Intra-Axonal Boundary that Controls Axon Initial Segment Assembly. Cell 149, 1125–1139.

Gallo, G, Yee, HF, Jr, and Letourneau, PC (2002). Actin turnover is required to prevent axon retraction driven by endogenous actomyosin contractility. J Cell Biol 158, 1219–1228.

Ganguly, A, Tang, Y, Wang, L, Ladt, K, Loi, J, Dargent, B, Leterrier, C, and Roy, S (2015). A dynamic formin-dependent deep F-actin network in axons. J Cell Biol 210, 401–417.

Gasser, HS, and Grundfest, H (1939). AXON DIAMETERS IN RELATION TO THE SPIKE DIMENSIONS AND THE CONDUCTION VELOCITY IN MAMMALIAN A FIBERS. Am J Physiol-Leg Content.

Gentile, JE, Carrizales, MG, and Koleske, AJ (2022). Control of Synapse Structure and Function by Actin and Its Regulators. Cells 11, 603.

Ghisleni, A, Bonilla-Quintana, M, Crestani, M, Lavagnino, Z, Galli, C, Rangamani, P, and Gauthier, NC (2024). Mechanically induced topological transition of spectrin regulates its distribution in the mammalian cell cortex. Nat Commun 15, 5711.

Glomb, O, Swaim, G, Munoz LLancao, P, Lovejoy, C, Sutradhar, S, Park, J, Wu, Y, Cason, SE, Holzbaur, ELF, Hammarlund, M, *et al.* (2023). A kinesin-1 adaptor complex controls bimodal slow axonal transport of spectrin in *Caenorhabditis elegans*. Dev Cell 58, 1847-1863.e12.

Götz, M, and Huttner, WB (2005). The cell biology of neurogenesis. Nat Rev Mol Cell Biol 6, 777–788.

Hammarlund, M, Jorgensen, EM, and Bastiani, MJ (2007). Axons break in animals lacking β-spectrin. J Cell Biol 176, 269–275.

Han, B, Zhou, R, Xia, C, and Zhuang, X (2017). Structural organization of the actin-spectrin–based membrane skeleton in dendrites and soma of neurons. Proc Natl Acad Sci U S A 114, E6678–E6685.

He, J, Zhou, R, Wu, Z, Carrasco, MA, Kurshan, PT, Farley, JE, Simon, DJ, Wang, G, Han, B, Hao, J, *et al.* (2016). Prevalent presence of periodic actin–spectrin-based membrane skeleton in a broad range of neuronal cell types and animal species. Proc Natl Acad Sci 113, 6029–6034.

He, L, Kooistra, R, Das, R, Oudejans, E, van Leen, E, Ziegler, J, Portegies, S, de Haan, B, van Regteren Altena, A, Stucchi, R, *et al.* (2020). Cortical anchoring of the microtubule cytoskeleton is essential for neuron polarity. eLife 9, e55111.

Heiman, MG, and Shaham, S (2010). Twigs into branches: How a filopodium becomes a dendrite. Curr Opin Neurobiol 20, 86–91.

Ho, J, Tumkaya, T, Aryal, S, Choi, H, and Claridge-Chang, A (2019). Moving beyond P values: data analysis with estimation graphics. Nat Methods 16, 565–566.

Hoffman, PN (2010). A conditioning lesion induces changes in gene expression and axonal transport that enhance regeneration by increasing the intrinsic growth state of axons. Exp Neurol 223, 11–18.

Hofmann, M, Biller, L, Michel, U, Bähr, M, and Koch, JC (2022). Cytoskeletal assembly in axonal outgrowth and regeneration analyzed on the nanoscale. Sci Rep 12, 14387.

Hotulainen, P, and Hoogenraad, CC (2010). Actin in dendritic spines: connecting dynamics to function. J Cell Biol 189, 619–629.

Huang, CY-M, Zhang, C, Ho, TS-Y, Oses-Prieto, J, Burlingame, AL, Lalonde, J, Noebels, JL, Leterrier, C, and Rasband, MN (2017). αII Spectrin Forms a Periodic Cytoskeleton at the Axon Initial Segment and Is Required for Nervous System Function. J Neurosci 37, 11311–11322.

Jessen, KR, and Mirsky, R (2016). The repair Schwann cell and its function in regenerating nerves. J Physiol 594, 3521–3531.

Kalil, K, and Dent, EW (2014). Branch management: mechanisms of axon branching in the developing vertebrate CNS. Nat Rev Neurosci 15, 7–18.

Kant, A, Johnson, VE, Arena, JD, Dollé, J-P, Smith, DH, and Shenoy, VB (2021). Modeling links softening of myelin and spectrin scaffolds of axons after a concussion to increased vulnerability to

repeated injuries. Proc Natl Acad Sci 118, e2024961118.

Kapitein, LC, and Hoogenraad, CC (2015). Building the Neuronal Microtubule Cytoskeleton. Neuron 87, 492–506.

Kim, IH, Racz, B, Wang, H, Burianek, L, Weinberg, R, Yasuda, R, Wetsel, WC, and Soderling, SH (2013). Disruption of Arp2/3 Results in Asymmetric Structural Plasticity of Dendritic Spines and Progressive Synaptic and Behavioral Abnormalities. J Neurosci 33, 6081–6092.

Korobova, F, and Svitkina, T (2008). Arp2/3 Complex Is Important for Filopodia Formation, Growth Cone Motility, and Neuritogenesis in Neuronal Cells. Mol Biol Cell 19, 1561–1574.

Krieg, M, Dunn, AR, and Goodman, MB (2014). Mechanical control of the sense of touch by β-spectrin. Nat Cell Biol 16, 224–233.

Krieg, M, Stühmer, J, Cueva, JG, Fetter, R, Spilker, K, Cremers, D, Shen, K, Dunn, AR, and Goodman, MB (2017). Genetic defects in β-spectrin and tau sensitize C. elegans axons to movement-induced damage via torque-tension coupling. eLife 6, e20172.

Krieger, CC, An, X, Tang, H-Y, Mohandas, N, Speicher, DW, and Discher, DE (2011). Cysteine shotgun–mass spectrometry (CS-MS) reveals dynamic sequence of protein structure changes within mutant and stressed cells. Proc Natl Acad Sci 108, 8269–8274.

Kriegstein, A, and Alvarez-Buylla, A (2009). The glial nature of embryonic and adult neural stem cells. Annu Rev Neurosci 32, 149–184.

Križ, J, Zhu, Q, Julien, J-P, and Padjen, AL (2000). Electrophysiological properties of axons in mice lacking neurofilament subunit genes: disparity between conduction velocity and axon diameter in absence of NF-H. Brain Res 885, 32–44.

Kumar, S, Maxwell, IZ, Heisterkamp, A, Polte, TR, Lele, TP, Salanga, M, Mazur, E, and Ingber, DE (2006). Viscoelastic Retraction of Single Living Stress Fibers and Its Impact on Cell Shape, Cytoskeletal Organization, and Extracellular Matrix Mechanics. Biophys J 90, 3762–3773.

Leite, SC, Sampaio, P, Sousa, VF, Nogueira-Rodrigues, J, Pinto-Costa, R, Peters, LL, Brites, P, and Sousa, MM (2016). The Actin-Binding Protein α-Adducin Is Required for Maintaining Axon Diameter. Cell Rep 15, 490–498.

Leterrier, C, Potier, J, Caillol, G, Debarnot, C, Rueda Boroni, F, and Dargent, B (2015). Nanoscale Architecture of the Axon Initial Segment Reveals an Organized and Robust Scaffold. Cell Rep 13, 2781–2793.

Levine, AJ, and Brivanlou, AH (2007). Proposal of a model of mammalian neural induction. Dev Biol 308, 247–256.

Liman, J, Bueno, C, Eliaz, Y, Schafer, NP, Waxham, MN, Wolynes, PG, Levine, H, and Cheung, MS (2020). The role of the Arp2/3 complex in shaping the dynamics and structures of branched actomyosin networks. Proc Natl Acad Sci U S A 117, 10825–10831.

Lorenzo, DN, Badea, A, Davis, J, Hostettler, J, He, J, Zhong, G, Zhuang, X, and Bennett, V (2014). A PIK3C3–Ankyrin-B–Dynactin pathway promotes axonal growth and multiorganelle transport. J Cell Biol 207, 735–752.

Lorenzo, DN, Badea, A, Zhou, R, Mohler, PJ, Zhuang, X, and Bennett, V (2019). βII-spectrin promotes mouse brain connectivity through stabilizing axonal plasma membranes and enabling axonal organelle transport.

Matusek, T, Gombos, R, Szécsényi, A, Sánchez-Soriano, N, Czibula, Á, Pataki, C, Gedai, A, Prokop, A, Raskó, I, and Mihály, J (2008). Formin Proteins of the DAAM Subfamily Play a Role during Axon Growth. J Neurosci 28, 13310–13319.

Micinski, D, and Hotulainen, P (2024). Actin polymerization and longitudinal actin fibers in axon initial segment plasticity. Front Mol Neurosci 17.

Moura, MLP (2023). Understanding the nucleation, assembly and dynamics of axonal actin rings.

Murillo, JR, Goto-Silva, L, Sánchez, A, Nogueira, FCS, Domont, GB, and Junqueira, M (2017). Quantitative proteomic analysis identifies proteins and pathways related to neuronal development in differentiated SH-SY5Y neuroblastoma cells. EuPA Open Proteomics 16, 1–11.

Nascimento, AI, Mar, FM, and Sousa, MM (2018). The intriguing nature of dorsal root ganglion neurons: Linking structure with polarity and function. Prog Neurobiol 168, 86–103.

Qu, Y, Hahn, I, Webb, SED, Pearce, SP, and Prokop, A (2017). Periodic actin structures in neuronal axons are required to maintain microtubules. Mol Biol Cell 28, 296–308.

Ran, FA, Hsu, PD, Wright, J, Agarwala, V, Scott, DA, and Zhang, F (2013). Genome engineering using the CRISPR-Cas9 system. Nat Protoc 8, 2281–2308.

Rief, M, Pascual, J, Saraste, M, and Gaub, HE (1999). Single molecule force spectroscopy of spectrin repeats: low unfolding forces in helix bundles1. J Mol Biol 286, 553–561.

Rust, MB, and Maritzen, T (2015). Relevance of presynaptic actin dynamics for synapse function and mouse behavior. Exp Cell Res 335, 165–171.

Sahasrabudhe, A, Ghate, K, Mutalik, S, Jacob, A, and Ghose, A (2016). Formin 2 regulates the stabilization of filopodial tip adhesions in growth cones and affects neuronal outgrowth and pathfinding in vivo. Dev Camb Engl 143, 449–460.

Şahin, M, Öncü, G, Yılmaz, MA, Özkan, D, and Saybaşılı, H (2021). Transformation of SH-SY5Y cell line into neuron-like cells: Investigation of electrophysiological and biomechanical changes. Neurosci Lett 745, 135628.

Sakaguchi, T, Okada, M, Kitamura, T, and Kawasaki, K (1993). Reduced diameter and conduction velocity of myelinated fibers in the sciatic nerve of a neurofilament-deficient mutant quail. Neurosci Lett 153, 65–68.

Schneider, F, Metz, I, and Rust, MB (2023). Regulation of actin filament assembly and disassembly in growth cone motility and axon guidance. Brain Res Bull 192, 21–35.

Theiss, C, and Meller, K (2000). Taxol impairs anterograde axonal transport of microinjected horseradish peroxidase in dorsal root ganglia neurons in vitro. Cell Tissue Res 299, 213–224.

Ulloa, F, and Martí, E (2010). Wnt won the war: Antagonistic role of Wnt over Shh controls dorso-ventral patterning of the vertebrate neural tube. Dev Dyn 239, 69–76.

Unsain, N, Bordenave, MD, Martinez, GF, Jalil, S, von Bilderling, C, Barabas, FM, Masullo, LA, Johnstone, AD, Barker, PA, Bisbal, M, *et al.* (2018). Remodeling of the Actin/Spectrin Membrane-associated Periodic Skeleton, Growth Cone Collapse and F-Actin Decrease during Axonal Degeneration. Sci Rep 8, 3007.

Varadarajan, SG, Hunyara, JL, Hamilton, NR, Kolodkin, AL, and Huberman, AD (2022). Central nervous system regeneration. Cell 185, 77–94.

Vassilopoulos, S, Gibaud, S, Jimenez, A, Caillol, G, and Leterrier, C (2019). Ultrastructure of the axonal periodic scaffold reveals a braid-like organization of actin rings. Nat Commun 10, 5803.

Verma, S, Kumar, N, and Verma, V (2016). Role of paclitaxel on critical nucleation concentration of tubulin and its effects thereof. Biochem Biophys Res Commun 478, 1350–1354.

Wang, G, Simon, DJ, Wu, Z, Belsky, DM, Heller, E, O'Rourke, MK, Hertz, NT, Molina, H, Zhong, G, Tessier-Lavigne, M, *et al.* (2019). Structural plasticity of actin-spectrin membrane skeleton and functional role of actin and spectrin in axon degeneration. eLife 8, e38730.

Wang, MS, Davis, AA, Culver, DG, Wang, Q, Powers, JC, and Glass, JD (2004). Calpain inhibition protects against Taxol-induced sensory neuropathy. Brain 127, 671–679.

Watanabe, K, Al-Bassam, S, Miyazaki, Y, Wandless, TJ, Webster, P, and Arnold, DB (2012). Networks of Polarized Actin Filaments in the Axon Initial Segment Provide a Mechanism for Sorting Axonal and Dendritic Proteins. Cell Rep 2, 1546–1553.

Witte, H, Neukirchen, D, and Bradke, F (2008). Microtubule stabilization specifies initial neuronal polarization. J Cell Biol 180, 619–632.

Xu, K, Zhong, G, and Zhuang, X (2013). Actin, Spectrin, and Associated Proteins Form a Periodic Cytoskeletal Structure in Axons. Science 339, 452–456.

Yang, P, Yang, Y, Sun, P, Tian, Y, Gao, F, Wang, C, Zong, T, Li, M, Zhang, Y, Yu, T, *et al.* (2021). βII spectrin (SPTBN1): biological function and clinical potential in cancer and other diseases. Int J Biol Sci 17, 32–49.

Yang, R, Walder-Christensen, KK, Kim, N, Wu, D, Lorenzo, DN, Badea, A, Jiang, Y-H, Yin, HH, Wetsel, WC, and Bennett, V (2019). ANK2 autism mutation targeting giant ankyrin-B promotes axon branching and ectopic connectivity. Proc Natl Acad Sci U S A 116, 15262–15271.

Yuan, A, Rao, MV, Veeranna, and Nixon, RA (2017). Neurofilaments and Neurofilament Proteins in Health and Disease.

Yuasa-Kawada, J, Kinoshita-Kawada, M, Tsuboi, Y, and Wu, JY (2023). Neuronal guidance genes in health and diseases. Protein Cell 14, 238–261.

Zhang, Y, Abiraman, K, Li, H, Pierce, DM, Tzingounis, AV, and Lykotrafitis, G Modeling of the axon membrane skeleton structure and implications for its mechanical properties.

Zhong, G, He, J, Zhou, R, Lorenzo, D, Babcock, HP, Bennett, V, and Zhuang, X (2014). Developmental mechanism of the periodic membrane skeleton in axons. eLife 3, e04581.

Zhou, R, Han, B, Nowak, R, Lu, Y, Heller, E, Xia, C, Chishti, AH, Fowler, VM, and Zhuang, X

(2022). Proteomic and functional analyses of the periodic membrane skeleton in neurons. Nat Commun 13, 3196.

Estimation Stats. Available at: https://www.estimationstats.com/#/. Accessed January 4, 2025.

Fin.